Development of Hypersphere World-Universe Model. Narrative

Part IV. Hypersphere World-Universe Model. New Physics

Solar System. Angular Momentum. New Physics

Abstract

The most widely accepted model of Solar System formation, known as the Nebular hypothesis, does not solve the Angular Momentum problem – why is the orbital momentum of Jupiter larger than rotational momentum of the Sun? The present manuscript introduces a Rotational Fission model of creation and evolution of Macrostructures of the World (Superclusters, Galaxies, Extrasolar Systems), based on Overspinning Cores of the World's Macroobjects, and the Law of Conservation of Angular Momentum. The Hypersphere World-Universe model is the only cosmological model in existence that is consistent with this Fundamental Law.

Keywords. "Hypersphere World-Universe Model" "Medium of the World" "Fifth Fundamental Force" "Dark Matter Particles" "Macroobjects Structure" "Rotational Fission" " Law of Conservation of Angular Momentum" "Dark Epoch" " Light Epoch" " Dark Matter Reactor" " Solar Corona" " Geocorona" " Planetary Corona" "Solar Wind"

1. Introduction

This paper is based on the World – Universe Model (WUM) [1]. To be consistent with the Law of Conservation of Angular Momentum, WUM is modified as follows:

- Overspinning Dark Matter Cores of Superclusters are the main players of the World's Macrostructures creation and evolution;
- New Dark Matter particles, named Dions, with mass 0.2 eV compose Outer shells of Supercluster's Cores;
- Dions with an energy density of 68.8% of the total energy density of the World are responsible for the gravitational interaction. In the modified WUM we came back to the standard neutrino cosmology;
- Proposed Fifth Fundamental force of Weak Interaction between Dark Matter particles provides the integrity of Dark Matter Cores of all Macroobjects;
- Dions outer shells of Supercluster's Cores are growing up to the maximum mass (see Section 4) during Dark Epoch lasting from the Beginning of the World (14.2 billion years ago) for 0.4 billion years;
- Light Galaxies and Extrasolar Systems arise due to Rotational Fission of Overspinning Supercluster's Cores and annihilation of Dark Matter particles;
- Macrostructures of the World form from the top (superclusters) down to galaxies, extrasolar systems, planets, and moons. Formation of galaxies and stars is not a process that concluded ages ago; instead, it is ongoing in the Light Epoch;
- Light Epoch spans from 0.4 billion years up to the present Epoch (during 13.8 billion years). The

Big Bang discussed in the standard cosmological model is, in our view, the transition from Dark Epoch to Light Epoch.

In Section 2 of this article we present a short history of Solar System formation. In Section 3 we develop the mathematical model of overspinning spherical objects. In Section 4 we introduce a new Dark Matter fermion, named "Dion," and a Fifth Fundamental Force that is responsible for a Weak Interaction between Dark Matter particles. In Section 5 we develop a Model of the formation and evolution of Macrostructures of the World from the Beginning of the World up to the present Epoch: Superclusters, Galaxies, Extrasolar Systems, Planets and Moons. In Section 6 we discuss main characteristics of Solar System: role of Dark Matter Cores in the Sun and in the gravitationally-rounded objects; composition of Corona, Geocorona, and Planetary Coronas; Solar wind; Planets activities and other features. In the Conclusion we postulate the principal role of Angular Momentum and Dark Matter in Cosmological theories of the World.

2. Short History of Solar System Formation

The most widely accepted model of Solar System formation, known as the Nebular hypothesis, was first proposed in 1734 by Emanuel Swedenborg [2], [3] and later elaborated and expanded upon by Immanuel Kant in 1755 in his "Universal Natural History and Theory of the Heavens" [4].

Nebular hypothesis maintains that 4.6 billion years ago, the Solar System formed from the gravitational collapse of a giant molecular cloud, which was light years across. Most of the mass collected in the Centre, forming the Sun; the rest of the mass flattened into a protoplanetary disc, out of which the planets and other bodies in the Solar System formed.

The Nebular hypothesis is not without its critics. In his "The Wonders of Nature", Vance Ferrell outlined the following counter-arguments [5]:

- It contradicts the obvious physical principle that gas in outer space never coagulates; it always spreads outward;
- Each planet and moon in solar system has unique structures and properties. How could each one be different if all of them came from the same nebula;
- A full 98 percent of all the angular momentum in the solar system is concentrated in the planets, yet a staggering 99.8 percent of all the mass in our Solar system is in our Sun;
- Jupiter itself has 60 percent of the planetary angular motion. Evolutionary theory cannot account for this. This strange distribution was the primary cause of the downfall of the Nebular hypothesis;
- There is no possible means by which the angular momentum from the Sun could be transferred to the planets. Yet this is what would have to be done if any of the evolutionary theories of Solar System origin are to be accepted. Speaking of the mass-angular momentum problem, Bergamini says: *"A theory of evolution that fails to account for this peculiar fact is ruled out before it starts"* [David Bergamini, The Universe, p. 93].

Lunar origin fission hypothesis was proposed by George Darwin in 1879 to explain the origin of the Moon by rapidly spinning Earth, on which equatorial gravitative attraction was nearly overcome by centrifugal force [6]. Donald U. Wise made a detailed analysis of this hypothesis in 1966 and concluded that "*it might seem prudent to include some modified form of rotational fission among our*

working hypothesis" [7].

Solar fission theory was proposed by Louis Jacot in 1951[8]. L. Jacot stated that:

- The planets were expelled from the Sun one by one from the equatorial bulge caused by rotation;
- One of these planets shattered to form the asteroid belt;
- The moons and rings of planets were formed from the similar expulsion of material from their parent planets.
  Tom Van Flandern further extended this theory in 1993 [9]. Flandern proposed that planets were expelled from the Sun in pairs at different times. Six original planets exploded to form the rest of the modern planets. It solves several problems the standard model does not:
- If planets fission from the Sun due to overspin while the proto-Sun is still accreting, this more easily explains how 98% of the solar system's angular momentum ended up in the planets;
- It solves the mystery of the dominance of prograde rotation for these original planets since they would have shared in the Sun's prograde rotation at the outset;
- It also explains coplanar and circular orbits;
- It is the only model that explains the twinning of planets (and moons) and difference of planet pairs because after each planet pair is formed in this way, it will be some time before the Sun and extended cloud reach another overspin condition.

The outstanding issues of the Solar fission are:

- It is usually objected that tidal friction between a proto-planet and a gaseous parent, such as the proto-Sun, ought to be negligible because the gaseous parent can reshape itself so that any tidal bulge has no lag or lead, and therefore transfers no angular momentum to the proto-planet;
- There would exist no energy source to allow for planetary explosions.

Neither L. Jacot nor T. Van Flandern proposed an origin for the Sun itself. It seems that they followed the standard Nebular hypothesis of formation of the Sun.

In this work, we will concentrate on furthering the Solar Fission theory.

Let's consider rotational and orbital angular momentum of all gravitationally-rounded objects in the Solar system, from Mimas, a small moon of Saturn ($3.75 \times 10^{19}\ kg$), to the Sun itself ($2 \times 10^{30}\ kg$). Their angular momenta are presented in **Table 1.**

From the point of view of Fission model, the prime object is transferring some of its rotational momentum to orbital momentum of the satellite. It follows that **the rotational momentum of the prime object should exceed the orbital momentum of its satellite**.

From **Table 1** we see that orbital momenta of most satellites are indeed substantially smaller than the rotational momenta of their prime objects, with three exceptions (explored in Section 6):

- The rotational momentum of the Sun is smaller than Jupiter's, Saturn's, Uranus's, and Neptune's orbital momentum;
- The rotational momentum of the Earth is substantially smaller than Moon's orbital momentum;
- The rotational momentum of Pluto is considerably smaller than Charon's orbital momentum.

In Section 5 we will address the origins of these angular momenta.

3. Rotational Angular Momentum of Overspinning Objects

Let's calculate rotational angular momentum for an overspinning spherical object L_{rot}. It can be found according to the following equation:

$$L_{rot} = I\omega$$

where I is momentum of inertia and ω is angular speed. Let's assume that a spherical object has a linear density distribution ρ:

$$\rho = \rho_{max} - (\rho_{max} - \rho_{min})\frac{r}{R} = \rho_{max}[1 - (1 - \delta)\frac{r}{R}]$$

where ρ_{max} and ρ_{min} are values of density at the center and the edge of the object, R is its radius, and δ is the density ratio:

$$\delta = \frac{\rho_{min}}{\rho_{max}}$$

Then mass M of the object is:

$$M = \frac{4\pi R^3}{3}\frac{\rho_{max}}{4}(1 + 3\delta)$$

and momentum of inertia I is:

$$I = 0.4 \times \frac{4\pi R^5}{3}\frac{\rho_{max}}{6}(1 + 5\delta) = 0.4 \times \frac{2}{3}MR^2\frac{1 + 5\delta}{1 + 3\delta}$$

In case of spherical objects with homogeneous density, $\delta = 1$, then momentum of inertia I is simply

$$I = 0.4 \times MR^2$$

In **Table 1**, we assumed homogeneous density when calculating the rotational momentum L_{rot} of gravitationally-rounded objects. When the density differential is large (which is the case of the Sun, discussed in Section 5), $\delta \ll 1$, the momentum of inertia I reduces to:

$$I = 0.4 \times \frac{2}{3}MR^2$$

It is worth noting that the linear approximation of density distribution is good enough when calculating the rotational angular momentum L_{rot}. In case of non-linear density distributions L_{rot} will not change substantially.

For overspinning spherical objects, the angular velocity equals to:

$$\omega = \frac{v_{esc}}{R} = \frac{(2GM/R)^{0.5}}{R} = \frac{(2GM)^{0.5}}{R^{1.5}}$$

where v_{esc} is an escape velocity of the object and G is a gravitational parameter. Then, the rotational angular momentum of overspinning objects equals to:

$$L_{rot} = \frac{4\sqrt{2}}{15}\frac{1 + 5\delta}{1 + 3\delta}G^{0.5}M^{1.5}R^{0.5}$$

In accordance with WUM, parameters G, M, R for Macroobjects Cores are time-varying: $G \propto \tau^{-1}$,

$M \propto \tau^{3/2}$ and $R \propto \tau^{1/2}$, where τ is a cosmological time. It follows that the rotational angular momentum of Cores is proportional to: $L_{rot} \propto \tau^2$

Table 1. Rotational and orbital angular momentum of gravitationally-rounded objects of the Solar System.

	Rotational Momentum (J s)	Orbital Momentum (J s)
Sun	1.10E+42	
Mercury	9.75E+29	9.15E+38
Venus	2.13E+31	1.85E+40
Earth	7.09E+33	2.66E+40
Moon	2.36E+29	2.89E+34
Mars	2.10E+32	3.53E+39
Jupiter	6.83E+38	1.93E+43
Io	4.84E+30	6.53E+35
Europa	9.68E+29	4.42E+35
Ganimede	4.18E+30	1.72E+36
Callisto	1.09E+30	1.66E+36
Saturn	1.35E+38	7.82E+42
Mimas	4.55E+25	9.96E+31
Enceladus	1.46E+26	3.25E+32
Tethys	2.70E+27	2.06E+33
Dione	3.67E+27	4.14E+33
Rhea	8.67E+27	1.03E+34
Titan	1.63E+30	9.16E+35
Lapetus	3.58E+26	2.10E+34
Uranus	2.30E+36	1.70E+42
Miranda	7.54E+25	5.67E+31
Ariel	5.22E+27	1.42E+33
Umbriel	2.88E+27	1.49E+33
Titania	7.28E+27	5.57E+33
Oberon	3.78E+27	5.54E+33
Neptune	2.72E+36	2.50E+42
Triton	1.94E+29	3.33E+34
Pluto	8.42E+28	3.66E+38
Charon	2.52E+27	5.32E+30
Ceres	1.62E+28	6.96E+36
Haumea	4.65E+29	1.18E+38
Eris	6.05E+29	6.12E+38

Let's introduce Age parameter θ_F that is a ratio of cosmological time of Core fission τ_F to the age of the World in present Epoch A_W: $\theta_F = \tau_F / A_W$. Finally, for L_{rot} at the time of Core fission we obtain the following equation:

$$L_{rot} = \frac{4\sqrt{2}}{15}\frac{1+5\delta}{1+3\delta} G^{0.5} M^{1.5} R^{0.5} \theta_F^2 \qquad 3.1$$

where for parameters G, M, R we use their values in the present Epoch. In the next Section we discuss the nature of overspinning spherical Cores of Macroobjects.

4. Macroobjects Cores Made up of Dark Matter Particles

According to WUM, **Macrostructures of the World** (Superclusters, Galaxies, Extrasolar Systems) have Nuclei made up of Dark Matter Fermions (DMFs) [10]. In the Dark Epoch from the Beginning of the World during 0.4 billion years these Nuclei are surrounded by Shells composed of Dark Matter Particles (DMPs).

The Shells envelope one another, like a Russian doll. The lighter a DMP, the greater the radius and the mass of its shell. Innermost shells are the smallest and are made up of heaviest particles; outer shells are larger and consist of lighter particles [11].

WUM postulates that masses of DMPs are proportional to a basic unit of mass m_0 multiplied by different exponents of α [12]:

- DMF1 (fermion): $m_{DMF1} = \alpha^{-2} m_0$
- DMF2 (fermion): $m_{DMF2} = \alpha^{-1} m_0$
- DIRAC (boson): $m_{DIRAC} = \alpha^{0} m_0$
- ELOP (boson): $m_{ELOP} = \frac{2}{3}\alpha^{1} m_0$
- DMF3 (fermion): $m_{DMF3} = \alpha^{2} m_0$
- DMF4 (fermion): $m_{DMF4} = \alpha^{4} m_0$

where α is Sommerfeld's constant and is, in fact, the ratio of electron mass m_e to the basic unit of mass m_0 : $\alpha = m_e/m_o$ and m_0 equals to: $m_0 = h/ac$, where h is Planck constant, c is the electrodynamic constant and a is the basic unit of length: $a = \alpha\lambda_e$ and λ_e is Compton wavelength of an electron: $\lambda_e = h/m_e c$ [12].

The values of Dark Matter Fermion masses DMF1, DMF2, DMF3 fall into the ranges estimated in literature for neutralinos, WIMPs, and sterile neutrinos respectively [10].

DMF1, DMF2 and DMF3 are Majorana fermions, which partake in the annihilation interaction with strength equals to α^{-2}, α^{-1}, and α^{2} respectively. The signatures of DMPs annihilation with expected masses of 1.3 TeV; 9.6 GeV; 3.7 keV are found in spectra of the diffuse gamma-ray background and the emission of various macroobjects in the World [10]. **Table 2** describes the parameters of Fermionic Compact Stars (FCSs) made up of different DMFs in the present Epoch.

The calculated parameters of the shells show that [11]:

- Nuclei made of annihilating DMF1 or DMF2 compose Cores of stars in extrasolar systems;

- Shells of annihilating DMF3 around Nuclei made up of annihilating DMF1 or DMF2 make up Cores of galaxies;
- Shells of DMF4 around Nuclei made up of annihilating DMF1, DMF2, DMF3 compose Cores of superclusters.

Table 2. Parameters of FCSs made up of different DMFs in the present Epoch.

Fermion	Fermion mass $m_f, MeV/c^2$	Macroobject mass M_{max}, kg	Macroobject radius R_{min}, m	Macroobject density $\rho_{max}, kg/m^3$
DMF1	$1{,}315 \times 10^3$	1.9×10^{30}	8.6×10^3	7.2×10^{17}
DMF2	9,596	1.9×10^{30}	8.6×10^3	7.2×10^{17}
DMF3	3.73×10^{-3}	1.2×10^{41}	5.4×10^{14}	1.8×10^{-4}
DMF4	2×10^{-7}	4.2×10^{49}	1.9×10^{23}	1.5×10^{-21}

Fermionic Compact Stars have the following properties:

- The maximum potential of interaction U_{max} between any particle or macroobject and FCS made up of any fermions does not depend on the nature of fermions;
$$U_{max} = \frac{GM_{max}}{R_{min}} = \frac{c^2}{6}$$
- The maximum orbit velocity v_o does not depend on the nature of fermions;
$$v_o = \sqrt{\frac{GM_{max}}{R_{min}}} = \frac{c}{\sqrt{6}}$$
- The minimum radius of FCS made of any fermion equals to three Schwarzschild radii R_{SH} and does not depend on the nature of the fermion;
$$R_{min} = 3R_{SH}$$
- FCS density does not depend on M_{max} and R_{min} and does not change in time while $M_{max} \propto \tau^{3/2}$ and $R_{min} \propto \tau^{1/2}$.

Fifth Fundamental Force. Dark Matter (DM) is among the most important open problems in both cosmology and particle physics. The widely discussed models for nonbaryonic DM are based on the Cold Dark Matter hypothesis, and corresponding particles are commonly assumed to be Weakly Interacting Massive Particles (WIMPs).

According to Wikipedia,

A WIMP is a new elementary particle which interacts via gravity and any other force (or forces), potentially not part of the standard model itself, which is as weak as or weaker than the weak nuclear force, but also non-vanishing in its strength.

It follows that a Fifth Fundamental force needs to exist, providing interaction between DMPs with strength far exceeding gravity, and with range considerably greater than that of the weak nuclear force.

According to WUM, strength of gravity is characterized by gravitational parameter

$$G = G_0 Q^{-1}$$

where $G_0 = \frac{a^2c^4}{8\pi hc}$ is an extrapolated value of G at the Beginning of the World and dimensionless time-varying quantity Q is a measure of the age of the World:

$$Q = \tau/t_0$$

where t_0 is a basic unit of time that equals to:

$$t_0 = a/c = 5.9059674 \times 10^{-23}\ s$$

Q in the present Epoch equals to [1]:

$$Q = 0.759972 \times 10^{40}$$

The range of the gravity equals to the size of the World R:

$$R = aQ = 1.34558 \times 10^{26}\ m$$

In WUM, weak interaction is characterized by the parameter G_W:

$$G_W = G_0 Q^{-1/4}$$

which is about 30 orders of magnitude greater than G. The range of the weak interaction R_W in the present Epoch equals to:

$$R_W = aQ^{1/4} = 1.65314 \times 10^{-4}\ m \qquad 4.1$$

that is much greater than the range of the weak nuclear force that is around $\sim 10^{-16} - 10^{-17}\ m$.

Calculated concentration of Dions n_D in the largest shell with the density $\rho_D \cong 1.5 \times 10^{-21} kg/m^3$:

$$n_D \cong 4.2 \times 10^{15}\ m^{-3}$$

shows that a distance between particles is around $\sim 10^{-5}\ m$, which is much smaller than R_W. Thus, the weak interaction between DMPs will provide integrity of DM shells.

It is worth noting that the critical density of the World in the present Epoch equals to [1]:

$$\rho_{cr} = 3\rho_0 Q^{-1} \cong 8.9 \times 10^{-27}\ kg/m^3$$

which is about 5 orders of magnitude smaller than ρ_D ($\rho_0 = \frac{h/c}{a^4}$ is a basic unit of density). Distance between particles in the Medium of the World is around $\sim 10^{-3}\ m$ that is larger than R_W.

5. Beginning of the World. Dark Epoch. Rotational Fission. Light Epoch

Beginning of the World. Before the Beginning there was nothing but an Eternal Universe. About 14.2 billion years ago the World was started by a fluctuation in the Eternal Universe, and the Nucleus of the World, which is a four-dimensional 4-ball, was born. An extrapolated Nucleus radius at the Beginning was equal to a that is chosen to fit the Age of the World. The 3D World is a hypersphere that is the surface of a 4-ball Nucleus. All points of the hypersphere are equivalent; there are no preferred centers or boundary of the World [1], [12].

Expansion. The 4-ball is expanding in the Eternal Universe, and its surface, the hypersphere, is likewise expanding so that the radius of the Nucleus R is increasing with speed c that is the gravitoelectrodynamic constant, for the absolute cosmological time τ from the Beginning and equals to $R = c\tau$. The expansion of the Hypersphere World can be understood by the analogy with an expanding 3D balloon: imagine small enough "flat" observer residing in a curved flatland on the surface of a balloon; as the balloon is blown up, the distance between all neighboring points grows; the two-dimensional world grows but there is no preferred center [1], [12].

Creation of Matter. The surface of the 4-ball is created in a process analogous to sublimation. It is a well-known endothermic process that occurs when surfaces are intrinsically more energetically favorable than the bulk of a material, and hence there is a driving force for surfaces to be created. Continuous creation of matter is the result of a similar process. Matter arises from the fourth spatial dimension. The Universe is responsible for the creation of Matter. Dark Matter particles carry new Matter in the World. Creation of Matter is a direct consequence of expansion. Creation of DM occurs homogeneously in all points of the hypersphere World [1], [12].

Dark Epoch started at the Beginning of the World and lasted for about 0.4 billion years. Hypersphere WUM is a classical model. According to the model, classical notions can be introduced only when the very first ensemble of particles was created at the cosmological time $\tau_q = t_0\alpha^{-2} \cong 10^{-18}s$ [1]. The World at cosmological times less than 10^{-18} s is best described by Quantum mechanics. The value of the parameter Q at that time was: $Q_q = \alpha^{-2}$; a size of the World R_q was $a \times \alpha^{-2} = 2\pi a_B$ (a_B is Bohr radius) and a total mass of the World:

$$M_W = 6\pi^2 m_0 \times Q^2 = 6\pi^2 m_0 \alpha^{-4} \cong 2.6 \times 10^{-18}\ kg$$

At time $\tau \gg \tau_q$ density fluctuations could happen in the Medium of the World filled out with DMF1, DMF2, DIRACs, ELOPs, DMF3 and DMF4. The heaviest DMF1 with mass $m_{DMF1} = m_0\alpha^{-2}$ could collect into a cloud of radius R_{cl} with distance between them equals to $R_W = aQ^{1/4}$. As the result of the weak interaction, clumps of DMF1 will arise with density $\rho_{cl} = \rho_0\alpha^{-2} \times Q^{-3/4}$, volume V_{cl} and mass M_{cl} :

$$M_{cl} = \rho_0\alpha^{-2}V_{cl} \times Q^{-3/4}$$

Considering the analogy between electromagnetic and gravitoelectromagnetic fields [1], we can write the following equation for the minimum product of objects masses to exert gravity on one another:

$$m_{DMF1}M_{cl} = m_0^2\alpha^{-4}a^{-3}V_{cl} \times Q^{-3/4} = 2m_0^2 \times Q$$

The volume of a clump V_{cl} then equals to

$$V_{cl} = 2\alpha^4 a^3 \times Q^{7/4}$$

and mass of a clump M_{cl} is:

$$M_{cl} = 2m_0\alpha^2 \times Q$$

A well-elaborated classical model can be introduced when the cosmological time was $\tau_{cl} = t_0\alpha^{-8} \cong 7 \times 10^{-6}\ s$. Taking the value of the parameter $Q_{cl} = \alpha^{-8}$ we get

$$M_{cl} = 2m_0\alpha^{-6} \cong 1.6 \times 10^{-15}\ kg$$

$$R_{cl} = a\,(3/2\pi)^{1/3}\alpha^{-10/3} \cong 1.8 \times 10^{-7}\ m$$

$$\rho_{cl} = \rho_0 a^4 \cong 6.4 \times 10^4\ kg/m^3$$

$$R_W^{cl} = a \times \alpha^{-2} \cong 3.3 \times 10^{-10}\ m$$

At that time, mass M_{World} and size R_{World} of the World were

$$M_{World} = 6\pi^2 m_0 \times Q^2 \cong 10^8\ kg$$

$$R_{World} = a \times \alpha^{-8} \cong 2 \times 10^3\ m$$

Analogous calculations for DMF2 produce the following results for clump mass M'_{cl} and density ρ'_{cl} :

$$M'_{cl} = 2m_0\alpha^{-7} \cong 2.2 \times 10^{-13}\ kg$$

$$\rho'_{cl} = \rho_0 a^5 \cong 4.7 \times 10^2\ kg/m^3$$

Larger clumps will attract smaller clumps and DMPs and initiate a process of expanding the DM Core to the maximum mass of the shell made up of Dions. Considering the Age parameter $\theta_{0.4} \cong 1/36$ and dependence of Core mass $M_{Core} \propto \tau^{3/2}$ and Core size $R_{Core} \propto \tau^{1/2}$, we obtain $M_{Core}^{0.4} = 2.3 \times 10^{47}\ kg$ and $R_{Core}^{0.4} = 3.2 \times 10^{22}\ m$ at the end of Dark Epoch (0.4 billion years). This is the Core of Supercluster. Considering the total mass of the World at that time $M_{tot}^{0.4}$:

$$M_{tot}^{0.4} = 6\pi^2 m_0 \times Q_{0.4}^2 = 3.3 \times 10^{50}\ kg$$

we estimate the number of Supercluster Cores to be around $\sim 10^3$. In our opinion, all Supercluster Cores had undergone rotational fission at approximately the same cosmological time.

Rotational Fission. Local Supercluster is a mass concentration of galaxies containing the Local Group, which in turn contains the Milky Way galaxy. At least 100 galaxy groups and clusters are located within its diameter of 110 million light-years.

Let's calculate the rotational angular momentum L_{rot}^{LSC} of Local Supercluster Core (LSC) before rotational fission based on the equation (3.1) and parameters of Dion shell (see **Table 2**) with the Age parameter $\theta_{0.4} \cong 1/36$:

$$L_{rot}^{LSC} = 3.7 \times 10^{77} J\ s$$

Milky Way (MW) is gravitationally bounded with Local Supercluster (LS) [13]. Let's compare L_{rot}^{LSC} with an orbital momentum of Milky Way L_{orb}^{MW} calculated based on the distance of 65 million light years from LSC and orbital speed of about 400 km/s [13]:

$$L_{orb}^{MW} = 2.5 \times 10^{71}\ J\ s$$

It means that as the result of rotational fission of LS Core, approximately $\sim 10^6$ galaxies like Milky Way could be generated at the same time. Considering that the number density of galaxies in the LS falls off with the square of the distance from its center near the Virgo Cluster, and the location of MW on the outskirts of the LS [14], the actual number of created galaxies could be much larger.

Analogous calculations for Milky Way Core (MWC) based on parameters of DMF3 shell produce the following value of rotational angular momentum L_{rot}^{MWC} :

$$L_{rot}^{MWC} = 2.4 \times 10^{60}\ J\ s$$

which far exceeds the orbital momentum of the Solar System L_{orb}^{SS} calculated based on the distance from the galactic center of 26,400 light years and orbital speed of about 220 km/s :

$$L_{orb}^{SS} = 1.1 \times 10^{56}\ J\ s \qquad 5.1$$

As the result of rotational fission of Milky Way's Core 13.8 billion years ago, approximately $\sim 10^4$ Extrasolar systems like Solar System could be created at the same time. Considering that MW has grown inside out (in the present Epoch, most old stars can be found in the middle, more recently formed ones on the outskirts [15]), the number of generated Extrasolar systems could be much larger.

Extrasolar system Cores can give birth to planet cores, and they can generate cores of moons by the same Rotational Fission mechanism (see next Section).

The mass-to-light ratio of the Local Supercluster is about 300 times larger than that of the Solar ratio. Similar ratios are obtained for other superclusters [16]. These facts support the rotational fission mechanism proposed above.

In 1933, Fritz Zwicky investigated the velocity dispersion of Coma cluster and found a surprisingly high mass-to-light ratio ($\sim$500). He concluded: *if this would be confirmed, we would get the surprising result that dark matter is present in much greater amount than luminous matter* [17]. These ratios are one of the main arguments in favor of presence of large amounts of Dark Matter in the World.

Light Epoch spans from 0.4 billion years up to the present Epoch (during 13.8 billion years). According to WUM, Cores of all Macroobjects (MO) of the World (Superclusters, Galaxies, Extrasolar systems) possess the following properties:

- Their Nuclei are made up of DMFs and contain other particles, including Dark Matter and baryonic matter, in shells surrounding the Nuclei;
- DMPs are continuously absorbed by Cores of all MOs. Light Matter (about 7.2% of the total Matter in the World) is a product of DMPs annihilation. Light Matter (LM) is re-emitted by Cores of MOs continuously;
- Nuclei and shells are growing in time: size $\propto \tau^{1/2}$; mass $\propto \tau^{3/2}$ and rotational angular momentum $\propto \tau^2$, until they reach the critical point of their stability, at which they detonate. Satellite cores and their orbital L_{orb} and rotational L_{rot} angular momenta released during detonation are produced by Overspinning Core (OC). The detonation process does not destroy OC; it's rather gravitational hyper-flares;
- Size, mass, composition, L_{orb} and L_{rot} of satellite cores depend on local density fluctuations at the edge of OC and cohesion of the outer shell. Consequently, the diversity of satellite cores has a clear explanation.

  This is a description of Gravitational Bursts (GBs) analogous to the description of Gamma Ray Bursts (GRBs) and Fast Radio Bursts (FRBs) [11]. In frames of WUM, the repeating GBs can be explained the following way:

- As the result of GB, the OC loses a small fraction of its mass and a large part of its rotational angular momentum;

- After GB the Core absorb new DMPs increasing its mass $\propto \tau^{3/2}$ and growing up L_{rot} much faster $\propto \tau^2$ until the next critical point of its stability at which it detonates again;
- Afterglow of GBs is a result of processes developing in the Nuclei and shells after detonation. In case of Extrasolar systems, a star wind is the afterglow of star detonation: star Core absorbs new DMPs, increase its mass $\propto \tau^{3/2}$ and gets rid of extra L_{rot} by star wind particles.

In frames of the developed Rotational Fission model it is easy to explain hyper-runaway stars unbound from the Milky Way with speeds of up to $\sim 700\ km/s$ [18]: they were launched by overspinning Core of the Large Magellanic Cloud with the speed higher than the escape velocity.

C. J. Clarke *et al.* observed CI Tau, a young 2 million years old star. CI Tau is located about 500 light years away in a highly-productive stellar 'nursery' region of the galaxy. They discovered that the Extrasolar System contains four gas giant planets that are only 2 million years old [19], amount of time that is too short for formation of gas giants according to prevailing theories.

In frames of the developed Rotational Fission model, this discovery can be explained by Gravitational Burst of the overspinning Core of the Milky Way two million years ago, which gave birth to CI Tau system with all planets generated at the same time.

To summarize,

- The rotational fission of macroobject cores is the most probable process that can generate satellite cores with large orbital momenta in a very short time;
- Macrostructures of the World form from the top (superclusters) down to galaxies, extrasolar systems, planets, and moons;
- Gravitational waves can be a product of rotational fission of overspinning Macroobject Cores;
- Hypersphere World-Universe model can serve as a basis for Transient Gravitational Astrophysics.

In the next Section we discuss main characteristics of Solar System considering the developed mechanism of Rotational Fission.

6. Solar System

Angular momentum. The Solar system was born 4.6 billion years ago as the result of the repeating Gravitational burst of Milky Way's Core. At that time, Age parameter $\theta_{9.6}$ equaled about $\cong 2/3$, and the rotational angular momentum of the Core L_{rot}^{MWC} was much larger than L_{orb}^{SS} (see equation (5.1)):

$$L_{rot}^{MWC} = 1.4 \times 10^{63}\ J\ s$$

At that time, the Galactic Core could generate approximately $\sim 10^7$ Extrasolar systems like the Solar system. Considering that Jupiter's orbital momentum is about 60% of the total angular momentum of Solar System L_{tot}^{SS}, we obtain

$$L_{tot}^{SS} \cong 3.2 \times 10^{43}\ J\ s \qquad 6.1$$

Let's calculate parameters of the Sun's Core necessary to provide this angular momentum. Substituting mass $M_{Sun} = 2 \times 10^{30}\ kg$ and radius $R_{Sun} = 7 \times 10^8\ m$ and using equation (3.1) we obtain

$$L_{rot}^{Sun} = 1.1 \times 10^{44}\ J\ s$$

which is 3.3 times greater than L_{tot}^{SS} . It follows that the Sun's Core can be smaller.

Let's consider the structure of the Sun. According to the standard Solar model it has:

- Core that extends from the center to about 20–25% of the solar radius, contains 34% of the Sun's mass with density $\rho_{max} = 1.5 \times 10^5\ kg/m^3$ and $\rho_{min} = 2 \times 10^4\ kg/m^3$. It produces all Sun's energy;
- Radiative zone from the Core to about 70% of the solar radius with density $\rho_{max} = 2 \times 10^4\ kg/m^3$ and $\rho_{min} = 2 \times 10^2\ kg/m^3$ in which convection does not occur and energy transfer occurs by means of radiation;
- Core and Radiative zone contain practically all Sun's mass [20].

In our opinion, the Sun has an Inner Core (Nucleus made up of DMF1) whose radius is 20–25% of the solar radius, and an Outer Core – the Radiative zone. We then calculate the Solar Core rotational angular momentum L_{rot}^{SC} :

$$L_{rot}^{SC} \cong 8.9 \times 10^{43}\ J\ s$$

which is 2.8 times larger than the overall angular momentum of the Solar System (6.1).

Let's follow the same procedure for the Earth – Moon pair. Considering the mass of Earth $M_{Earth} = 6 \times 10^{24} kg$ and radius $R_{Earth} = 6.4 \times 10^6 m$ and using (3.1) ($\theta_{9.6} \cong 2/3$ and $\delta = 2.9/13.1$) we calculate $L_{rot}^{Earth} = 6.6 \times 10^{34}\ J\ s$ that is 2.3 times larger than the Moon's orbital momentum $L_{orb}^{Moon} = 2.9 \times 10^{34}$ J s (see **Table 1**).

Let's look at the structure of the Earth. According to the standard model it has:

- An inner core and an outer core that extend from the center to about 45% of the Earth radius with density $\rho_{max} = 1.3 \times 10^4\ kg/m^3$ and $\rho_{min} = 9.9 \times 10^3\ kg/m^3$;
- Lower mantle, spanning from the outer core to about 90% of the Earth radius (below 660 km) with density $\rho_{max} = 5.6 \times 10^3\ kg/m^3$ and $\rho_{min} = 4.4 \times 10^3\ kg/m^3$;
- Inner core, outer core, and lower mantle contain practically all of the Earth's mass [21].

Very little is known about the lower mantle apart from that it appears to be relatively seismically homogeneous. Outer core – lower mantle boundary has a sharp drop of density $(9.9 \rightarrow 5.6) \times 10^3\ kg/m^3$ [21].

In our opinion, lower mantle is a part of the Earth's core. It could be significantly different 4.6 billion years ago, since during this time it was gradually filled with all chemical elements produced by Earth's core due to DMF1 annihilation. Considering the Earth's core (EC) with radius $R_{core}^{Earth} = 5.7 \times 10^6\ m$ ($\theta_{9.6} \cong 2/3$ and $\delta = 4.4/13.1$), the rotational angular momentum equals to:

$$L_{rot}^{EC} = 6.5 \times 10^{34}\ J\ s$$

which is 2.2 times larger than the orbital momentum of the Moon.

As for the Pluto – Charon pair, it is definitely a binary system. Charon was not generated by Pluto's core; instead, they are two independent objects that happened to be bounded together by gravity.

Earth's internal heat. According to the standard model, the Earth's internal heat is produced mostly through radioactive decay. The major heat-producing isotopes within Earth are K-40, U-238, and Th-232 with half-lives of $(1.25; 4.47; 14.0) \times 10^9$ $year$ respectively, and with the calculated mean mantle concentrations of $(36.9;\ \ 30.8;\ 124)\ \times 10^{-9}$ $\frac{kg\ isotope}{kg\ mantle}$ respectively [22]. The mean global heat loss from Earth is 44.2 TW [23]. The Earth's Uranium has been thought to be produced in one or more supernovae over 6 billion years ago [24].

Radiogenic decay can be estimated from the flux of geoneutrinos that are emitted during radioactive decay. The KamLAND Collaboration combined precise measurements of the geoneutrino flux from the Kamioka Liquid-Scintillator Antineutrino Detector, Japan, with existing measurements from the Borexino detector, Italy. They found that decay of U-238 and Th-232 together contribute about 20 TW to the total heat flux from the Earth to space 44.2 ± 1.0 TW. The neutrinos emitted from the decay of K-40 were below the limits of detection in their experiments but are known to contribute 4 TW. Based on the observations the KamLAND Collaboration made a conclusion *that heat from radioactive decay contributes about half of Earth's total heat flux* [25].

Plutonium-244. According to the Wikipedia article,

Pu-244 has a half-life of 80 million years. Unlike other plutonium isotopes, Pu-244 is not produced in quantity by the nuclear fuel cycle, because it needs very high neutron flux environments. A nuclear weapon explosion can produce some Pu-244 by rapid successive neutron capture.

Nevertheless, D. C. Hoffman *et al.* in 1971 obtained the first indication of Pu-244 present existence in Nature [26].

In our opinion, all chemical products of the Earth including isotopes K-40, U-238, Th-232, and Pu-244, are produced within the Earth as the result of DMF1 annihilation. They arrive in the Crust of the Earth due to convection currents in the mantle carrying heat and isotopes from the interior to the planet's surface [27].

Gravitationally-rounded objects internal heat. The analysis of Sun's heat for planets in Solar system yields the effective temperature of Earth of 255 K [28]. The actual mean surface temperature of Earth is 288 K [29]. The higher actual temperature of **Earth** is due to energy generated internally by the planet itself.

Jupiter radiates more heat than it receives from the Sun [30]. Giant planets like Jupiter are hundreds of degrees warmer than current temperature models predict. Until now, the extremely warm temperatures observed in Jupiter's atmosphere (about 970 degrees C [31]) have been difficult to explain, due to lack of a known heat source [12].

Saturn radiates 2.5 times more energy than it receives from the Sun [32]; **Uranus** – 1.1 times [33]; **Neptune** – 2.6 times [34].

The most fascinating result was obtained for the smallest gravitationally-rounded object – **Mimas.** **Figure 1** illustrates the unexpected and bizarre pattern of daytime temperatures found on it.

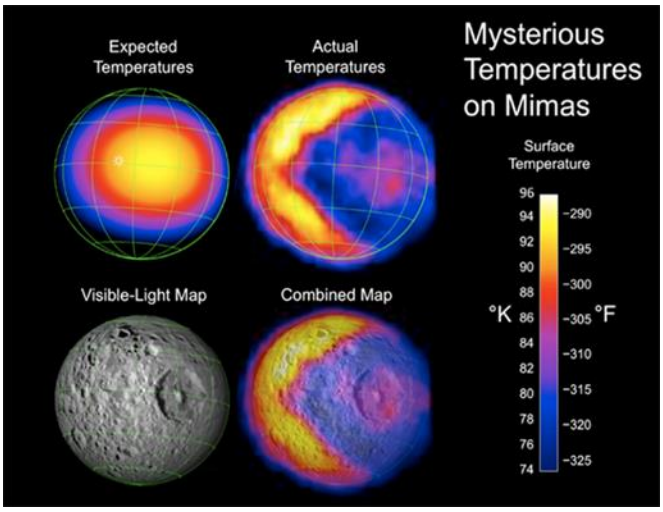

Figure 1. Mimas pattern of daytime temperatures. Adapted from [35].

Dark Matter Cores. The following facts support the existence of DM Cores in Macroobjects:

- Fossat *et al.* found that Solar Core rotates 3.8 ± 0.1 faster than the surrounding envelope [36];
- By analyzing the earthquake doublets, Zhang *et al.* concluded that the Earth's inner core is rotating faster than its surface by about 0.3 - 0.5 degrees per year [37];
- T. Guillot *et al.* found that a deep interior of Jupiter rotates nearly as a rigid body, with differential rotation decreasing by at least an order of magnitude compared to the atmosphere [38].

The fact that Macroobject Cores rotate faster than surrounding envelopes, despite high viscosity of the internal medium, is intriguing. WUM explains this phenomenon through absorption of DMPs by Cores. Dark Matter Particles supply not only additional mass ($\propto \tau^{3/2}$), but also additional angular momentum ($\propto \tau^{2}$). Cores irradiate products of annihilation, which carry away excessive angular momentum. The Solar wind is the result of this mechanism.

WUM explanation. The internal heating of all gravitationally-rounded objects of the Solar system is due to DMPs annihilation in their Nuclei made up of DMF1 with mass 1.3 TeV (compare to proton mass: 938 MeV). The amount of energy produced due to this process is sufficiently high to heat up the objects. New DMF1 freely penetrate through the entire objects' envelope, get absorbed into the nucleus and support DMF1 annihilation continuously. Objects' nuclei are "DM Reactors" fueled by DMF1 [12].

In our opinion, all chemical elements, compositions, substances, rocks, etc. are produced by Macroobjects themselves as the result of DMPs annihilation. The diversity of all gravitationally-rounded objects of the Solar System is explained by their distance from the Sun, and the differences in their Cores (mass, size, composition).

The "DM Reactor" inside of all gravitationally-rounded objects (including Earth) provides sufficient energy for all geological processes on planets and satellites. All gravitationally-rounded objects in hydrostatic equilibrium, down to Mimas in Solar system, prove the validity of WUM [12].

The evolution of the Sun. By 1950s, stellar astrophysicists had worked out the physical principles governing the structure and evolution of stars [39]. According to these principles, the Sun's

luminosity had to change over time, with the young Sun being about 30% less luminous than today [40], [41], [42], [43]. The long-term evolution of the bolometric solar luminosity $L(\tau)$ as a function of cosmological time τ can be approximated by a simple linear law: $L(\tau) \propto \tau$ [39].

One of the consequences of WUM holds that all stars were fainter in the past. As their cores absorb new DM, size of MO cores R_{MO} and their luminosity L_{MO} are increasing in time: $R_{MO} \propto \tau^{1/2}$ and $L_{MO} \propto R_{MO}^2 \propto \tau$ respectively. Taking the age of the World $A_W \cong 14.2\ Byr$ and the age of the solar system $A_{SS} \cong 4.6\ Byr$, it is easy to find that the young Suns' output was 67% of what it is today. Literature commonly refers to the value of 70% [42], [43]. This result supports the developed model of the structure and evolution of the Sun [39].

Pioneer anomaly. According to Fractal Cosmology, Macroobject Cores are surrounded by a transitional region. In this region, the density decreases rapidly to the point of the zero level of the fractal structure [44] characterized by radius R_f and density ρ_f, that satisfy the following equation for $r \geq R_f$:

$$\rho(r) = \frac{\rho_f R_f}{r} \tag{6.2}$$

According to Yu. Baryshev: *For a structure with fractal dimension $D = 2$ the constant $\rho_f R_f$ may be actually viewed as a new fundamental physical constant* [44]. In WUM, it is natural to connect this constant with a basic unit of energy density $\sigma_0 = hc/a^3$:

$$\rho_f R_f = 4\sigma_0/c^2 \tag{6.3}$$

The value of 4 above follows from the ratio for all MOs of the World: 1/3 of the total energy is in the central macroobject and 2/3 of the total energy is in the structure around it [10].

Wikipedia describes the so-called Pioneer anomaly as

observed deviation from predicted accelerations of the Pioneer 10 and Pioneer 11 spacecraft after they passed about 20 astronomical units on their trajectories out of the Solar System. An unexplained force appeared to cause an approximately constant sunward acceleration of $a_P = 8.74 \pm 1.33 \times 10^{-10}\ m/s^2$ for both spacecraft. The magnitude of the Pioneer effect a_P is numerically quite close to the product of the speed of light c and the Hubble constant H_0 hinting at cosmological connection.

Let us calculate deceleration a_P at the distance $r_P \gg R_f$ due to additional mass of the structure $M_{FS} \propto r_P^2$ with the following equation for gravitational parameter in the present Epoch $G = \frac{c^4}{8\pi\sigma_0 R_0}$ [10]:

$$a_P = \frac{GM_{FS}}{r_P^2} = \frac{c^4}{8\pi\sigma_0 R_0} \times \frac{8\pi\sigma_0}{c^2} = \frac{c^2}{R_0} = cH_0 = 6.68 \times 10^{-10}\ m/s^2$$

which is in good agreement with the experimentally measured value (R_0 and H_0 are the values of the World's size R and Hubble's parameter H at the present Epoch). It is important to notice that the calculated deceleration does not depend on r_P and equals to cH_0 for all objects around the Macroobject at the distance $r \gg R_f$.

Mass of the structure around Sun M_V at distances $R_V \gg R_f$ is: $M_V = \frac{8\pi R_V^2 \sigma_0}{c^2}$. At distance to Voyager 1 : $R_V \cong 1.8 \times 10^{13}\ m$ [45], the structure mass is: $M_V \cong 3.3 \times 10^{27} kg$ that is ~ 0.15% M_{Sun}.

Structure of the Solar atmosphere. Let's take a look at the structure of Solar atmosphere, its density and temperature depicted in **Figure 2**.

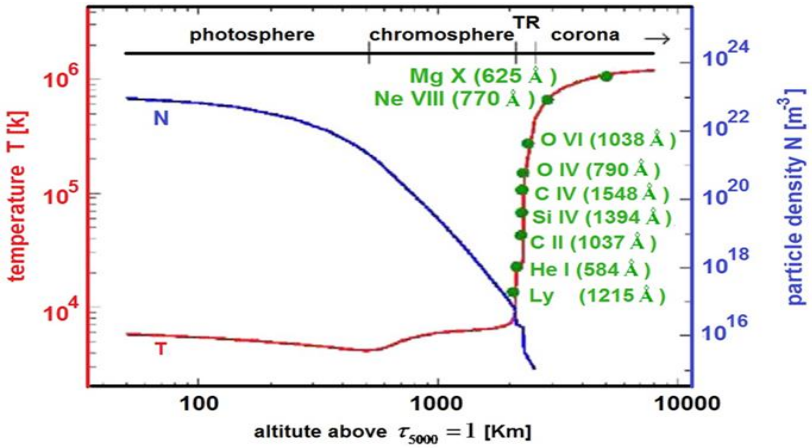

Figure 2. Height variations of the temperature and density of solar atmosphere. Adapted from H. Peter [46].

According to the standard model, the visible surface of the Sun, the **photosphere**, is the layer below which the Sun becomes opaque to visible light [43]. Above the photosphere visible sunlight is free to propagate into space, and almost all of its energy escapes the Sun entirely. The sunlight has the spectrum of a black-body radiating at about 5,800 K.

Above the photosphere lies the **chromosphere** that is about 2,500 km thick, dominated by a spectrum of emission and absorption lines. The temperature of the chromosphere increases gradually with altitude, ranging up to around 20,000 K near the top [47]. The particle density decreases rapidly from 10^{22} to $10^{17} m^{-3}$.

Above the chromosphere, in a thin (about 200 km) **transition region**, the temperature rises rapidly from around 20,000 K in the upper chromosphere to coronal temperatures closer to 1,000,000 K. The particle density decreases from 10^{17} up to $10^{16}-10^{15}\ m^{-3}$ in the low corona.

In our opinion, this is a zero level of the fractal structure. The calculated density according to (6.3) is:

$$\rho_f \cong 2.3 \times 10^{-9}\ kg/m^3 \qquad 6.4$$

Corona is an aura of plasma that surrounds the Sun and other stars. The Sun's corona extends at least 8 million kilometers into outer space [48] and is most easily seen during a total solar eclipse. Spectroscopy measurements indicate strong ionization and plasma temperature in excess of 1,000,000 K [49]. The corona emits radiation mainly in the X-rays, observable only from space. The plasma is transparent to its own radiation and to that one coming from below, therefore we say that it is optically-thin. The gas, in fact, is very rarefied and the photon mean free-path overcomes by far all the other length-scales, including the typical sizes of the coronal features.

J. T. Schmelz has this to say about composition of Solar corona:

Along with temperature and density, the elemental abundance is a basic parameter required by astronomers to understand and model any physical system. The abundances of the solar corona are known to differ from those of the solar photosphere [50].

Wikipedia has this to say about the coronal heating problem:

Coronal heating problem in solar physics relates to the question of why the temperature of the Sun's corona is millions of kelvins higher than that of the surface. The high temperatures require energy to be carried from the solar interior to the corona by non-thermal processes, because the second law of thermodynamics prevents heat from flowing directly from the solar photosphere (surface), which is at about 5800 K, to the much hotter corona at about 1 to 3 MK (parts of the corona can even reach 10 MK).

In our opinion, the origin of the Solar corona plasma is not the coronal heating. Plasma particles (electrons, protons, multicharged ions) are so far apart that its temperature in the usual sense is not very meaningful. This plasma is the result of the annihilation of Dark Matter particles DMF1 with mass 1.3 TeV . The Solar corona resembles a honeycomb filled with plasma.

The following experimental results speak in favor of this model:

- The corona emits radiation mainly in the X-rays;
- The plasma is transparent to its own radiation and to that one coming from below;
- The abundances of the solar corona are known to differ from those of the solar photosphere;
- During the impulsive stage of Solar flares, radio waves, hard x-rays, and gamma rays with energy above 100 GeV are emitted (one photon emitted during the solar minimum had an energy as high as 467.7 GeV) [51];
- Assuming the particle density in the low corona $10^{15}\,m^{-3}$ and mass of DMF1: $m_{DMF1} = 2.3 \times 10^{-24}\ kg$ we can find mass density $\rho^{in}_{DMF1} = 2.3 \times 10^{-9}\ kg/m^3$ that is equal to the density of the fractal structure (6.4);
- A distance between particles DMF1 is about $10^{-5}\ m$ that is much smaller than the range of the weak interaction of DMPs R_W (4.1). It means that the Solar corona is a stable Shell around the Sun with density decreasing according to equation (6.2) with inner radius about $R_{in} \cong 7 \times 10^8\ m$ and outer radius R_{out} :

$$R_{out} = \frac{4\sigma_0/c^2}{m_{MDF1} n_{out}}$$

  where n_{out} is the particle density of the Shell at the outer radius: $n_{out} = R_W^{-3} = a^{-3} \times Q^{-3/4}$.

Considering this value of n_{out} we can calculate R_{out} :

$$R_{out} = 4\alpha^2 a \times Q^{3/4} \cong 3 \times 10^{12}\ m \qquad 6.5$$

The total mass of the Shell M_{DMF1} is about:

$$M_{DMF1} = \frac{8\pi\sigma_0}{c^2} R_{out}^2 \cong 9 \times 10^{25}\ kg \qquad 6.6$$

Observable outer radius of the Solar corona $8 \times 10^9\ m$ [46] depends on the concentration of DMPs, the strength of their annihilation interaction, and a sensitivity of the measuring instrument.

Geocorona. According to Wikipedia,

The geocorona is the luminous part of the outermost region of the Earth's atmosphere, the exosphere. It is seen primarily via far-ultraviolet light (Lyman-alpha) from the Sun that is scattered from neutral hydrogen. It extends to at least 15.5 Earth radii.

Let's take a look at structure of Earth atmosphere, its density and temperature depicted in **Figure 3**.

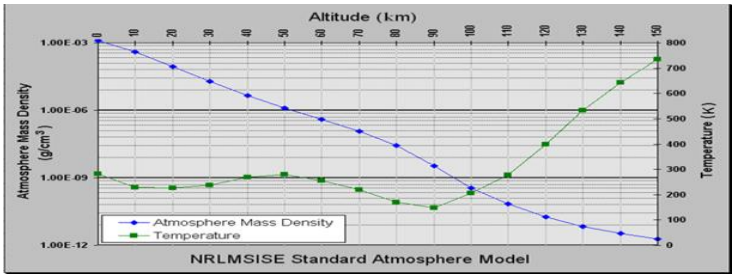

Figure 3. Temperature and mass density against altitude from NRLMSISE-00 standard atmosphere model. Adapted from M. Picone, A. E. Hedin, D. Drob [52].

The atmosphere consists of five primary layers: the troposphere, stratosphere, mesosphere, thermosphere, and exosphere [53], [54], [55]:

- Troposphere: 0 to 12 km . It contains roughly 80% of the mass of Earth's atmosphere [56];
- Stratosphere: 12 to 50 km. The atmospheric pressure at the top of the stratosphere is roughly 1/1000 the pressure at sea level;
- Mesosphere: 50 to 80 km. The top of Mesosphere is the coldest place on Earth and has an average temperature around −85 °C [57], [58];
- Thermosphere: 80 to 700 km. The highly diluted gas in this layer can reach 2,500 °C. The lower part of it, from 80 to 550 kilometers contains the ionosphere;
- Exosphere: 700 to 10,000 km. The top of exosphere merges into the solar wind.

The mesopause is the temperature minimum at the boundary between the mesosphere and the thermosphere. It consists of two minima - one at about 85 km and a stronger minimum at about 100 km [59] with temperatures below −143 °C .

Far-ultraviolet photons in the exosphere have been observed out to a distance of approximately 100,000 km from the Earth (15.5 Earth radii) [60]. The first high-quality and wide-field-of-view image of Earth's corona of 38 Earth radii (243,000 km) obtained by the first interplanetary microspacecraft [61].

The Hisaki satellite with the extreme ultraviolet spectrometer EXCEED acquires spectral images (52–148 nm) of the atmospheres/magnetospheres of planets from Earth orbit. Due to its low orbital altitude (~1000 km), the images taken by the instrument also contain the geocoronal emissions. In this context, EXCEED has provided quasi-continuous remote sensing observations of the geocorona with high temporal resolution (~1 min) since 2013 [62]. The most popular explanation of this geocoronal emission is the scattering of Solar Far-Ultraviolet (FUV) photons by exospheric hydrogen.

X-rays from Earth's geocorona were first detected by Chandra X-ray Observatory in 1999 [63]. X-rays were observed in the range of energies $0.08 - 10\ keV$ [63]. The main mechanism explaining the geocoronal X-rays is that they are caused by collisions between neutral atoms in the geocorona with carbon, oxygen and nitrogen ions that are streaming away from the Sun in the solar wind [63], [64], [65]. This process is called "charge exchange", since an electron is exchanged between neutral atoms in geocorona and ions in the solar wind.

X-rays from Planets were also observed by Chandra [63]. According to NASA:

- *The X-rays from Venus and, to some extent, the Earth, are due to the fluorescence of solar X-rays striking the atmosphere;*
- *Fluorescent X-rays from oxygen atoms in the Martian atmosphere probe heights similar to those on Venus. A huge Martian dust storm was in progress when the Chandra observations were made. Since the intensity of the X-rays did not change when the dust storm rotated out of view, astronomers were able to conclude that the dust storm did not affect Mars's upper atmosphere;*
- *Jupiter has an environment capable of producing X-rays in a different manner because of its substantial magnetic field. X-rays are produced when high-energy particles from the Sun get trapped in its magnetic field and accelerated toward the polar regions where they collide with atoms in Jupiter's atmosphere. Chandra's image of Jupiter shows strong concentrations of X-rays near the north and south magnetic poles. The weak equatorial X-ray emission is likely due to reflection of solar X-rays;*
- *Like Jupiter, Saturn has a strong magnetic field, so it was expected that Saturn would also show a concentration of X-rays toward the poles. However, Chandra's observation revealed instead an increased X-ray brightness in the equatorial region. Furthermore, Saturn's X-ray spectrum, or the distribution of its X-rays according to energy, was found to be similar to that of X-rays from the Sun.*

V. I. Shematovich and D. V. Bisikalo gave the following explanation of the planetary coronas [66]:

The measurements reveal that planetary coronas contain both a fraction of thermal neutral particles with a mean kinetic energy corresponding to the exospheric temperature and a fraction of hot neutral particles with mean kinetic energy much higher than the exospheric temperature. These suprathermal (hot) atoms and molecules are a direct manifestation of the non-thermal processes taking place in the atmospheres. These hot particles lead to the atmospheric escape, determine the coronal structure, produce non-thermal emissions, and react with the ambient atmospheric gas triggering hot atom chemistry.

Let's summarize the obtained results for Geocorona and Planetary Coronas:

- FUV radiation has been observed out to a distance of approximately 243,000 km from the Earth;
- FUV radiation was observed in the wavelength range down to 52 nm;
- X-rays were observed in the range of energies $0.08 - 10\ keV$;
- X-rays from Venus are due to the fluorescence of solar X-rays striking the atmosphere;
- Fluorescent X-rays from oxygen atoms in the Martian atmosphere probe heights similar to those on Venus. Dust storm did not affect Mars's upper atmosphere;
- Jupiter's X-rays are produced when high-energy particles from the Sun get trapped in its

magnetic field and accelerated toward the polar regions where they collide with atoms in Jupiter's atmosphere;
- Saturn's X-ray spectrum was found to be similar to that of X-rays from the Sun;
- Suprathermal (hot) atoms and molecules are a direct manifestation of the non-thermal processes taking place in the atmospheres. These hot particles produce non-thermal emissions.

In our opinion, the described picture of Geo and Planetary Coronas is similar to the picture of the Solar Corona:

- The Earth thermosphere and exosphere composed of DMF1 explains the difference in the size of the Geocorona and the size of the Earth: The Sun and Solar corona have the same ratio of sizes;
- At the distance of 243,000 km from the Earth, atoms and molecules are so far apart that they can travel hundreds of kilometers without colliding with one another. Thus, the exosphere no longer behaves like a gas, and the particles constantly escape into space. In our view, FUV radiation and X-rays are the consequence of DMF1 annihilation;
- All planets and some observed satellites (Europa, Io, Io Plasma Torus, Titan) have X-rays in upper atmosphere of the planets, similar to the Solar Corona;
- The calculated density of the Earth's fractal structure $\rho_f \cong 2.5 \times 10^{-7}\ kg/m^3$ (6.3) is in good agreement with experimental results for atmosphere density at the lowest temperature (below -143 °C) at 100 km altitude, similar to that of the Solar Corona;
- The most impressive result is that Saturn's X-ray spectrum is similar to that of X-rays of the Sun;
- Suprathermal atoms and molecules proposed by V. I. Shematovich and D. V. Bisikalo are the result of DMF1 annihilation in Geocorona, similar to that of Solar corona.

We suppose that not only gravitationally-rounded objects in the Solar System have Coronas made up of Dark Matter particles, but so do all gravitationally-rounded Macroobjects of the World.

7. Conclusion

Dark Matter is abundant:

- 2.4 % of Light Matter is in Superclusters, Galaxies, Stars, Planets, etc.
- 4.8% of Light Matter is in the Medium of the World;
- The remaining 92.8 % of mass is Dark Matter.

Dark Matter is omnipresent:

- Dark Matter Reactors in Cores of all gravitationally-rounded Macroobjects;
- Coronas of all Macroobjects of the World;
- The Medium of the World.

In the present paper we develop the Rotational Fission model of creation and evolution of Macrostructures of the World (Superclusters, Galaxies, Extrasolar Systems), based on Overspinning Cores of the World's Macroobjects, and the Law of Conservation of Angular Momentum. To be consistent with this Fundamental Law, we develop New Physics of the World:

- The main players of the World are overspinning Dark Matter Cores of Superclusters;
- Milky Way galaxy was born 13.8 billion years ago as the result of a Gravitational Burst of the Local

Supercluster Core due to its rotational fission;

- Proposed Fifth Fundamental force of Weak Interaction between Dark Matter particles provides the integrity of Dark Matter Cores of all Macroobjects;
- Proposed new Dark Matter particles Dions with mass 0.2 eV compose outer Shell of Supercluster's Cores and are responsible for the gravitational interaction.

It is time to adopt the existence of the Dark Matter in the World from the Classical Physics point of view.

Acknowledgements

Special thanks to my son Ilya Netchitailo, who questioned every aspect of the Model, gave valuable suggestions and helped shape it to its present form.

References

[1] Netchitailo, V. (2016) Overview of Hypersphere World-Universe Model. *Journal of High Energy Physics, Gravitation and Cosmology*, **2**, 593-632. doi: 10.4236/jhepgc.2016.24052.
[2] Swedenborg, E. (1734) Latin: Opera Philosophica et Mineralia (English: Philosophical and Mineralogical Works). Principia, 1. http://www.swedenborg.org.uk/bookshop/swedenborg_a-z/the_principia_2_vols .
[3] Baker, G. L. (1983) Emanuel Swedenborg–An 18th century cosmologist. The Physics Teacher, October, 441. http://www.newchurchhistory.org/articles/glb2007/baker.pdf.
[4] Brush, S. G. (2014) A History of Modern Planetary Physics: Nebulous Earth. p. 7. ISBN 0521441714.
[5] Ferrell, V. (1996) The Wonders of Nature. Harvestime Books. Altamont, TN 37301 U.S.A.
[6] Darwin, G. H. (1879) On the Bodily Tides of Viscous and Semi-Elastic Spheroids, and on the Ocean Tides upon a Yielding Nucleus. Phil. Trans. Roy. Soc., 170, 1.
[7] Wise, D. U. (1966) Origin of the Moon by Fission. http://adsabs.harvard.edu/full/1966ems..conf..213W .
[8] Jacot, L. (1986) Heretical Cosmology (transl. of Science et bon sense, 1981). Exposition-Banner.
[9] Van Flandern, T. (1999) Dark Matter, Missing Planets, and New Comets. North Atlantic.
[10] Netchitailo, V. (2015) 5D World-Universe Model. Multicomponent Dark Matter. *Journal of High Energy Physics, Gravitation and Cosmology*, **1**, 55-71. doi: 10.4236/jhepgc.2015.12006.
[11] Netchitailo, V. (2017) Astrophysics: Macroobject Shell Model. *Journal of High Energy Physics, Gravitation and Cosmology*, **3**, 776-790. doi: 10.4236/jhepgc.2017.34057.
[12] Netchitailo, V. (2018) Hypersphere World-Universe Model. Tribute to Classical Physics. *Journal of High Energy Physics, Gravitation and Cosmology*, **4**, 441-470. doi: 10.4236/jhepgc.2018.43024.
[13] NASA (2015) The Cosmic Distance Scale. https://imagine.gsfc.nasa.gov/features/cosmic/local_supercluster_info.html.
[14] Tully, R. B. (1982) The Local Supercluster. Astrophysical Journal **257**, 389. Bibcode:1982ApJ...257..389T. doi:10.1086/159999.
[15] Ness, M., *et al.* (2015) The Cannon: A data-driven approach to Stellar Label Determination. The Astrophysical Journal, **808**, 1. doi:10.1088/0004-637X/808/1/16.
[16] Heymans, C., *et al.* (2008) The dark matter environment of the Abell 901/902 supercluster: a weak lensing analysis of the HST STAGES survey. arXiv:0801.1156.
[17] Zwicky, F. (1933) Die Rotverschiebung von extragalaktischen Nebeln. Helvetica Physica Acta, **6**, 110.
[18] Marchetti, T., Rossi, E. M., Brown. A. G. A. (2018) Gaia DR2 in 6D: Searching for the fastest stars in the Galaxy. *Monthly Notices of the Royal Astronomical Society*, sty2592,https://doi.org/10.1093/mnras/sty2592.
[19] Clarke, C. J., *et al.* (2018) High-resolution Millimeter Imaging of the CI Tau Protoplanetary Disk: A Massive Ensemble of Protoplanets from 0.1 to 100 au. The Astrophysical Journal Letters, **866**, L6.
[20] Djorgovski, S. G. (2016) Stellar Structure and the Sun.

http://www.astro.caltech.edu/~george/ay1/lec_pdf/Ay1_Lec08.pdf.
[21] Dziewonski, A. M., Anderson, D. L. (1981) Preliminary Reference Earth Model. Physics of the Earth and Planetary Interiors. **25**, 297. Bibcode:1981PEPI...25..297D. doi:10.1016/0031-9201(81)90046-7. ISSN 0031-9201.
[22] Turcotte, D. L.; Schubert, G. (2002) Geodynamics. Cambridge, England, UK: Cambridge University Press, 137. ISBN 978-0-521-66624-4.
[23] Pollack, H. N., Hurter, S. J., Johnson, J. R. (1993) Heat flow from the Earth's interior: Analysis of the global data set. *Reviews of Geophysics*. **31** (3): 267–80. Bibcode:1993RvGeo..31..267P. doi:10.1029/93RG01249.
[24] Arculus, R. (2016) The Cosmic Origins of Uranium. http://www.world-nuclear.org/information-library/nuclear-fuel-cycle/uranium-resources/the-cosmic-origins-of-uranium.aspx.
[25] Gando, A., *et al.* (2011) Partial radiogenic heat model for Earth revealed by geoneutrino measurements. Nature Geoscience, **4**, 647.
[26] Hoffman, D. C., *et al.* (1971) Detection of Plutonium-244 in Nature. Nature, **234**, 132.
[27] Ricard, Y. (2009) 2. Physics of Mantle Convection. In David Bercovici and Gerald Schubert. Treatise on Geophysics: Mantle Dynamics, **7**. Elsevier Science. ISBN 9780444535801.
[28] Cole, G.H.A. and Woolfson, M.M. (2002) Planetary Science: The Science of Planets around Stars. Institute of Physics Publishing, 36-37, 380-382. https://doi.org/10.1887/075030815X.
[29] Kinver, M. (2009) Global Average Temperature May Hit Record Level in 2010. BBC. Retrieved 22 April 2010.
[30] Elkins-Tanton, Linda T. (2006). *Jupiter and Saturn*. New York: Chelsea House. ISBN 978-0-8160-5196-0.
[31] O'Donoghue, J., Moore, L., Stallard, T. S., and Melin, H. (2016) Heating of Jupiter's upper atmosphere above the Great Red Spot. Nature, 18940.
[32] de Pater, I., Lissauer, J. J. (2010) Planetary Sciences (2nd ed.). Cambridge University Press. pp. 254–255. ISBN 978-0-521-85371-2.
[33] Class 12 – Giant Planets – Heat and Formation. 3750 – Planets, Moons & Rings. Colorado University, Boulder. 2004. Retrieved 13 March 2008.
[34] Pearl, J. C.; Conrath, B. J. (1991). "The albedo, effective temperature, and energy balance of Neptune, as determined from Voyager data". Journal of Geophysical Research: Space Physics. 96: 18, 921–18, 930. Bibcode:1991JGR....9618921P. doi:10.1029/91ja01087.
[35] Goddard Space Flight Center (2010) Goddard Instrument Aboard Cassini Spacecraft Sees 'Pac-Man' on Saturn Moon. https://www.nasa.gov/centers/goddard/news/features/2010/pac-man-mimas.html.
[36] Fossat, E., *et al.* (2017) Asymptotic g modes: Evidence for a rapid rotation of the solar core. arXiv:1708.00259.
[37] Zhang, J., *et al.* (2005) Inner Core Differential Motion Confirmed by Earthquake Waveform Doublets. Science , 309, 1357-1360. https://doi.org/10.1126/science.1113193.
[38] Guillot, T., *et al.* (2018) A Suppression of Differential Rotation in Jupiter's Deep Interior. Nature, 555, 227-230. https://www.nature.com/articles/nature25775.
[39] Feulner, G. (2012) The Faint Young Sun Problem. arXiv:1204.4449.
[40] Hoyle, F. (1958) Remarks on the Computation of Evolutionary Tracks, Ricerche Astronomiche, **5**, 223.
[41] Schwarzschild, M. (1958) Structure and evolution of the stars. Princeton University Press, New Jersey.
[42] Newman, M. J. and Rood, R. T. (1977) Implications of solar evolution for the earth's early atmosphere. Science, **198**, 1035. doi:10.1126/science.198.4321.1035.
[43] Gough, D. O. (1981) Solar interior structure and luminosity variations. Solar Physics, 74, 21.
[44] Baryshev, Yu. (2008) Field Fractal Cosmological Model as an Example of Practical Cosmology Approach. arXiv: gr-qc/0810.0162.
[45] Agle, D. C., Brown, D. (2012) Data from NASA's Voyager 1 Point to Interstellar Future. http://www.nasa.gov/mission_pages/voyager/voyager20120614.html.

[46] Peter, H. (2004) Structure and dynamics of the low corona of the Sun. Reviews in Modern Astronomy **17**, 87.
[47] Abhyankar, K. D. (1977) A Survey of the Solar Atmospheric Models. Bulletin of the Astronomical Society of India. **5**,40. Bibcode:1977BASI....5...40A.
[48] Karen C. Fox (2014) NASA's STEREO Maps Much Larger Solar Atmosphere Than Previously Observed. https://www.nasa.gov/content/goddard/nasas-stereo-maps-much-larger-solar-atmosphere-than-previously-observed/.
[49] Aschwanden, M. J. (2004) Physics of the Solar Corona. An Introduction. Praxis Publishing. ISBN 978-3-540-22321-4.
[50] Schmelz, J. T., *et al.* (2012) Composition of the Solar Corona, Solar Wind, and Solar Energetic Particles. The Astrophysical Journal, **755**, 1. http://iopscience.iop.org/article/10.1088/0004-637X/755/1/33/pdf.
[51] Grossman, L. (2018) Strange gamma rays from the sun may help decipher its magnetic fields. Science News, **194,** 9. https://www.sciencenews.org/article/strange-gamma-rays-sun-magnetic-fields.
[52] M. Picone, A.E. Hedin, D. Drob (2017) NRL MSISE-00 (Mass Spectrometer - Incoherent Scatter) Model of the Upper Atmosphere. https://www.ukssdc.ac.uk/wdcc1/nrlmsise00.html.
[53] Zell, H. (2015) Earth's Upper Atmosphere. NASA. https://www.nasa.gov/mission_pages/sunearth/science/mos-upper-atmosphere.html
[54] Russell, R. (2008) The Thermosphere. Windows to the Universe. https://www.windows2universe.org/?page=/earth/Atmosphere/thermosphere.html
[55] Geerts, B. and Linacre, E. (1997) The height of the tropopause. http://www-das.uwyo.edu/~geerts/cwx/notes/chap01/tropo.html
[56] Troposphere. Concise Encyclopedia of Science & Technology. McGraw-Hill. 1984.
[57] States, R. J., Gardner, C. S. (2000) Thermal Structure of the Mesopause Region (80–105 km) at 40°N Latitude. Part I: Seasonal Variations. Journal of the Atmospheric Sciences. **57**, 66. Bibcode:2000JAtS...57...66S. https://doi.org/10.1175/1520-0469(2000)057%3C0066:TSOTMR%3E2.0.CO;2
[58] Buchdahl, J. (2010) Atmosphere, Climate & Environment Information Programme. http://www.ace.mmu.ac.uk/eae/atmosphere/older/mesosphere.html
[59] Xu, J., *et al.* (2007) Mesopause Structure from Thermosphere, Ionosphere, Mesosphere, Energetics, and Dynamics (TIMED)/Sounding of the Atmosphere Using Broadband Emission Radiometry (SABER) observations. Journal of Geophysical Research, **112** (D9). Bibcode:2007JGRD..112.9102X. https://agupubs.onlinelibrary.wiley.com/doi/full/10.1029/2006JD007711.
[60] Reyes, R. Exploring the Sun-Earth Connection. Southwest Research Institute. http://pluto.space.swri.edu/image/glossary/geocorona.html.
[61] Kameda, S., *et al.* (2017) Ecliptic North-South Symmetry of Hydrogen Geocorona. Geophysical Research Letter, **44**, 11706. https://doi.org/10.1002/2017GL075915.
[62] Kuwabara, M., *et al.* (2017) The Geocoronal Responses to the Geomagnetic Disturbances. Journal of Geophysical Research: Space Physics, **122**, 1269. https://agupubs.onlinelibrary.wiley.com/doi/pdf/10.1002/2016JA023247.
[63] NASA (2012) Solar System. http://chandra.harvard.edu/xray_sources/solar_system.html.
[64] Wargelin, B. J., *et al.* (2014) Observation and Modeling of Geocoronal Charge Exchange X-Ray Emission During Solar Wind Gusts. The Astrophysical Journal, **796**, 1. http://dx.doi.org/10.1088/0004-637X/796/1/28.
[65] Cravensa, T. E., *et al.* (2009) Solar Wind Charge Exchange Contributions to the Diffuse X-Ray Emission. AIP Conference Proceedings **1156**, 37. https://doi.org/10.1063/1.3211832.
[66] Shematovich, V. I. and Bisikalo, D. V. (2018) Hot Planetary Coronas. Planetary Science. http://planetaryscience.oxfordre.com/view/10.1093/acrefore/9780190647926.001.0001/acrefore-9780190647926-e-104.

High-Energy Atmospheric Physics. Ball Lightning

Abstract

This article proposes an explanation for High-Energy Atmospheric phenomena through the frames of Hypersphere World – Universe Model (WUM). In WUM, Terrestrial Gamma-Ray Flashes (TGFs) are, in fact, Gamma-Ray Bursts (GRBs). The spectra of TGFs at very high energies are explained by Dark Matter particles annihilation in Geocorona. Lightning initiation problem is solved by GRBs that slam into thunderclouds and carve a conductive path through a thunderstorm. We introduce Multiworld consisting of Macro-World, Large-World, Small-World, and Micro-World, characterized by suggested Gravitational, Extremely-Weak, Super-Weak, and Weak interaction respectively. We propose a new model of Ball Lightning formation based on the Dark Matter Core surrounded by electron-positron plasma in the Small-World.

Keywords. "Hypersphere World – Universe Model"; "High-Energy Atmospheric Physics"; "Ball Lightning"; "Geocorona": "Lightning Initiation Problem"; "Terrestrial Gamma-Ray Flashes"; "Gamma-Ray Bursts"; "Dark Matter Core"; "Electron-Positron Plasma"; "Multiworld"

1. Introduction

This paper is based on the revised World – Universe Model (WUM) [1]. To be consistent with the Law of Conservation of Angular Momentum, WUM is modified as follows:

- New Dark Matter particles, named Dions, with mass 0.2 eV and energy density of 68.8% of the total energy density of the World compose outer shells of Supercluster's Cores. They are responsible for the Le Sage's mechanism of the gravitation [2];
- Proposed Fifth Fundamental force of Weak Interaction between Dark Matter Particles (DMPs) provides the integrity of Dark Matter Cores of all Macroobjects;
- The origin of the Solar corona plasma is the result of the annihilation of DMPs with mass 1.3 TeV. The Solar corona made up of DMPs resembles a honeycomb filled with plasma;
- The composition and characteristics of Geocorona and Planetary Coronas are similar to those of the Solar Corona.

In the present article we develop a new Model of High-Energy Atmospheric Physics based on the approach to Geocorona suggested by WUM [1]. To explain the formation of Ball Lightnings and their characteristics we introduce the Small-World characterized by the proposed Super-Weak interaction between DMPs. We calculate main parameters of different Worlds in the suggested Multiworld.

In Section 2 we present a short history of Ball Lightning hypothesis. In Section 3 we present experimental results and existing theories in High-Energy Atmospheric Physics concerning Lightning initiation problem and Terrestrial Gamma-Ray Flashes (TGFs). In Section 4 we provide a short description of the Geocorona model and propose that TGFs are, in fact, Gamma-Ray Bursts (GRBs). Spectra of TGFs at very high energies are produced by DMPs annihilation in Geocorona. Lightning initiation problem is solved by GRBs that slam into the thunderclouds. In Section 5 we introduce Multiworld consisting of Macro-World, Large-World, Small-World, and Micro-World

characterized by proposed Gravitational, Extremely-Weak, Super-Weak, and Weak interaction respectively. In Section 6 we propose a new model of Ball Lightning formation based on the Dark Matter (DM) Core surrounded by electron-positron plasma in the Small-World.

2. Short History of Ball Lightning Hypothesis

Ball lightning is an unexplained atmospheric phenomenon that is usually associated with thunderstorms and lasts considerably longer than the split-second flash of a lightning bolt. Ball Lightning (BL) usually appears during thunderstorms, sometimes within a few seconds of lightning, but sometimes without apparent connection to a lightning bolt. In some cases, BL appears after a thunderstorm – or even before it. In 1972, Neil Charman published a review in which he identified the properties of a "typical" BL [3]:

- They frequently appear almost simultaneously with cloud-to-ground lightning discharge;
- They are generally spherical or pear-shaped with fuzzy edges;
- Their diameters range from 1cm to several meters, most commonly 10–20 cm;
- They can be seen clearly in daylight;
- The lifetime of each event is from 1 second to over a minute with the brightness remaining fairly constant during that time;
- They tend to move, most often in a horizontal direction at a few meters per second, but may also move vertically, remain stationary or wander erratically;
- Many of them are described as having rotational motion;
- It is rare that observers report the sensation of heat, although in some cases the disappearance of the ball is accompanied by the liberation of heat;
- Some display an affinity for metal objects and may move along conductors such as wires;
- Some appear within buildings passing through closed doors and windows;
- Some have appeared within metal aircraft and have entered and left without causing damage;
- The disappearance of a ball is generally rapid and may be either silent or explosive.

Vacuum hypothesis. An attempt to explain ball lightning was made by Nikola Tesla in 1904 [4], but there is at present no widely accepted explanation for the phenomenon. Tesla's thoughts on BL production are presented in a review "Tesla and Ball Lightning" [5]:

When sudden and very powerful discharges pass through the air, the tremendous expansion of some portions of the latter and subsequent rapid cooling and condensation gives rise to the creation of partial vacua in the places of greatest development of heat. These vacuous spaces, owing to the properties of the gas, are most likely to assume the shape of hollow spheres when, upon cooling, the air from all around rushes in to fill the cavity created by the explosive dilatation and subsequent contraction.

Suppose now that this result would have been produced by one spark or streamer discharge and that now a second discharge, and possible many more, follows in the path of the first. What will happen? Let us now assume that such a powerful streamer or spark discharge, in its passage through the air, happens to come upon vacuous sphere or space formed in the manner described. This space, containing gas highly rarefied, may be just in the act of contracting, at any rate, the intense current,

passing through the rarefied gas suddenly raises the same to an extremely high temperature, all the higher as the mass of the gas is very small.

Tesla considers that the initial energy of the nucleus is not sufficient to maintain the fireball, but that there must be an external source of energy. According to Tesla, "*this energy comes from other lightnings passing through the nucleus*", and the concentration of energy occurs because of the resistance of the nucleus, i.e. the greater energy-absorbing capacity of the rarefied gas than the surrounding gas through which the discharge passes [5].

Microwave cavity hypothesis. Peter Kapitsa proposed that BL is a glow discharge driven by microwave radiation that is guided to the ball along lines of ionized air from lightning clouds where it is produced. The ball serves as a resonant microwave cavity, automatically adjusting its radius to the wavelength of the microwave radiation so that resonance is maintained [6].

Maser-Soliton hypothesis was proposed by Peter H. Handel in 1975 [7]. According to this hypothesis, outdoor BL is caused by an atmospheric maser – analogous to a laser but operating at a much lower energy – having a volume of the order of many cubic kilometers.

Antimatter hypothesis. In 1971, fragments of antimatter comets or meteoroids were hypothesized, by David Ashby and Colin Whitehead, as a possible cause for BL [8] . They monitored the sky with gamma-ray detection apparatus and reported unusual surges of radiation at 511 keV, which is the characteristic gamma ray frequency of a collision between an electron and a positron. The authors noted that there were no thunderstorms present at the times that the gamma-ray readings were observed. They proposed that BL was caused by tiny grains of antimatter. These grains arrived from space and slowly filtered down through the Earth's atmosphere, shielded from immediate annihilation by a kind of quantum barrier. The grains would tend to become negatively charged through the emission of positrons and so would be drawn to the ground as it became positively charged during thunderstorms [9].

Scientists using NASA's Fermi Gamma-ray Space Telescope have detected beams of antimatter produced above thunderstorms on Earth, a phenomenon never seen before. Members of Fermi's team think the antimatter particles were formed in a TGF, a brief burst produced inside thunderstorms and shown to be associated with lightning. They have detected gamma rays with energies of 511 keV [10].

Black hole hypothesis. Another hypothesis is that some BL is the passage of microscopic primordial black holes through the Earth's atmosphere. This possibility was mentioned in a patent application in 1996 by Leendert Vuyk [11]:

A reactor chamber for containing and exploiting ball lightning discharges consists of vessels with a symmetrical axis and a mating surface perpendicular to the axis. Also claimed is a method for containing, developing and exploiting two black holes or ball lightning discharges using the chamber described above. The two black holes are placed in one part of the vessel following which the vessel is sealed to the second part.

The first detailed scientific analysis of this hypothesis was made by Mario Rabinowitz in 1999 [12]: *Small, quiescent black holes can be considered as candidates for the missing dark matter of the universe, and as the core energy source of ball lightning. By means of gravitational tunneling, directed*

radiation is emitted from black holes in a process much attenuated from that of Hawking radiation which has proven elusive to detect. Gravitational tunneling emission is similar to electric field emission of electrons from a metal in that a second body is involved which lowers the barrier and gives the barrier a finite rather than infinite width. Hawking deals with a single isolated black hole.

Extreme Ball Lightning hypothesis. Van Devender distinguished Extreme Ball Lightning (EBL) from ordinary Ball Lightning (BL) by the following characteristics [13]:

- It glows in air;
- It originates from nothing visible;
- It lasts between 10 and 1200 seconds;
- It is lethal or potentially lethal;
- It causes significant damage;
- It contains energy estimated at 100,000 to 1 billion Joules, far in excess of the energy density attributable to chemicals or electrostatics;
- It penetrates walls, glass and metal, generally without leaving a hole;
- It leaves black streaks on corpses without the spasm of electrocution;
- It can excavate tons of earth.

According to Van Devender, to date no theory addresses the characteristics of EBL. He said, "*It seems to require new physics*" [14].

In view of Wal Thornhill, explaining EBL doesn't require new physics. The clue of his hypothesis comes from the observed ability of EBL to penetrate solid material. According to Thornhill, there is one stable particle that has the ability to pass through solids without any appreciable effect – neutrino, which in the presence of an excited nucleus may accept a lower level of energy than required for pair production and form a stable "heavy neutrino" [13].

Microwave Bubble hypothesis. H.-C. Wu proposed the following explanation of a formation of BL:

- A relativistic electron bunch can be produced by the stepped leader of lightning and coherently emit high-power microwave when striking the ground;
- The intense microwave ionizes the local air and evacuates the resulting plasma by its radiation pressure, thereby forming a spherical plasma cavity that traps the microwave [15].

Observation of the Optical and Spectral Characteristics of Ball Lightning was made by Jianyong Cen, *et al.* in 2012 [16]. At a distance of 900 m a total of 1.64 seconds of digital video of the BL and its spectrum was obtained, from the formation of the BL after the ordinary lightning struck the ground, up to the optical decay of the phenomenon. The BL traveled horizontally across the video frame at an average speed of 8.6 m/s . It had a diameter of 5 m.

Oscillations in the light intensity and in the oxygen and nitrogen emission at a frequency of 100 Hz, possibly caused by the electromagnetic field of the 50 Hz high-voltage power transmission line in the vicinity, were observed. From the spectrum, the temperature of the BL was assessed as being lower than the temperature of the parent lightning (<15,000–30,000 K). The observed data are consistent with vaporization of soil as well as with ball lightning's sensitivity to electric fields [16].

3. High-Energy Atmospheric Physics

In his "The mystery of Lightning" review [17], a leading lightning physicist Joseph R. Dwyer provides an excellent overview of the main experimental observations and leading models of thunderstorms and lightnings. Many mysteries remain about how thunderstorms and lightnings work, including how lightnings get started. It is established that thunderstorms and lightnings produce intense bursts of x-rays and gamma-rays. These high-energy radiations may be important for understanding how lightning works.

Lightning initiation problem. Years of balloon, aircraft, and rocket observations have never found large enough electric fields inside thunderstorms to make a spark. And yet lightnings strike the Earth about 4 million times per day. This has led to the cosmic-ray model of lightning initiation [17]:

- Cosmic ray slams into atmosphere and carves a conductive path through a thunderstorm;
- Air showers alone will not increase the conductivity enough to initiate lightning;
- A mechanism of runaway electron avalanche was proposed in order to increase ionization [18];
- Strong electric fields accelerate electrons to nearly the speed of light;
- These electrons emit x-rays and gamma-rays, which were observed by G. Fishman, *et al.* [19];
- A gamma-ray flash descends from the overhead thundercloud;
- It is not clear why some discharges make x-rays and others do not;
- Gamma-rays are produced inside of thunderstorms;
- Explosive production of energetic particles were observed from space [19];
- Thunderstorms create electron and positron beams;
- Thunderstorms produce Terrestrial Gamma-ray Flashes (TGFs).

Terrestrial Gamma-Ray Flashes were first detected by chance by NASA's Earth-orbiting Compton gamma ray telescope. Compton was searching for GRBs from exploding stars, when it unexpectedly began detecting very strong bursts of high energy x-rays and gamma rays, coming from Earth. Detectors observed an unexplained terrestrial phenomenon: brief (lasting about a millisecond), intense flashes of gamma rays. According to G. J. Fishman, *et al.*, *"These flashes must originate in the atmosphere at altitudes above at least 30 kilometers in order to escape atmospheric absorption and reach the orbiting detectors. The photon spectra from the events are very hard (peaking in the high-energy portion of the spectrum) and are consistent with bremsstrahlung emission from energetic MeV electrons. The most likely origin of these high-energy electrons, although speculative at this time, is a rare type of high-altitude electrical discharge above thunderstorm regions"* [19].

A paper by Joseph R. Dwyer, *et al.* provides a brief review of TGFs [20]: "*They have durations ranging from a few tens of microseconds to a few milliseconds [21], [22] and produce the highest energy emission of natural phenomena originating from within the Earth's atmosphere [23], [24], [25]. TGFs are relatively common, with a thousand or more produced around the planet each day [22], [26]. Spacecraft measurements have found that the source altitudes of the gamma rays must be below 20 km [23], [27], [28], [29], within the altitude range of thunderstorms. The spectra of TGFs (up to a few tens of MeV) are consistent with bremsstrahlung emissions from energetic electrons accelerated by strong electric fields within the thunderclouds [23], [27], [28], although there is currently some debate about the spectra at very high energies (~40–100 MeV) [24], [30]. It is a challenge to develop*

models that can explain how large numbers of high-energy electrons are generated so rapidly deep within the atmosphere [31]".

There are two leading models of TGF formation[17]:

1. Lightning leader emission, similar to x-ray emission seen near the ground;
2. Dark Lightning, which:

- Generates so many high-energy particles that it discharges the thunderstorm faster than normal lightning;
- Makes currents > 100,000 amps;
- Emits very little visible light, i.e. appears dark;
- Can explain TGFs;
- Cosmic rays are not needed.

But how can we explain a new mystery: a bright TGF was seen by spacecraft in the middle of Sahara Desert on a nice day. The nearest thunderstorms were ~ 1000 miles away [19].

4. Geocorona

Let's summarize the obtained results, which are difficult to explain in frames of the existing models:

- Sometimes BL appears without apparent connection to a lightning bolt;
- Unusual surges of radiation at 511 keV when there were no thunderstorms;
- Beams of antimatter (positrons) produced above thunderstorms on Earth;
- A gamma-ray flash coming down from the overhead thundercloud;
- Some discharges make x-rays and others do not;
- Explosive production of energetic particles observed from space;
- Thunderstorms make electron and positron beams;
- Thunderstorms produce TGFs;
- A bright TGF was seen by spacecraft in the middle of Sahara Desert on a nice day;
- The spectra of TGFs at very high energies (~40–100 MeV).

Geocorona is the luminous part of the outermost region of the Earth's atmosphere. It extends to at least 640,000 km from the Earth. X-rays from Earth's Geocorona in the range of energies 0.08-10 keV were first detected in 1999. The main mechanism explaining the geocoronal X-rays is that they are caused by collisions between neutral atoms in the Geocorona with carbon, oxygen and nitrogen ions in the solar wind [32], [33], [34]. This process is called "charge exchange", since an electron is exchanged between neutral atoms in Geocorona and ions in the solar wind.

According to WUM, the characteristics of Geocorona are similar to the characteristics of the Solar Corona [1]:

- The Geocorona composed of Dark Matter Fermions DMF1 with mass 1.3 TeV has the size that is much larger than the size of the Earth;
- At the distance of 640,000 km from the Earth, atoms and molecules are so far apart that the outermost region of the Earth's atmosphere no longer behaves like a gas;

- X-rays and gamma-rays are the consequence of DMF1 annihilation;
- The Geocorona made up of DMPs resembles a honeycomb filled with plasma including the ionosphere from about 60 km to 1,000 km altitude;
- The calculated density of the Geocorona near the surface of the Earth is $\cong 2.5 \times 10^{-7}\ kg/m^3$.

As the result of DMPs annihilation, X-rays and gamma-rays are going not only up and out of the Earth, but also down to the Earth's surface. In case they were produced at altitudes of above at least 30 km, they can reach the orbiting detectors [19]. In case the source altitudes of the gamma rays is below about 20 km [23], [27], [28], [29] (within the altitude range of thunderstorms), they can reach the surface of the Earth (see **Figure 1**).

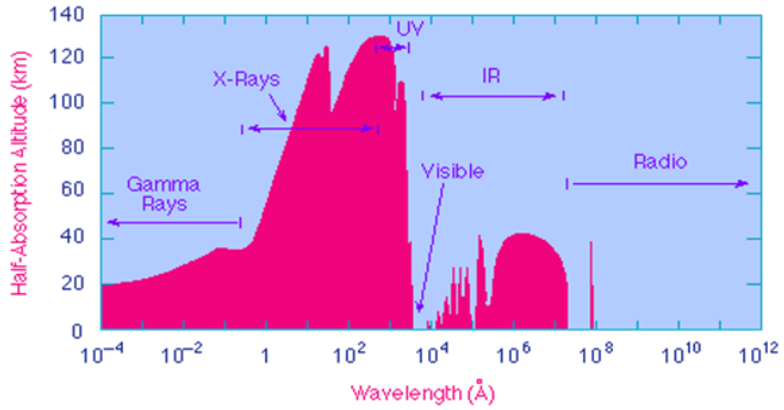

Figure 1. Atmospheric Windows. Adapted from "Atmospheric Windows" by Eric G. Blackman [35].

In our view, TGFs are, in fact, well-known GRBs [36]. The spectra of TGFs at very high energies can be explained by DMF1 annihilation. Lightning initiation problem can be solved by X-rays and gamma-rays, which slam into the thunderclouds and carve a conductive path through a thunderstorm. From this point of view, it is easy to explain all experimental results summarized above.

5. Multiworld

According to A. G. Oreshko, "*P. L. Kapitsa supposed that a ball lightning is a window in another world*" [37]. We analyzed possibility of the existence of other worlds: Micro-World, Small-World, and Large-World based on the proposed Weak, Super-Weak and Extremely-Weak interaction respectively [38]. It was suggested that BL is an object of the Small-World. Below we discuss main characteristics of the proposed new Worlds in the Multiworld.

Macro-World. According to WUM, strength of gravity is characterized by gravitational parameter G_g:

$$G_g = G_0 \times Q^{-1} \propto \tau^{-1}$$

where $G_0 = \frac{a^2 c^4}{8\pi hc}$ is an extrapolated value of G_g at the Beginning of the World ($Q = 1$), c is the electrodynamic constant, h is Planck constant, a is a basic unit of length: $a = \alpha\lambda_e$, λ_e is the Compton wavelength of an electron and α is Sommerfeld's constant that is, in fact, the ratio of electron mass m_e to the basic unit of mass m_0 : $\alpha = m_e/m_0$ and m_0 equals to: $m_o = h/ac$ [1]. Dimensionless time-

varying quantity Q is a measure of the Age of the World: $Q = \tau/t_0$ where τ is a cosmological time and a basic unit of time t_0 equals to:

$$t_0 = a/c = 5.9059674 \times 10^{-23}\ s$$

In the present epoch, Q equals to [39]:

$$Q = 0.759972 \times 10^{40}$$

The range of gravity equals to the size of the World R :

$$R = aQ = 1.34558 \times 10^{26}\ m$$

The total mass of the Macro-World M_{tot} is:

$$M_{tot} = 6\pi^2 m_0 \times Q^2 = 4.26943 \times 10^{53}\ kg$$

WUM foresees three additional types of interactions: Weak, Super-Weak, and Extremely-Weak, characterized by the following parameters respectively:

$$G_W = G_O \times Q^{-1/4} \propto \tau^{-1/4}$$

$$G_{SW} = G_O \times Q^{-1/2} \propto \tau^{-1/2}$$

$$G_{EW} = G_O \times Q^{-3/4} \propto \tau^{-3/4}$$

In our view, each type of interaction provides integrity of the corresponding world (see **Table 1**).

Table 1. Parameters of Multiworld (ρ_0 is a basic unit of density: $\rho_0 = h/ca^4$).

Type of world	**Type of Interaction**	**Relative Interaction Parameter** G/G_0	**Relative Range of Interaction** r/a	**Relative Total Mass** $M_{max}/4\pi m_0$	**Relative Density of World** $\rho/3\rho_0$
Macro-World	Gravity	Q^{-1}	Q	$1.5\pi \times Q^2$	Q^{-1}
Large-World	Extremely-Weak	$Q^{-3/4}$	$Q^{3/4}$	$Q^{3/2}$	$Q^{-3/4}$
Small-World	Super-Weak	$Q^{-1/2}$	$Q^{1/2}$	Q	$Q^{-1/2}$
Micro-World	Weak	$Q^{-1/4}$	$Q^{1/4}$	$Q^{1/2}$	$Q^{-1/4}$

Micro-World is characterized by the parameter G_W , which is about 30 orders of magnitude greater than G_g . The range of the weak interaction R_W in the present epoch equals to:

$$R_W = a \times Q^{1/4} = 1.65314 \times 10^{-4}\ m$$

that is much greater than the range of the weak nuclear force (around $\sim 10^{-16} - 10^{-17}\ m$) .

With Nikola Tesla's principle at heart – *There is no energy in matter other than that received from the environment* – we apply to the Micro-World the following equation for a maximum total mass M_W :

$$M_W = 4\pi\sigma_0 R_W^2/c^2 = 4\pi m_0 \times Q^{1/2} = 1.36752 \times 10^{-7}\ kg$$

where σ_0 is a basic unit of surface energy density: $\sigma_0 = hc/a^3$. The average density of the Micro-World ρ_W is:

$$\rho_W = 3\rho_0 \times Q^{-1/4} = 7.22621 \times 10^3\ kg/m^3$$

In our opinion, Micro-World objects with mass about Planck mass are the building blocks of all Macroobjects.

Large-World is characterized by the parameter G_{EW}, which is about 10 orders of magnitude greater than G_g . The range of the extremely-weak interaction R_{EW} in the present epoch equals to:

$$R_{EW} = a \times Q^{3/4} = 1.44115 \times 10^{16}\ m$$

In our view, Extrasolar Systems (ESSs) are Large-World objects with spherical boundary between ESS and Intergalactic Medium. This boundary has a surface energy density σ_0 . Maximum total mass of ESS equals to:

$$M_{EW} = 4\pi\sigma_0 R_{EW}^2/c^2 = 4\pi m_0 \times Q^{3/2} = 1.03928 \times 10^{33}\ kg$$

and average density ρ_{EW} equals to:

$$\rho_{EW} = 3\rho_0 \times Q^{-3/4} = 8.28918 \times 10^{-17}\ kg/m^3$$

which is about 10 orders of magnitude greater than the critical density [1]. In WUM, ESSs have Cores made up of DMPs surrounded by shells composed of DM and baryonic matter. Extremely-weak interaction between DM Cores and all particles around them provide integrity of ESSs.

Small-World is characterized by the parameter G_{SW} , which is about 20 orders of magnitude greater than G_g . The range of the super-weak interaction R_{SW} in the present epoch equals to:

$$R_{SW} = a \times Q^{1/2} = 1.54351 \times 10^6\ m$$

A maximum total mass of Small-World M_{SW} is:

$$M_{SW} = 4\pi m_0 \times Q = 1.19215 \times 10^{13}\ kg$$

and average density ρ_{SW} equals to:

$$\rho_{SW} = 3\rho_0 \times Q^{-1/2} = 7.73947 \times 10^{-7}\ kg/m^3$$

which is about 20 orders of magnitude greater than critical density [1]. **Table 2** describes parameters of Small-World objects made up of different fermions taking part in the super-weak interaction.

In WUM, BLs have Cores made up of DMPs surrounded by shells composed of electron-positron plasma. Super-weak interaction between DM Cores and all particles around them provide integrity of BLs (see next Section).

Table 2. Parameters of Small-World objects made up of different fermions DMF1, DMF2, and electron-positron plasma.

Fermion	Fermion mass, $m_f, MeV/c^2$	Macroobject mass, M_{max}, kg	Macroobject radius, R_{min}, m	Macroobject density, $\rho_{max}, kg/m^3$
Interacting DMF1	$1{,}315\times10^3$	2.3	9.2×10^{-7}	7.2×10^{17}
Interacting DMF2	9,596	2.3	9.2×10^{-7}	7.2×10^{17}
Electron-positron plasma	0.511	$8\text{x}10^6$	3.1	$6.4\text{x}10^4$

6. Ball Lightning Formation

The clue of our model comes from the observed ability of BLs to penetrate solid materials. It means that the Core of BL should be composed of DMPs. In WUM, they are DMF1 and DMF2. Fermion small-stars made up of DMF1 or DMF2 can form Cores of BLs in the Small-World characterized by super-weak interaction.

Following Tesla vacuum hypothesis [4], [5], we suppose that when sudden and very powerful TGF passes through the air and strike the surface of the Earth, "*the tremendous expansion of some portions of the air and subsequent rapid cooling and condensation gives rise to the creation of partial vacua in the places of greatest development of heat. These vacuous spaces, owing to the properties of the gas, are most likely to assume the shape of hollow spheres when, upon cooling, the air from all around rushes in to fill the cavity created by the explosive dilatation and subsequent contraction*".

In our Model, the places of greatest development of heat are the spots on the Earth's surface struck by TGFs. As the result, the ablation of the soil takes place and vaporized chemical elements of soil and the oxygen and nitrogen from the air can be absorbed by BLs and observed experimentally [16].

Very powerful gamma quants with energy at least 1.02 MeV in the vicinity of atomic nuclei of the ground can produce electron-positron pairs with high concentration. This collisionless unmagnetized electron-positron plasma, whose properties are very well studied, composes a shell around DM core of BL made up of DMF1 and provides their affinity for metal objects such as wires.

The most important part of the BL formation is a DM core. The calculated density of the Geocorona composed of DMF1 ρ_{DMF1} near the surface of the Earth is [1]:

$$\rho_{DMF1} \cong 2.5 \times 10^{-7}\ kg/m^3$$

According to WUM, in the Small-World DMF1 and a microobject will exert super-weak interaction on one another when the minimum product of their masses m_{DMF1} and M_{micro} equals to [39]:

$$m_{DMF1} \times M_{micro} = 2m_0^2 \times Q^{1/2} = 2.71692 \times 10^{-36}\ kg^2$$

Dark Matter particle DMF1 has a mass m_{DMF1} :

$$m_{DMF1} = 2.34419 \times 10^{-24}\ kg$$

Then the minimum mass of microobject should be

$$M_{micro} \approx 1.16 \times 10^{-12}\ kg$$

Let's calculate a radius of a sphere in Geocorona r_{micro} having minimum mass M_{micro}: $r_{micro} \cong 10^{-2}\ m$. When powerful TGF strikes the surface of the Earth, the explosive dilatation of this portion of Geocorona with radius r_{micro} gives rise to the creation of hollow sphere with partial vacua and all DMPs outside of the sphere. The subsequent rapid contraction induces DMPs rush in to fill the cavity. As the result, at the center of the sphere arises microobject with minimum mass M_{micro} and density high enough for the beginning of the DMPs annihilation.

The estimations, based on the average density of the moon Mimas about $\sim 10^3\ kg/m^3$ with the Core made up of annihilating DMF1 [1], show that the size of the microobject should be about $\sim 10^{-5}\ m$. The described microobject attracts new DMPs from Geocorona due to super-weak interaction and grows up to the next value of a mass of the macroobject M_{macro}, which can be calculated in accordance with the following equation:

$$m_e \times M_{macro} = 2m_0^2 \times Q^{1/2}$$

where m_e is a mass of electron: $m_e \approx 9.11 \times 10^{-31}\ kg$. Mass of the macroobject equals to:

$$M_{macro} \cong 3 \times 10^{-6}\ kg$$

This macroobject will start attracting electron-positron pairs produced by TGF. Considering the density of the atmosphere $\rho_{atm} \cong 1.25\ kg/m^3$ we can calculate the minimum radius of the BL r_{min}:

$$r_{min} \cong 0.83 \times 10^{-2}\ m$$

that is in good agreement with experimentally observed value of BL minimum size about $\sim 1\ cm$ [3]. We take density of the atmosphere ρ_{atm} for the average BL density to explain movement of BL in air.

According to WUM, mass of BL's core can grow up to 2.3 kg and the radius of plasma shell can be a few meters (see **Table 2**). Mass of the small BLs is mostly in the DM cores. Then they can easily penetrate through walls, glass and metal, generally without leaving a hole. Practically all mass of the EBLs is in the plasma. EBL with diameter 5 m observed in [16] had the mass of about 83 kg. In our opinion, Nuclear Fireball is a huge EBL.

As the conclusion:

- BL has the core made up of DMF1 surrounded by the electron-positron plasma contaminated by chemical elements of soil and air as the result of TGF strike of the ground;
- The core of BL irradiates quants with different energies and attracts new DMPs from Geocorona due to super-weak interaction. It explains the observed result that the brightness of BL remains fairly constant during its lifetime;
- DMPs supply not only additional mass, but also additional angular momentum [1]. It explains the fact that many of BLs are described as having rotational motion;
- World – Universe Model can serve as a basis for High-Energy Atmospheric Physics.

It is important to emphasize that the initial energy required for a BL/EBL creation is insufficient for its sustenance of up to 1200 seconds. Additional energy, therefore, must be consumed by a BL/EBL once it had been formed. Once we master the creation of BLs and EBLs in a controlled environment, we can concentrate our efforts on harvesting that energy.

Acknowledgements

I am a Doctor of Sciences in Physics. I belong to the school of physicists established by Alexander Prokhorov – Nobel Prize Laureate in Physics. I am an author of more than 150 published papers, mostly in the area of Laser Physics. I'm eternally grateful to Prof. A. M. Prokhorov and Prof. A. A. Manenkov, whose influence on my scientific life has been decisive.

I started to work on World – Universe Model 17 years ago, having published 11 papers on viXra and 12 articles in the Journal of High Energy Physics, Gravitation and Cosmology (JHEPGC).

Many thanks to Prof. C. Corda for publishing my manuscripts in JHEPGC. Special thanks to my son Ilya Netchitailo who questioned every aspect of the Model, gave valuable suggestions and helped shape it to its present form.

References

[1] Netchitailo, V. S. (2019) Solar System. Angular Momentum. New Physics. JHEPGC **5**, 112-139. 10.4236/jhepgc.2019.51005.
[2] Netchitailo, V. S. (2016) 5D World–Universe Model. Gravitation. Journal of High Energy Physics, Gravitation and Cosmology, **2**, 328.
[3] Charman, N. (1972) The enigma of ball Lightning. New Scientist. **56** (824): 632–635. https://books.google.com/books?id=TCTpu1UVFsYC&pg=PA633#v=onepage&q&f=false.
[4] Tesla, N. (1904) The Transmission of Electrical Energy without Wires. Electrical World and Engineer. http://web.archive.org/web/20051222121927/http://tfcbooks.com/tesla/wireless01.htm.
[5] Tesla and Ball Lightning (1988).
https://www.bibliotecapleyades.net/tesla/esp_tesla_20.htm
[6] Kapitsa, P. L. (1955) The Nature of Ball Lightning. In Donald J. Ritchie. Ball Lightning: A Collection of Soviet Research in English Translation (1961 ed.). Consultants Bureau, New York. pp. 11–16.
[7] Handel, P. H. (1975) Maser Theory of Ball Lightning. Bulletin of the American Physical Society Series II, **20**, No. 26.
[8] Ashby, D. E. T. F. and Whitehead, C. (1971) Is Ball Lightning caused by Antimatter Meteorites? Nature. **230** (5290): 180–182. Bibcode:1971Natur. **230**, 180A. doi:10.1038/230180a0.
[9] Are antimatter meteorites optical illusions? New Scientist. **49** (744). 1971-03-25. ISSN 0262-4079. https://books.google.com/books?id=yXq8b86qFLQC&pg=PA661&lpg=PA661&dq=Are+antimatter+meteorites+optical+illusions?%22&source=bl&ots=5aH0iPzKNj&sig=gVpclonPkexWBhhzoIKi6AVEEk8&hl=en&sa=X&ved=2ahUKEwje9vCt1avfAhWqJTQIHR3eCv8Q6AEwAHoECAgQAQ#v=onepage&q=Are%20antimatter%20meteorites%20optical%20illusions%3F%22&f=false.
[10] NASA's Fermi Catches Thunderstorms Hurling Antimatter into Space. https://www.nasa.gov/mission_pages/GLAST/news/fermi-thunderstorms.html.
[11] Vuyk, L. (1996) Practical containment, development and exploitation of energy contained in ball lightning discharges or black holes. https://nl.espacenet.com/publicationDetails/biblio?II=0&ND=3&adjacent=true&locale=nl_NL&FT=D&date=19970912&CC=NL&NR=1002570C1&KC=C1.
[12] Rabinowitz, M. (2002) Little Black Holes: Dark Matter and Ball Lightning. arXiv:0212251.
[13] Thornhill, W. (2006) The IEEE, Plasma Cosmology and Extreme Ball Lightning. https://www.holoscience.com/wp/the-ieee-plasma-cosmology-and-extreme-ball-lightning/
[14] Van Devender, P. (2011) Extreme Ball Lightning: New Physics, New Energy Source, or Just Great Fun. https://www.osti.gov/servlets/purl/1107768.
[15] H.-C. Wu, H. C. (2014) Theory of ball lightning. arXiv:1411.4784.
[16] Cen, J., Yuan, P. and Xue, S. (2014) Observation of the Optical and Spectral Characteristics of Ball Lightning. Physical Review Letters **112**, 035001.

[17] Dwyer, J. R. (2012) The mystery of Lightning.
http://www.insightcruises.com/events/sa24/PDF/The_Mysteries_of_Lightning.pdf
[18] Gurevich, A. V., Milikh, G. M., and Roussel-Dupre, R. (1992) Runaway electron mechanism of air breakdown and preconditioning during a thunderstorm. Phys. Lett. A, **165**, 463 – 468.
[19] Fishman, G. J., *et al.* (1994) Discovery of Intense Gamma-Ray Flashes of Atmospheric Origin. Science **264** (5163), 1313-1316. DOI: 10.1126/science.264.5163.1313.
[20] Dwyer, J. R., Liu, N. and Rassoul, H. K. (2013) Properties of the thundercloud discharges responsible for terrestrial gamma-ray flashes. Geophysical Research Letters. https://doi.org/10.1002/grl.50742.
[21] Fishman, G. J., *et al.* (2011) Temporal properties of terrestrial gamma-ray flashes from the gamma-ray burst monitor on the Fermi observatory. J. Geophys. Res., **116**, A07304. doi:10.1029/2010JA016084.
[22] Briggs, M. S., *et al.* (2013) Terrestrial gamma-ray flashes in the Fermi Era: Improved observations and analysis methods. J. Geophys. Res. Space Physics, **118**, 1–26. doi:10.1002/jgra.50205.
[23] Dwyer, J. R. and Smith, D. M. (2005) A comparison between Monte Carlo simulations of runaway breakdown and terrestrial gamma-ray flash observations. Geophys. Res. Lett., **32**, L22804. doi:10.1029/2005GL023848.
[24] Tavani, M., *et al.* (2011) Terrestrial gamma-ray flashes as powerful particle accelerators. Phys. Rev. Lett., **106**(1), 018501, 5.
[25] Dwyer, J. R. (2012) The relativistic feedback discharge model of terrestrial gamma ray flashes. J. Geophys. Res., **117**, A02308. doi:10.1029/2011JA017160.
[26] Østgaard, N., Gjesteland, T., Hansen, R. S., Collier, A. B., Carlson, B. (2012) The true fluence distribution of terrestrial gamma flashes at satellite altitude, J. Geophys. Res., **117**, A03327. doi:10.1029/2011JA017365.
[27] Carlson, B., N. Lehtinen, and U. Inan (2007), Constraints on terrestrial gamma-ray flash production derived from satellite observations, Geophys. Res. Lett.,34, L08809, doi:10.1029/2006GL029229.
[28] Gjesteland, T., Østgaard, N., Connell, P. H., Stadsnes, J. and Fishman G. J. (2010) Effects of dead time losses on terrestrial gamma ray flash measurements with the Burst and Transient Source Experiment. J. Geophys. Res., **115**, A00E21. doi:10.1029/2009JA014578.
[29] Xu, W., Celestin, S., and Pasko, V. (2012) Source altitudes of terrestrial gamma-ray flashes produced by lightning leaders. Geophys. Res. Lett. **39**, L08801. doi:10.1029/2012GL051351.
[30] Celestin, S., Xu, W., and Pasko, V. (2012) Terrestrial gamma ray flashes with energies up to 100 MeV produced by nonequilibrium acceleration of electrons in lightning. J. Geophys. Res., **117**, A05315. doi:10.1029/2012JA017535.
[31] Dwyer, J. R. (2008) The source mechanisms of terrestrial gamma-ray flashes(TGFs). J. Geophys. Res., **113**, D10103. doi:10.1029/2007JD009248.
[32] NASA (2012) Solar System. http://chandra.harvard.edu/xray_sources/solar_system.html.
[33] Wargelin, B. J., *et al.* (2014) Observation and Modeling of Geocoronal Charge Exchange X-Ray Emission During Solar Wind Gusts. The Astrophysical Journal, **796**, 1. http://dx.doi.org/10.1088/0004-637X/796/1/28.
[34] Cravensa, T. E., *et al.* (2009) Solar Wind Charge Exchange Contributions to the Diffuse X-Ray Emission. AIP Conference Proceedings **1156**, 37. https://doi.org/10.1063/1.3211832.
[35] Atmospheric Windows http://www.pas.rochester.edu/~blackman/ast104/windows.html.
[36] Netchitailo, V.S. (2017) Burst Astrophysics. Journal of High Energy Physics, Gravitation and Cosmology, 3, 157-166. https://doi.org/10.4236/jhepgc.2017.32016.
[37] Oreshko, A. G. (2012) Observation of Dark Spherical Area after Passage of Ball Lightning through Thick Absorbers.
https://www.researchgate.net/profile/Alexander_Oreshko/publication/312218738_Observation_of_Dark_Spherical_Area_After_Passage_of_Ball_Lightning_Through_Thick_Absorbers/links/5877307808ae329d6226e786/Observation-of-Dark-Spherical-Area-After-Passage-of-Ball-Lightning-Through-Thick-Absorbers.pdf
[38] Netchitailo, V. S. (2013) World-Universe Model. viXra:1303.0077.
[39] Netchitailo, V. S. (2016) Overview of Hypersphere World-Universe Model. Journal of High Energy Physics, Gravitation and Cosmology, **2**, 593.

Dark Matter Cosmology and Astrophysics

Abstract

Hypersphere World-Universe Model (WUM) envisions Matter carried from Universe into World from fourth spatial dimension by Dark Matter Particles (DMPs). Luminous Matter is byproduct of Dark Matter (DM) annihilation. WUM introduces Dark Epoch (spanning from Beginning of World for 0.4 billion years) when only DMPs existed, and Luminous Epoch (ever since for 13.8 billion years). Big Bang discussed in standard cosmological model is, in our view, transition from Dark Epoch to Luminous Epoch due to Rotational Fission of Overspinning DM Supercluster's Cores and annihilation of DMPs. WUM solves a number of physical problems in contemporary Cosmology and Astrophysics through DMPs and their interactions: **Angular Momentum problem** in birth and subsequent evolution of Galaxies and Extrasolar systems – how do they obtain it; **Fermi Bubbles** – two large structures in gamma-rays and X-rays above and below Galactic center; **Mysterious Star KIC 8462852** with irregular dimmings; **Coronal Heating problem** in solar physics – temperature of Sun's corona exceeding that of photosphere by millions of degrees; **Cores of Sun and Earth** rotating faster than their surfaces; Diversity of **Gravitationally-Rounded Objects** in Solar system and their **Internal Heat**; **Lightning Initiation problem** – electric fields observed inside thunderstorms are not sufficient to initiate sparks; **Terrestrial Gamma-Ray Flashes** – bursts of high energy X-rays and gamma rays emanating from Earth. Model makes predictions pertaining to **Masses of DMPs**, proposes **New Types of their Interactions**. WUM reveals **Inter-Connectivity of Primary Cosmological Parameters** and calculates their values, which are in good agreement with the latest results of their measurements.

Keywords. "Hypersphere World-Universe Model"; "Law of Conservation of Angular Momentum; Dark Epoch"; "Rotational Fission"; "Luminous Epoch"; "Multiworld"; "Dark Matter Particles"; "Macroobject Shell Model"; "Dark Matter Core"; "Medium of the World"; "Mysterious Star KIC 8462852"; "Dark Matter Fermi Bubbles"; "Solar Corona"; "Geocorona"; "Planetary Corona"; "Galactic Wind"; "Solar Wind"; "High-Energy Atmospheric Physics"; "Lightning Initiation Problem"; "Terrestrial Gamma-Ray Flashes"; "Gamma-Ray Bursts"; "Gravitational Bursts"; "Ball Lightning"

1. Introduction

Hypersphere World-Universe Model (WUM) is proposed as an alternative to the prevailing Big Bang Model of standard physical cosmology. WUM is a classical model, and is described by classical notions, which define emergent phenomena. By definition, an emergent phenomenon is a property that is a result of simple interactions that work cooperatively to create a more complex interaction. Physically, simple interactions occur at a microscopic level, and the collective result can be observed at a macroscopic level. WUM introduces classical notions once the very first ensemble of particles has been created at the cosmological time $\cong 10^{-18}\ s$ (state of the World at cosmological times $< 10^{-18}\ s$ is best described by Quantum Mechanics). WUM is a natural continuation of Classical Physics.

The Hypersphere World-Universe model is the only cosmological model in existence that

- Is consistent with the Law of conservation of angular momentum, and answers the following questions: why is the orbital momentum of Jupiter larger than rotational momentum of Sun,

and how did Milky Way galaxy and Solar system obtain their substantial orbital angular momentum?

- Reveals the Inter-connectivity of primary cosmological parameters of the World (Age, Size, Hubble's parameter, Newtonian parameter of gravitation, Critical energy density, Concentration of Intergalactic Plasma, Temperature of the Microwave Background Radiation, Temperature of the Far-Infrared Background Radiation peak) and calculates their values, which are in good agreement with experimental results;
- Considers Fermi Bubbles (FBs) built up from Dark Matter Particles (DMPs), and explains X-rays and gamma-rays radiated by FBs as a result of DMPs annihilation;
- Solves Coronal heating problem that relates to the question of why the temperature of the Solar corona is millions of degrees higher than that of the photosphere. In WUM, the Solar corona is made up of DMPs, and the plasma is the result of their annihilation. The Solar corona resembles a honeycomb filled with plasma. The Geocorona and Planetary Coronas possess features similar to these of the Solar Corona;
- Explains the diversity of Very High Energy gamma-ray sources in the World in frames of the proposed Macroobject (MO) Shell Model, which describes Cores of MOs as Nuclei made up of annihilating Dark Matter Fermions (DMFs) surrounded by shells containing other DMPs;
- Explains the diversity of gravitationally-rounded objects (planets and moons in Solar system) and their internal heat through annihilation of DMFs in their Cores.

WUM paints the following picture of creation and evolution of the World:

- Overspinning (surface speed at equator exceeding escape velocity) DM Cores of Superclusters initiate creation of all World's Macrostructures;
- The outer shells of Supercluster's Cores are composed of DMFs named Dions, with mass of 0.2 eV and total energy density of 68.8% of the overall energy density of the World;
- Proposed Weak Interaction between DMPs provides the integrity of Dark Matter (DM) Cores of all MOs;
- Dions' outer shells of Supercluster's Cores are growing to the critical mass during Dark Epoch lasting from the Beginning of the World (14.2 billion years ago) for 0.4 billion years;
- Luminous Galaxies and Extrasolar Systems arise due to Rotational Fission of Overspinning Supercluster's Cores and annihilation of DMPs;
- Macrostructures of the World form from Superclusters down to Galaxies, Extrasolar systems, planets, and moons. Formation of galaxies and stars is not a process that concluded ages ago; instead, it is ongoing in the Luminous Epoch;
- Luminous Epoch spans from 0.4 billion years up to the present Epoch (13.8 billion years). The Big Bang discussed in the standard cosmological model is, in our view, the transition from Dark Epoch to Luminous Epoch.

A number of ideas presented in this paper are not new, and we don't claim credit for them. In fact, several ideas belonging to classical scientists such as Riemann, Maxwell, Heaviside, Planck, and Dirac are revisited in a new light. In the present manuscript we are attempting to describe the World while unifying and simplifying existing models and results into a cohesive physical picture of Dark Matter Cosmology and Astrophysics.

This manuscript concludes the series of papers on World-Universe Model published by "Journal of

High Energy Physics, Gravitation and Cosmology" journal [1]-[12]. Many results obtained there are quoted in the current work without a full justification; an interested reader is encouraged to view the referenced papers in such cases. In this manuscript we discuss the proposed Multiworld and Dark Matter Fermi Bubbles for the first time.

In **Chapter 2** we consider the origin, evolution, structure, ultimate fate, and primary cosmological parameters of the World. In **Chapter 3** we discuss the main physical phenomena of Luminous Matter Astrophysics: Intergalactic Plasma, Microwave Background Radiation, Energy-Varying Photons, Mass-Varying Neutrinos, Cosmic Far-Infrared Background, and Time Delay of Fast Radio Bursts. **Chapter 4** deals with the proposed Multicomponent DM, Macroobjects Cores made up of DMPs, and Weak Interaction providing integrity of all DM Cores. **Chapter 5** discusses Dark Matter Cosmology including Dark Epoch, Rotational Fission, Luminous Epoch, and Distribution of the World's Energy Density. In **Chapter 6** we explain different phenomena of DM Astrophysics: Multiwavelength Pulsars, Binary Millisecond Pulsars, Gamma-Ray Bursts, and Young Stellar Object Dippers in frames of the proposed Macroobject Shell Model. We also discuss the proposed Multiworld and Dark Matter Fermi Bubbles. **Chapter 7** debates different physical phenomena of Solar System: Angular momentum, Gravitationally-Rounded Objects Internal Heat, Dark Matter Cores of Macroobjects, Evolution of the Sun, Solar Corona, Geocorona, Planetary Coronas, and High-Energy Atmospheric Physics including Ball Lightning.

2. Cosmology

WUM utilizes the following Basic ideas:

Hypersphere World as a model of a finite universe was proposed by Georg Riemann in 1854 [13]. WUM views the World as a 3-dimensional Hypersphere that expands along the fourth spatial dimension in the Universe. A Hypersphere is an example of a 3-Manifold which locally behaves like regular Euclidean 3-dimensional space, just as the surface of a sphere looks like a plane to small enough observers.

Principal role of Maxwell's Equations (ME) that form the foundation of classical electrodynamics. Gravitoelectromagnetism (GEM) refers to a gravitational and electromagnetic analogy. The equations for GEM were first published by O. Heaviside in 1893 as a separate theory expanding Newton's law [14]. WUM follows this theory [5]. Maxwell's equations produce only two physically measurable quantities: energy density and energy flux density [9].

Existence of the Medium of the World stated by Nikola Tesla: "*All attempts to explain the workings of the universe without recognizing the existence of the ether and the indispensable function it plays in the phenomena are futile and destined to oblivion*" [15]. Paul Dirac stated in 1951 in an article in Nature, titled "Is there an Aether?" that "*we are rather forced to have an aether*" [16].

Variable gravitational parameter. The hypothesis was first proposed by P. Dirac in 1937 [17].

Continuous creation of Matter. In 1964 F. Hoyle and J. V. Narlikar explained the appearance of new matter by postulating the existence of what they dubbed the "creation field", or just the "C-field"[18]. P. Dirac in 1974 discussed the mechanisms of the additive and multiplicative creation of Matter [19].

Mach's principle. A very general statement of Mach's principle is "*Local physical laws are determined*

by the large-scale structure of the universe".

Fundamental parameters. Two Fundamental parameters in various rational exponents define all macro and micro features of the World: constant α (Sommerfeld's constant, see Section 2.5 for details) and dimensionless quantity Q, which increases in time, and is, in fact, a measure of the Size and Age of the World (see Section 2.6).

Key concepts and observations of WUM are the following:

- Expansion and Creation of Matter;
- Content of the World;
- Structure of Macroobjects;
- Inter-Connectivity of Primary Cosmological Parameters;
- Gravity, Space and Time are all emergent phenomena.

WUM makes reasonable assumptions in each of these areas. The remarkable agreement of the calculated values of the primary cosmological parameters with the observational data gives us considerable confidence in the Model.

2.1. Expansion and Creation of Matter

Before the Beginning of the World there was nothing but an Eternal Universe. About 14.2 billion years ago the World was started by a fluctuation in the Eternal Universe, and the Nucleus of the World, which is a four-dimensional ball, was born. An extrapolated Nucleus radius at the Beginning was equal to a basic unit of size a (see Section 2.5). 4-ball is the interior of a three-dimensional hypersphere. All points of the hypersphere are equivalent; there are no preferred centers or boundary of the World [5].

The 4-ball is expanding in the Eternal Universe, and its surface, the hypersphere, is likewise expanding. The radius of the Nucleus R is increasing with speed c (gravitoelectrodynamic constant) for the absolute cosmological time τ from the Beginning and equals to $R = c\tau$. The expansion of the Hypersphere World can be understood through the analogy with an expanding 3D balloon: imagine an ant residing on a seemingly two-dimensional surface of a balloon. As the balloon is blown up, its radius increases, and its surface grows. The distance between any two points on the surface increases. The ant sees her world expand but does not observe a preferred center.

According to WUM, the surface of the 4-ball is created in a process analogous to sublimation. Continuous creation of matter is the result of such process (see Section 2.8). Sublimation is a well-known endothermic process that happens when surfaces are intrinsically more energetically favorable than the bulk of a material, and hence there is a driving force for surfaces to be created. Matter arises from the fourth spatial dimension. The Universe is responsible for the creation of Matter. Dark Matter Particles (DMPs) carry new Matter into the World [5].

It is important to emphasize that

- Creation of Matter is a direct consequence of expansion;
- Creation of Dark Matter (DM) occurs homogeneously in all points of the hypersphere World;
- Luminous Matter is a byproduct of DM annihilation. Consequently, the matter-antimatter asymmetry problem discussed in literature does not arise (since antimatter does not get

created by DM annihilation).

2.2. Content of the World

The existence of the Medium is a principal point of WUM. It follows from the observations of Intergalactic Plasma; Cosmic Microwave Background Radiation (MBR); Far-Infrared Background Radiation (FIRB). Inter-galactic voids discussed by astronomers are in fact examples of the Medium in its purest. Cosmic MBR is part of the Medium; it then follows that the Medium is the absolute frame of reference. Relative to MBR rest frame, Milky Way galaxy and Sun are moving with the speed of 552 and 370 km/s respectively [5].

Theory of a Rotationally Elastic Medium. Long time ago it was realized that there are no transverse waves in the Aether, and hence the Aether could not be an elastic matter of an ordinary type. In 1846 James McCullagh proposed a theory of a rotationally elastic medium, i.e. a medium in which every particle resists absolute rotation [20]. This theory produces equations analogous to ME. WUM is based on Maxwell's equations, and McCullagh's theory is a good fit for description of the Medium.

The Medium consists of stable elementary particles with lifetimes longer than the age of the World: protons, electrons, photons, neutrinos, and dark matter particles. For all particles under consideration we use the following characteristics:

- Type of particle (fermion or boson);
- "Mass" that is equivalent to "Rest energy" with the constant c^2 ;
- Electrical charge.

The total energy density of the Medium is 2/3 of the overall energy density of the World (see Section 2.8). Superclusters, Galaxies, Extrasolar systems, planets, moons, etc. are made of the same particles. The energy density of Macroobjects adds up to 1/3 of the total energy density of the World throughout the World's evolution [5].

2.3. Structure of Macroobjects

In our view, all Macroobjects (MOs) of the World (galaxies, extrasolar systems, planets, and moons) possess the following properties [8]:

- Macroobject nuclei are made up of self-annihilating DMFs;
- MOs contain other particles, including DM and baryonic matter, in shells surrounding their nuclei.

WUM predicts existence of 5 types of self-annihilating DMPs with masses of 1.3 TeV, 9.6 GeV, 70 MeV, 340 keV, and 3.7 keV (see Section 4.1). The signs of annihilation of these particles are found in the observed gamma-ray spectra which we connect with the structure of MOs (nuclei and shells composition). Annihilation of those DMPs can give rise to any combination of gamma-ray lines. Thus, the diversity of Very High Energy gamma-ray sources in the World has a clear explanation in frames of WUM [8].

2.4. Nucleosynthesis. Large-Scale Structures. Ultimate Fate

Nucleosynthesis of all luminous elements (including light elements) occurs inside of DM Cores of all Macroobjects during their evolution. The theory of Stellar nucleosynthesis is well developed, starting with the publication of a celebrated B^2FH review paper [21]. With respect to WUM, this theory should

be expanded to include annihilation of heavy DMFs in MOs' Cores (see Section 4.1). The amount of energy produced due to this process is sufficiently high to create all elements inside of MOs' [5].

Formation and Evolution of Large-Scale Structures. All Macroobjects of the World have Cores made up of different DMPs. The matter creation is occurring homogeneously in all points of the World. It follows that new stars can be created inside of galaxies, new galaxies can be created inside of superclusters, which can arise in the World. Structures form in parallel around different Cores made of different DMPs. Formation of galaxies and stars is not a process that concluded ages ago; instead, it is ongoing [5].

Ultimate Fate of the World. The Universe is continuously creating Matter in the World. Assuming an Eternal Universe, the numbers of cosmological structures and their size on all levels will increase. The temperature of the Medium will asymptotically reach zero [1].

2.5. Fundamental Parameters and Basic Units

It is the main goal of WUM to develop a Model based on two dimensionless Fundamental Parameters only: the constant α and the time-varying parameter Q, which is a measure of the Size and Age of the World. In WUM we often use well-known physical parameters, keeping in mind that all of them can be expressed through the Basic Units. Taking the relative values of physical parameters in terms of the Basic Units we can express all dimensionless parameters of the World through two Fundamental Parameters α and Q in various rational exponents, as well as small integer numbers and π.

To define the values of the constant α and a we analyze the history of the Classical Physics [10]:

- The electrodynamic constant c in Maxwell's equations was measured by Weber and Kohlrausch in 1857 [22];
- Rydberg constant $R_\infty = \alpha^3/2a$ is a physical constant relating to atomic spectra. The constant first arose in 1888 as an empirical fitting parameter in the Rydberg formula for the hydrogen spectral series [23]. As of 2018, R_∞ is the most accurately measured Fundamental constant;
- Electron Charge-to-Mass Ratio e/m_e is a Quantity in experimental physics. It bears significance because the electron mass m_e cannot be measured directly. The e/m_e ratio of an electron was successfully calculated by J. J. Thomson in 1897 [24]. We define it after Thomson: $R_T \equiv e/m_e$;
- Planck constant h, which is generally associated with the behavior of microscopically small systems, was introduced and measured by Max Planck in 1901 based on statistical thermodynamic analysis of the black-body radiation [25];
- The magnetic constant: $\mu_0 = 4\pi \times 10^{-7}\ H/m$.

Based on the experimentally measured values of the constants c, R_∞, R_T, h we calculate the most important Fundamental constants as follows:

$$\alpha = [2(\mu_0 h/c)R_\infty^2 R_T^2]^{1/5}$$

$$a = [\frac{(\mu_0 h/c)^3 R_\infty R_T^6}{4}]^{1/5}$$

$$m_e = \frac{h}{c}\left[\frac{8R_\infty}{(\mu_0 h/c)^2 R_T^4}\right]^{1/5}$$

$$e = \left(\frac{2\alpha h/c}{\mu_0}\right)^{1/2}$$

All these Fundamental constants, including classical electron radius $a_o = a/2\pi$, were measured and could be calculated before Quantum Mechanics. The calculated constant a is the basic unit of size in WUM. It is worth to note that the constant α was later named "Sommerfeld's constant" and then "Fine-structure constant".

Below we will refer to the following Basic Units:

- energy $E_0 = \frac{hc}{a}$;
- energy density $\rho_0 = \frac{hc}{a^4}$;
- surface energy density $\sigma_0 = \frac{hc}{a^3}$;
- mass $m_0 = \frac{h}{ac}$;
- time $t_0 = \frac{a}{c}$;
- frequency $\nu_0 = \frac{c}{a}$.

2.6. Inter-Connectivity of Primary Cosmological Parameters

The constancy of the universe fundamental constants, including Newtonian constant of gravitation and Planck mass, is now commonly accepted, although has never been firmly established as a fact. All conclusions on the (almost) constancy of the Newtonian parameter of gravitation are model-dependent. A commonly held opinion states that gravity has no established relation to other fundamental forces, so it does not appear possible to calculate it from other constants that can be measured more accurately, as is done in some other areas of physics. WUM holds that there indeed exist relations between all primary cosmological parameters that depend on dimensionless time-varying quantity Q, which equals to: $Q = \tau/t_0$ [4].

The model develops a mathematical framework that allows for direct calculation of the following primary cosmological parameters through Q [7]:

- Newtonian parameter of gravitation G:

$$G = \frac{a^2 c^4}{8\pi hc} \times Q^{-1}$$

- Hubble's parameter H:

$$H = \nu_0 \times Q^{-1}$$

- Age of the World A_τ :

$$A_\tau = t_0 \times Q$$

- The Worlds' radius of curvature in the fourth spatial dimension R:

$$R = a \times Q$$

- Critical energy density ρ_{cr} :

$$\rho_{cr} = 3\rho_0 \times Q^{-1}$$

- Concentration of Intergalactic Plasma n_{IGP} :

$$n_{IGP} = \frac{2\pi^2}{a^3}\frac{m_e}{m_p} \times Q^{-1}$$

- Minimum Energy of Photons E_{ph} :

$$E_{ph} = \left(\frac{m_e}{m_p}\right)^{1/2} E_0 \times Q^{-1/2}$$

- Temperature of the Microwave Background Radiation T_{MBR} :

$$T_{MBR} = \frac{E_0}{k_B}\left(\frac{15\alpha}{2\pi^3}\frac{m_e}{m_p}\right)^{1/4} \times Q^{-1/4}$$

- Temperature of the Far-Infrared Background Radiation peak T_{FIRB} :

$$T_{FIRB} = \frac{E_0}{k_B}\left(\frac{15}{4\pi^5}\right)^{1/4} \times Q^{-1/4}$$

where k_B is the Boltzmann constant that was measured by Planck in 1901 [25]; m_e/m_p is electron-to-proton mass ratio.

In frames of WUM, we calculate the values of these parameters, which are in good agreement with the latest results of their measurements. For example, calculating the value of Hubble's parameter H_0 based on the average value of the gravitational parameter G we find $H_0 = 68.7457\ km/s\ Mpc$, which is in good agreement with $H_0 = 69.32 \pm 0.8\ km/s\ Mpc$ obtained using WMAP data [26]. Note that the precision of H_0 value has increased by three orders of magnitude. Similar precision enhancement holds for other parameters' values as well.

The remarkable agreement of the calculated values of the primary cosmological parameters with the observational data (see Sections 3.1, 3.2, 3.3, and 3.5) gives us considerable confidence in the Model. We propose to introduce Q as a new Fundamental Parameter tracked by CODATA and use its value in calculation of all Q-dependent parameters.

2.7. Hypersphere World

The physical laws we observe appear to be independent of the Worlds' curvature in the fourth spatial dimension due to the very small value of the dimension-transposing gravitomagnetic parameter of the Medium [1]. Consequently, direct observation of the Worlds' curvature would appear to be a hopeless goal.

One way to prove the existence of the Worlds' curvature is direct measurement of truly large-scale parameters of the World: Gravitational, Hubble's, Temperature of the Microwave Background Radiation. Conducted at various points of time, these measurements would give us varying results, providing insight into the curved nature of the World. Unfortunately, the accuracy of the measurements is quite poor. Measurement errors far outweigh any possible "curvature effects", rendering this technique useless in practice. To be conclusive, the measurements would have to be conducted billions of years apart [5].

In WUM, Local Physics is linked with the large-scale structure of the Hypersphere World through the dimensionless quantity Q. The proposed approach to the fourth spatial dimension agrees with Mach's principle: "*Local physical laws are determined by the large-scale structure of the universe*". Applied to WUM, it follows that all parameters of the World depending on Q are a manifestation of the Worlds' curvature in the fourth spatial dimension [5].

2.8. Critical Energy Density

The principal idea of WUM is that the energy density of the World ρ_W equals to the critical energy density ρ_{cr} necessary for 3-Manifold at any cosmological time. ρ_{cr} can be found by considering a sphere of radius R_M and enclosed mass M that can be calculated by multiplication of critical density by the volume of the sphere. When the World has the critical density, the Hubble velocity $H \times R_M$ is equal to the escape velocity, which gives an equation for the mass M leading to the equation for ρ_{cr} [27]:

$$\rho_{cr} = \frac{3H^2c^2}{8\pi G}$$

This equation can be rewritten as [1]:

$$\frac{4\pi G}{c^2} \times \frac{2}{3}\rho_{cr} = \mu_g \times \rho_M = H^2 = \frac{c^2}{R^2}$$

where $\mu_g = \frac{4\pi G}{c^2}$ is a gravitomagnetic parameter and $\rho_M = \frac{2}{3}\rho_{cr}$ is the energy density of the Medium.

According to WUM, creation of Matter in the Hypersphere World occurs continually through a process analogous to sublimation (see Section 2.1). The Eternal Universe is responsible for the creation of Matter. The physical conditions at the expanding 4-ball Nucleus of the World and Universe boundary remain constant in all times. If we assume that the content of Matter in 4-ball Nucleus is proportional to the surface of the 4-ball (hypersphere) and basic unit of surface energy density σ_0, then an energy density of the Nucleus ρ_N:

$$\rho_N = \frac{2\pi^2R^3\sigma_0}{0.5\pi^2R^4} = \frac{4hc}{a^3R} = 4\rho_0 \times Q^{-1}$$

is higher than the critical energy density of the World: $\rho_{cr} = 3\rho_0 \times Q^{-1}$. It means that the surface of the 4-ball Nucleus is intrinsically more energetically favorable than the bulk and hence there is a driving force for surface to be created. It is worth to note that energy density of the Nucleus $\rho_N \propto R^{-1}$, and hence the surface energy density of the hypersphere $\rho_{cr} \propto R^{-1}$. Considering that $H \propto R^{-1}$, it is easy to see that the gravitational parameter $G \propto R^{-1}$ [1].

2.9. Gravity, Space and Time

In frames of WUM, the parameter G can be calculated based on the value of the energy density of the Medium ρ_M of the World [1]:

$$G = \frac{\rho_M}{4\pi} \times P^2$$

where a dimension-transposing parameter P equals to:

$$P = \frac{a^3 c^2}{2hc}$$

Then the Newton's law of universal gravitation can be rewritten in the following way:

$$F = G\frac{m \times M}{r^2} = \frac{\rho_M}{4\pi}\frac{\frac{a^3}{2L_{Cm}} \times \frac{a^3}{2L_{CM}}}{r^2}$$

where we introduced the measurable parameter of the Medium ρ_M instead of the phenomenological coefficient G; and gravitoelectromagnetic charges $\frac{a^3}{2L_{Cm}}$ and $\frac{a^3}{2L_{CM}}$ instead of macroobjects masses m and M (L_{Cm} and L_{CM} are Compton length of mass m and M respectively). The gravitoelectromagnetic charges have a dimension of "Area", which is equivalent to "Energy", with the constant that equals to the basic unit of surface energy density σ_0 .

Following WUM approach , we can find a gravitomagnetic parameter of the Medium μ_M [1]:

$$\mu_M = R^{-1}$$

and the impedance of the Medium Z_M :

$$Z_M = \mu_M c = H = \tau^{-1}$$

These parameters are analogous to the magnetic constant μ_0 and impedance of electromagnetic field $Z_0 = \mu_0 c$.

It follows that measuring the value of Hubble's parameter anywhere in the World and taking its inverse value allows us to calculate the absolute Age of the World. The Hubble's parameter is then the most important characteristic of the World, as it defines the Worlds' Age. While in our Model Hubble's parameter H has a clear physical meaning, the gravitational parameter $G = \frac{a^3 c^3}{8\pi hc}H$ is a phenomenological coefficient in the Newton's law of universal gravitation.

The second important characteristic of the World is the gravitomagnetic parameter μ_M . Taking its inverse value, we can find the absolute radius of curvature of the World in the fourth spatial dimension. We emphasize that the above two parameters (Z_M and μ_M) are principally different physical characteristics of the Medium that are connected through the gravitoelectrodynamic constant c . It means that Time is not a physical dimension and is absolutely different entity than Space. Time is a factor of the World.

In WUM, Time and Space are closely connected with Mediums' impedance and gravitomagnetic parameter. It follows that neither Time nor Space could be discussed in absence of the Medium. The gravitational parameter G that is proportional to the Mediums' energy density can be introduced only for the Medium filled with Matter. In frames of WUM, the Gravitation is a result of simple interactions of Dark Matter Fermions Dions with Matter that work cooperatively to create a more complex interaction. Dions are responsible for the Le Sage's mechanism of the gravitation [4].

As the conclusion, Gravity, Space and Time are all emergent phenomena [5]. In this regard, it is worth to recall the Albert Einstein quote: "*When forced to summarize the theory of relativity in one sentence: time and space and gravitation have no separate existence from matter*".

3. Luminous Matter Astrophysics

3.1. Intergalactic Plasma

In our Model, the World consists of stable elementary particles with lifetimes longer than the age of the World. Protons with mass m_p and electrons with mass m_e have identical concentrations in the World: $n_p = n_e$. Low density intergalactic plasma consisting of protons and electrons has the lowest plasma frequency ω_{pl} [1]:

$$\omega_{pl}^2 = \frac{4\pi n_p e^2}{4\pi\varepsilon_0 m_p} = \frac{m_e}{m_p}\frac{4\pi n_e e^2}{4\pi\varepsilon_0 m_e} = \frac{m_e}{m_p}\omega_e^2 \qquad 3.1.1$$

where e is the elementary charge, ε_0 is the electric constant, and ω_e is electron plasma frequency. If we assume that ω_e is proportional to $Q^{-1/2}$, then n_e is proportional to Q^{-1}. Energy densities of protons and electrons are then proportional to Q^{-1}, similar to the critical energy density $\rho_{cr} \propto Q^{-1}$. Considering $\omega_e = 2\pi\nu_0 \times Q^{-1/2}$, we can calculate concentration of protons and electrons:

$$n_p = n_e = \frac{2\pi^2}{a^3}\frac{m_e}{m_p} \times Q^{-1} = 0.25480\ m^{-3}$$

A. Mirizzi, *et al.* found that the mean diffuse intergalactic plasma density is bounded by $n_e \lesssim 0.27\ m^{-3}$ [28]. The calculated Mediums' plasma density is in good agreement with the estimated value [28].

$\rho_p = n_p m_p c^2$ is the energy density of protons in the Medium. The relative energy density of protons Ω_p is then the ratio of ρ_p/ρ_{cr} :

$$\Omega_p = \frac{\rho_p}{\rho_{cr}} = \frac{2\pi^2\alpha}{3} = 0.048014655 \qquad 3.1.2$$

This value is in good agreement with experimentally found value of 0.049 ± 0.013 [29]. It is worth to note that the relative energy density of protons in Luminous Epoch is constant all time and proportional to the Fundamental constant α.

3.2. Microwave Background Radiation

According to WUM, the black body spectrum of MBR is due to thermodynamic equilibrium of photons with low density intergalactic plasma consisting of protons and electrons. $\rho_e = n_e m_e c^2$ is the energy density of electrons in the Medium. We assume that the energy density of MBR ρ_{MBR} equals to twice the value of ρ_e (considering two polarizations of photons) [1]:

$$\rho_{MBR} = 2\rho_e = 4\pi^2\alpha\frac{m_e}{m_p}\rho_0 \times Q^{-1} = \frac{8\pi^5}{15}\frac{k_B^4}{(hc)^3}T_{MBR}^4$$

where T_{MBR} is MBR temperature. We can now calculate the value of T_{MBR}:

$$T_{MBR} = \frac{E_0}{k_B}\left(\frac{15\alpha}{2\pi^3}\frac{m_e}{m_p}\right)^{1/4} \times Q^{-1/4} = 2.72518\ K \qquad 3.2$$

which is in excellent agreement with experimentally measured value of $2.72548 \pm 0.00057\ K$ [30]. We are not aware of any other model that allows calculation of MBR temperature with such accuracy.

3.3. Energy-Varying Photons

From equation (3.1.1) we obtain the value of the lowest frequency ν_{pl} [1]:

$$\nu_{pl} = \frac{\omega_{pl}}{2\pi} = \left(\frac{m_e}{m_p}\right)^{1/2}\nu_0 \times Q^{-1/2} = 4.5322\ Hz$$

Photons with energy smaller than $E_{ph} = h\nu_{pl}$ cannot propagate in plasma, thus $h\nu_{pl}$ is the smallest amount of energy a photon may possess. Following L. Bonetti, *et al.* [31] we can call this amount of energy the rest energy of photons that equals to

$$E_{ph} = \left(\frac{m_e}{m_p}\right)^{1/2} E_0 \times Q^{-1/2} = 1.8743 \times 10^{-14}\ eV \qquad 3.3$$

The above value is in good agreement with the value $E_{ph} \lesssim 2.2 \times 10^{-14}\ eV$ estimated by L. Bonetti, *et al.* [31]. It is more relevant to call E_{ph} the minimum energy of photons which can pass through the Intergalactic plasma. It is worth to note that E_{ph} is varying in time: $E_{ph} \propto \tau^{-1/2}$.

3.4. Mass-Varying Neutrinos

It is now established that there are three different types of neutrino: electronic ν_e, muonic ν_μ, and tauonic ν_τ. Neutrino oscillations imply that neutrinos have non-zero masses. Let's take neutrino masses m_{ν_e}, m_{ν_μ}, m_{ν_τ} that are near [3]:

$$m_\nu = m_0 \times Q^{-1/4}$$

Their concentrations n_ν are then proportional to

$$n_\nu \propto \frac{1}{a^3} \times Q^{-3/4}$$

and their energy density ρ_ν is then proportional to Q^{-1}, similar to critical energy density $\rho_{cr} \propto Q^{-1}$. Experimental results obtained by M. Sanchez [32] show $\nu_e \to \nu_{\mu,\tau}$ neutrino oscillations with parameter Δm^2_{sol} given by

$$2.3 \times 10^{-5}\ eV^2/c^4 \le \Delta m^2_{sol} \le 9.3 \times 10^{-5}\ eV^2/c^4$$

and $\nu_\mu \to \nu_\tau$ neutrino oscillations with parameter Δm^2_{atm}:

$$1.6 \times 10^{-3}\ eV^2/c^4 \le \Delta m^2_{atm} \le 3.9 \times 10^{-3}\ eV^2/c^4$$

where Δm^2_{sol} and Δm^2_{atm} are mass splitting for solar and atmospheric neutrinos respectively. Significantly more accurate result was obtained by P. Kaus, *et al.* [33] for the ratio of the mass splitting:

$$\sqrt{\frac{\Delta m^2_{sol}}{\Delta m^2_{atm}}} \cong 0.16 \cong \frac{1}{6} \qquad 3.4$$

Let's assume that muonic neutrino's mass indeed equals to

$$m_{\nu_\mu} = m_\nu = m_0 \times Q^{-1/4} \cong 7.5 \times 10^{-3}\ eV/c^2$$

From equation (3.4) it then follows that

$$m_{\nu_\tau} = 6m_\nu \cong 4.5 \times 10^{-2}\ eV/c^2$$

Then the squared values of the muonic and tauonic neutrino masses fall into the experimentally found ranges:

$$m^2_{\nu_\mu} \cong 5.6 \times 10^{-5}\ eV^2/c^4$$

$$m^2_{\nu_\tau} \cong 2 \times 10^{-3}\ eV^2/c^4$$

We assume that electronic neutrino mass equals to [3]:

$$m_{\nu_e} = \frac{1}{24} m_\nu \cong 3.1 \times 10^{-4}\ eV/c^2$$

The sum of the calculated neutrino masses

$$\Sigma m_\nu \cong 0.053\ eV/c^2$$

is in good agreement with the value of $0.06\ eV/c^2$ discussed in literature [34].

3.5. Cosmic Far-Infrared Background

The cosmic Far-Infrared Background (FIRB), which was announced in 1998, is part of the Cosmic Infrared Background, with wavelengths near 100 microns that is the peak power wavelength of the black-body radiation at temperature 29 K. According to WUM, large cosmic grains are responsible for the FIRB [3].

It was experimentally found that the size of large grains D_G is roughly equal to the length $L_F = a \times Q^{1/4}$, and their mass M_G is close to the Planck mass: $M_P = 2m_0 \times Q^{1/2}$ [35], [36], [37]. A grain of mass $B_1 M_P$ and radius $B_2 L_F$ is receiving energy at the following rate:

$$\frac{d}{d\tau}(B_1 M_P c^2) = \frac{B_1 M_P c^2}{2\tau}$$

where B_1 and B_2 are parameters. The received energy will increase the grain's temperature T_G, until equilibrium is achieved: power received equals to the power irradiated by the surface of a grain in accordance with the Stefan-Boltzmann law

$$\frac{B_1 M_P c^2}{2\tau} = \sigma_{SB} T_G^4 \times 4\pi B_2^2 L_F^2$$

where σ_{SB} is Stefan-Boltzmann constant: $\sigma_{SB} = \frac{2\pi^5 k_B^4}{15h^3 c^3}$. With Nikola Tesla's principle at heart – *There is no energy in matter other than that received from the environment* – we get:

$$B_1 M_P c^2 = 4\pi B_2^2 L_F^2 \sigma_0$$

We then calculate the grain's stationary temperature T_G to be [3]:

$$T_G = (\frac{15}{4\pi^5})^{1/4} \frac{hc}{k_B L_F} = 28.955\ K \qquad 3.5$$

This result is in an excellent agreement with experimentally measured value of $29\ K$ [38]-[49]. The total flux of the FIRB radiation is the sum of the contributions of all individual grains. Comparing equations (3.2) and (3.5), we can find the relation between the grains' temperature and the temperature of the MBR:

$$T_G = (3\Omega_e)^{-1/4} \times T_{MBR}$$

where electron relative energy density Ω_e equals to $\Omega_e = \frac{m_e}{m_p}\Omega_p$.

3.6. Time Delay of Fast Radio Bursts

Fast Radio Burst (FRB) is a high-energy astrophysical phenomenon manifested as a transient radio pulse lasting only a few milliseconds. The component frequencies of each burst are delayed by different amounts of time depending on the wavelength. This delay is described by a value referred to as a Dispersion Measure which is the total column density of free electrons between the observer and the source of FRB. Fast radio bursts have Dispersion measures which are consistent with propagation through ionized plasma [29].

Consider a photon with initial frequency ν_{emit} and energy E_{emit} emitted at time τ_{emit} when the radius of the hypersphere World in the fourth spatial dimension was R_{emit}. The photon is continuously losing kinetic energy on its way to Earth until time τ_{obsv} when the radius is $R_{obsv} = R_0$. An observer will measure ν_{obsv} and energy E_{obsv} and calculate a redshift z. Recall that τ_{emit} and τ_{obsv} are cosmological times (ages of the World at the moments of emitting and observing).

A light-travel time distance to the source of FRB d_{LTT} equals to [7]:

$$d_{LTT} = c(\tau_{obsv} - \tau_{emit}) = ct_{LTT} = R_0 - R_{emit}$$

Let's calculate photons' traveling time $\boldsymbol{t_{ph}}$ considering that the minimum energy of photons $\boldsymbol{E_{ph}}$ is much smaller than the energy of photons $\boldsymbol{E_{\gamma}}$:

$$t_{ph} = \frac{1}{c}\int_{R_{emit}}^{R_0}(1-\frac{E_{ph}^2}{E_\gamma^2})^{-1/2}\,dr = t_{LTT} + \Delta t_{ph}$$

where Δt_{ph} is photons' time delay relative to the light-travel time t_{LTT} that equals to

$$\Delta t_{ph} = \frac{1}{2c}\int_{R_{emit}}^{R_0}\frac{E_{ph}^2}{E_\gamma^2}\,dr \qquad 3.6.1$$

All observed FRBs have redshifts $z < 1$. It means that we can use the Hubble's law: $d_{LTT} = R_0 z$. Then

$$R_{emit} = (1-z)R_0 \qquad 3.6.2$$

Photons' minimum energy squared at radius r between R_{emit} and R_0 equals to (see equation (3.3)):

$$E_{ph}^2 = \frac{m_e}{m_p}\frac{a}{r}E_0^2 \qquad 3.6.3$$

According to WUM, photons' energy E_γ on the way to the observer can be expressed by the following equation [6]:

$$E_\gamma = zE_{obsv} + (1-z)\frac{R_0}{r}E_{obsv} \qquad 3.6.4$$

which reduces to E_{emit} at (3.6.2) and to E_{obsv} at $r = R_0$. Placing the values of the parameters (3.6.2), (3.6.3), (3.6.4) into (3.6.1), we have for photons' time delay [6]:

$$\Delta t_{ph} = \frac{4.61}{z^2}\left[ln\left(\frac{1}{1-z^2}\right) - \frac{z^2}{1+z}\right] \times (\frac{\nu}{1GHz})^{-2}$$

Taking z=0.492 [29] we get the calculated value of photons' time delay

$$\Delta t_{ph}^{cal} = 2.189 \times (\frac{\nu}{1GHz})^{-2}$$

which is in good agreement with experimentally measured value [29]:

$$\Delta t_{ph}^{exp} = 2.438 \times (\frac{\nu}{1GHz})^{-2}$$

It is worth to note that in our calculations there is no need in the dispersion measure, and time delay depends on the redshift only.

4. Dark Matter

4.1. Multicomponent Dark Matter

DMPs might be observed in Centers of Macroobjects has drawn many new researchers to the field in the last forty years. Indirect effects in cosmic rays and gamma-ray background from the annihilation of cold DM in the form of heavy stable neutral leptons in Galaxies were considered in pioneer articles [50]-[55]. A mechanism whereby DM in protostellar halos plays the role in the formation of the first stars is discussed by D. Spolyar, K. Freese, and P. Gondolo [56]. Heat from neutralino DM annihilation is shown to overwhelm any cooling mechanism, consequently impeding the star formation process. A "dark star'' powered by DM annihilation instead of nuclear fusion may result. Dark stars are in hydrostatic and thermal equilibrium, but with an unusual power source. Weakly Interacting Massive Particles (WIMPs) are among the best candidates for DM [57]. Important cosmological problems like Dark Matter and Dark Energy could be, in principle, solved through extended gravity. This is stressed, for example, in the famous paper of Prof. C. Corda [58].

Two-component DM system consisting of bosonic and fermionic components is proposed for the explanation of emission lines from the bulge of Milky Way galaxy. C. Boehm, P. Fayet, and J. Silk analyze the possibility of two coannihilating neutral and stable DMPs: a heavy fermion for example, like the lightest neutralino (> 100 GeV) and the other one a possibly light spin-0 particle (~ 100 MeV) [59].

WUM proposes multicomponent DM system consisting of two couples of coannihilating DMPs: a heavy DM fermion – DMF1 (1.3 TeV) and a light spin-0 boson – DIRAC (70 MeV) that is a dipole of Dirac's monopoles; a heavy fermion – DMF2 (9.6 GeV) and a light spin-0 boson – ELOP (340 keV) that is a dipole of preons with electrical charge e/3; a self-annihilating fermion – DMF3 (3.7 keV) and a fermion DMF4 named Dion (0.2 eV).

WUM postulates that masses of DMFs and bosons are proportional to m_0 multiplied by different exponents of α and can be expressed with the following formulae [11]:

DMF1 (fermion): $m_{DMF1} = \alpha^{-2} m_0 = 1.3149950\ TeV$
DMF2 (fermion): $m_{DMF2} = \alpha^{-1} m_0 = 9.5959823\ GeV$
DIRAC (boson): $m_{DIRAC} = \alpha^{0} m_0 = 70.025267\ MeV$
ELOP (boson): $m_{ELOP} = 2/3\alpha^{1} m_0 = 340.66606\ keV$
DMF3 (fermion): $m_{DMF3} = \alpha^{2} m_0 = 3.7289402\ keV$
DMF4 (fermion): $m_{DMF4} = \alpha^{4} m_0 = 0.19857111\ eV$

The values of mass of DMF1, DMF2, DMF3 fall into the ranges estimated in literature for neutralinos, WIMPs, and sterile neutrinos respectively [2]. DMF1, DMF2 and DMF3 partake in the self-annihilation interaction with strength equals to α^{-2}, α^{-1} and α^{2} respectively.

4.2. Macroobjects Cores Made up of Dark Matter Particles

According to WUM, Macrostructures of the World (Superclusters, Galaxies, Extrasolar Systems) have Nuclei made up of DMFs, which are surrounded by Shells composed of DM and baryonic matter. The shells envelope one another, like a Russian doll. The lighter a particle, the greater the radius and the mass of its shell. Innermost shells are the smallest and are made up of heaviest particles; outer shells are larger and consist of lighter particles [11]. **Table 1** describes the parameters of Macroobjects Cores (which are Fermionic Compact Stars in WUM) in the present Epoch made up of different DM fermions: self-annihilating DMF1, DMF2, DMF3 and the fermion DMF4 named Dion.

Table 1. Parameters of Macroobjects Cores made up of different DMFs in the present Epoch.

Fermion	Fermion mass m_f, MeV	Macroobject mass M_{max}, kg	Macroobject radius R_{min}, m	Macroobject density $\rho_{max}, kg/m^3$
DMF1	1.3×10^{6}	1.9×10^{30}	8.6×10^{3}	7.2×10^{17}
DMF2	9.6×10^{3}	1.9×10^{30}	8.6×10^{3}	7.2×10^{17}
DMF3	3.7×10^{-3}	1.2×10^{41}	5.4×10^{14}	1.8×10^{-4}
DMF4	2×10^{-7}	4.2×10^{49}	1.9×10^{23}	1.5×10^{-21}

The calculated parameters of the shells show that [11]:

- Nuclei made of self-annihilating DMF1 and/or DMF2 compose Cores of stars in extrasolar systems;
- Shells of DMF3 around Nuclei made up of self-annihilating DMF1 and/or DMF2 make up Cores of galaxies;
- Nuclei made of DMF1 and/or DMF2 surrounded by shells of DMF3 and DMF4 compose Cores of superclusters.

Macroobjects Cores have the following properties [2]:

- The minimum radius of Core R_{min} made of any fermion equals to three Schwarzschild radii;
- Core density does not depend on M_{max} and R_{min} and does not change in time while $M_{max} \propto \tau^{3/2}$ and $R_{min} \propto \tau^{1/2}$.

K. Mehrgan, *et al.* observed a supergiant elliptical galaxy Holmberg 15A about 700 million light-years from Earth. They found an extreme core with a mass of 4×10^{10} solar masses at the center of Holm 15A [60]. The calculated maximum mass of galaxy Core of 6×10^{10} solar masses (see **Table 1**) is in good agreement with the experimentally found value [60].

4.3. Weak Interaction

The widely discussed models for nonbaryonic DM are based on the Cold DM hypothesis, and corresponding particles are commonly assumed to be WIMPs, *which interact via gravity and any other force (or forces), potentially not part of the standard model itself, which is as weak as or weaker than the weak nuclear force, but also non-vanishing in its strength* [Wikipedia. Weakly interacting massive particles]. It follows that a new weak force needs to exist, providing interaction between DMPs. The strength of this force exceeds that of gravity, and its range is considerably greater than that of the weak nuclear force.

According to WUM, strength of gravity is characterized by gravitational parameter [11]:

$$G = G_0 \times Q^{-1}$$

where $G_0 = \frac{a^2 c^4}{8\pi hc}$ is an extrapolated value of G at the Beginning of the World ($Q=1$). Q in the present Epoch equals to [5]:

$$Q = 0.759972 \times 10^{40}$$

The range of the gravity equals to the size of the World R:

$$R = a \times Q = 1.34558 \times 10^{26}\ m$$

In WUM, weak interaction is characterized by the parameter G_W:

$$G_W = G_0 \times Q^{-1/4}$$

which is about 30 orders of magnitude greater than G. The range of the weak interaction R_W in the present Epoch equals to:

$$R_W = a \times Q^{1/4} = 1.65314 \times 10^{-4}\ m \qquad 4.3$$

that is much greater than the range of the weak nuclear force. Calculated concentration of Dions n_D

in the largest shell of Superclusters: $n_D \cong 4.2 \times 10^{15}\, m^{-3}$ shows that a distance between particles is around $\sim 10^{-5}\, m$, which is much smaller than R_W. Thus, the introduced weak interaction between DMPs will provide integrity of all DM shells. In our view, weak interaction between particles DMF3 provides integrity of Fermi Bubbles (see Section 6.7).

5. Dark Matter Cosmology

5.1. Dark Epoch

Dark Epoch started at the Beginning of the World and lasted for about 0.4 billion years. WUM is a classical model, therefore classical notions can be introduced only when the very first ensemble of particles was created at the cosmological time $\cong 10^{-18} s$. At time $\tau \gg 10^{-18} s$ density fluctuations could happen in the Medium of the World filled with DMF1, DMF2, DIRACs, ELOPs, DMF3 and DMF4. The heaviest Dark Matter particles DMF1 could collect into a cloud with distances between particles smaller than R_W. As the result of the weak interaction, clumps of DMF1 will arise. Larger clumps will attract smaller clumps and DMPs and initiate a process of expanding the DM clump followed by growth of surrounding shells made up of other DMPs, up to the maximum mass of the shell made up of Dions at the end of Dark Epoch (0.4 billion years).

The process described above is the formation of the DM Core of a Supercluster [11]. We estimate the number of Supercluster Cores at present Epoch to be around $\sim 10^3$. DMPs supply not only additional mass ($\propto \tau^{3/2}$) to Cores, but also additional angular momentum ($\propto \tau^2$) fueling the overspinning of Dark Matter Cores (see next Section). In our opinion, all Supercluster Cores had undergone rotational fission at approximately the same cosmological time [11].

5.2. Rotational Fission

According to WUM, the rotational angular momentum of overspinning objects before rotational fission equals to [11]:

$$L_{rot} = \frac{4\sqrt{2}}{15}\frac{1+5\delta}{1+3\delta} G^{0.5} M^{1.5} R^{0.5}$$

where M is a mass of overspinning object, R is its radius, δ is the density ratio inside of the object: $\delta = \rho_{min}/\rho_{max}$. Parameters G, M, R for Macroobjects Cores are time-varying: $G \propto \tau^{-1}$, $M \propto \tau^{3/2}$ and $R \propto \tau^{1/2}$. It follows that the rotational angular momentum of Cores L_{rot} is proportional to τ^2.

Let's introduce Age parameter θ_F that is a ratio of cosmological time of Core fission τ_F to the age of the World in present Epoch A_W: $\theta_F = \tau_F / A_W$. Finally, for L_{rot} at the time of Core fission we obtain the following equation:

$$L_{rot} = \frac{4\sqrt{2}}{15}\frac{1+5\delta}{1+3\delta} G^{0.5} M^{1.5} R^{0.5} \theta_F^2 \qquad 5.2$$

where for parameters G, M, R we use their values in the present Epoch.

Local Supercluster (LS) is a mass concentration of galaxies containing the Local Group, which in turn contains the Milky Way galaxy. At least 100 galaxy groups and clusters are located within its diameter of 110 million light-years. Considering parameters of Dions' shell (see **Table 1**), we calculate the

rotational angular momentum L_{rot}^{LSC} of LS Core before rotational fission with the age parameter $\theta_{0.4} \cong 1/36$:

$$L_{rot}^{LSC} = 3.7 \times 10^{77} J\ s$$

Milky Way (MW) is gravitationally bounded with LS [61]. Let's compare L_{rot}^{LSC} with an orbital momentum of Milky Way L_{orb}^{MW} calculated based on the distance of 65 million light years from LS Core and orbital speed of about 400 km/s [61]:

$$L_{orb}^{MW} = 2.5 \times 10^{71}\ J\ s$$

It means that as the result of rotational fission of LS Core, approximately $\sim 10^6$ galaxies like Milky Way could be generated at the same time. Considering that density of galaxies in the LS falls off with the square of the distance from its center near the Virgo Cluster, and the location of MW on the outskirts of the LS [62], the actual number of created galaxies could be much larger.

The mass-to-light ratio of the LS is about 300 times larger than that of the Solar ratio. Similar ratios are obtained for other superclusters [63]. These facts support the rotational fission mechanism proposed above. In 1933, Fritz Zwicky investigated the velocity dispersion of Coma cluster and found a surprisingly high mass-to-light ratio ($\sim$500). He concluded: *if this would be confirmed, we would get the surprising result that dark matter is present in much greater amount than luminous matter* [64]. These ratios are one of the main arguments in favor of presence of large amounts of Dark Matter in the World.

Analogous calculations for MW Core based on parameters of DMF3 shell (see **Table 1**) produce the following value of rotational angular momentum L_{rot}^{MWC} [11]:

$$L_{rot}^{MWC} = 2.4 \times 10^{60}\ J\ s$$

which far exceeds the orbital momentum of the Solar System L_{orb}^{SS} calculated based on the distance from the galactic center of 26,400 light years and orbital speed of about 220 km/s :

$$L_{orb}^{SS} = 1.1 \times 10^{56}\ J\ s$$

As the result of rotational fission of MW Core 13.8 billion years ago, approximately $\sim 10^4$ Extrasolar systems like Solar System could be created at the same time. Considering that MW has grown inside out (in the present Epoch, most old stars can be found in the middle, more recently formed ones on the outskirts [65]), the number of generated Extrasolar systems could be much larger. Extrasolar system Cores can give birth to planetary cores, which in turn can generate cores of moons by the same Rotational Fission mechanism (see Section 7.1).

The oldest known star HD 140283 (Methuselah star) is a subgiant star about 190 light years away from Earth for which a reliable age has been determined [66]. H. E. Bond, *et al.* found its age to be 14.46 +/- 0.8 Gyr that does not conflict with the age of the Universe, 13.77 +/- 0.06 Gyr, based on the microwave background and Hubble constant [66]. It means that this star must have formed between 13.66 and 13.83 Gyr, amount of time that is too short for formation of second generation of stars according to prevailing theories. In our Model this discovery can be explained by generation of HD 140283 by overspinning Core of the MW 13.8 billion years ago.

In frames of the developed Rotational Fission model it is easy to explain hyper-runaway stars

unbound from the Milky Way with speeds of up to $\sim 700\, km/s$ [67]: they were launched by overspinning Core of the Large Magellan Cloud with the speed higher than the escape velocity [11].

5.3. Luminous Epoch

Luminous Epoch spans from 0.4 billion years up to the present Epoch (during 13.8 billion years). According to WUM, Cores of all Macroobjects (MOs) of the World (Superclusters, Galaxies, Extrasolar systems) possess the following properties [11]:

- Their Nuclei are made up of DMFs and contain other particles, including Dark Matter and baryonic matter, in shells surrounding the Nuclei;
- DMPs are continuously absorbed by Cores of all MOs. Luminous Matter (about 7.2% of the total Matter in the World) is a byproduct of DMPs annihilation. Luminous Matter is re-emitted by Cores of MOs continuously;
- Nuclei and shells are growing in time: size $\propto \tau^{1/2}$; mass $\propto \tau^{3/2}$; and rotational angular momentum $\propto \tau^2$, until they reach the critical point of their stability, at which they detonate. Satellite cores and their orbital L_{orb} and rotational L_{rot} angular momenta released during detonation are produced by Overspinning Core (OC). The detonation process does not destroy OC; it's rather gravitational hyper-flares;
- Size, mass, composition, L_{orb} and L_{rot} of satellite cores depend on local density fluctuations at the edge of OC and cohesion of the outer shell. Consequently, the diversity of satellite cores has a clear explanation.

WUM refers to OC detonation process as Gravitational Burst (GB), analogous to Gamma Ray Burst [6]. In frames of WUM, the repeating GBs can be explained the following way:

- As the result of GB, the OC loses a small fraction of its mass and a large part of its rotational angular momentum;
- After GB, the Core absorbs new DMPs. Its mass increases $\propto \tau^{3/2}$, and its angular momentum L_{rot} increases much faster $\propto \tau^2$, until it detonates again at the next critical point of its stability;
- Afterglow of GBs is a result of processes developing in the Nuclei and shells after detonation;
- In case of Extrasolar systems, a star wind is the afterglow of star detonation: star Core absorbs new DMPs, increases its mass $\propto \tau^{3/2}$ and gets rid of extra L_{rot} by star wind particles;
- Solar wind is the afterglow of Solar Core detonation 4.6 billion years ago. It creates the bubble of the heliosphere continuously (see Section 6.6);
- In case of Galaxies, a galactic wind is the afterglow of repeating galactic Core detonations. In Milky Way it continuously creates two Dark Matter Fermi Bubbles (see Section 6.7).

S. E. Koposov, *et al.* present the discovery of the fastest Main Sequence hyper-velocity star S5-HVS1 with mass about 2.3 solar masses that is located at a distance of ~9 kpc from the Sun. When integrated backwards in time, the orbit of the star points unambiguously to the Galactic Centre, implying that S5-HVS1 was kicked away from Sgr A* with a velocity of ~1800 km/s and travelled for 4.8 Myr to the current location. So far, this is the only hyper-velocity star confidently associated with the Galactic Centre [68]. In frames of the developed Model this discovery can be explained by Gravitational Burst of the overspinning Core of the Milky Way 4.8 million years ago, which gave birth to S5-HVS1 with the speed higher than the escape velocity of the Core.

C. J. Clarke, *et al.* observed CI Tau, a young 2 million years old star. CI Tau is located about 500 light years away in a highly-productive stellar 'nursery' region of the galaxy. They discovered that the Extrasolar System contains four gas giant planets that are only 2 million years old [69], amount of time that is too short for formation of gas giants according to prevailing theories. In frames of the developed Rotational Fission model, this discovery can be explained by Gravitational Burst of the overspinning Core of the Milky Way two million years ago, which gave birth to CI Tau system with all planets generated at the same time [11].

To summarize,

- The rotational fission of macroobject Cores is the most probable process that can generate satellite cores with large orbital momenta in a very short time;
- Macrostructures of the World form from the top (superclusters) down to galaxies, extrasolar systems, planets, and moons;
- Gravitational waves can be a product of rotational fission of overspinning Macroobject Cores;
- Hypersphere World-Universe model can serve as a basis for Transient Gravitational Astrophysics.

5.4. Distribution of the World's Energy Density

According to WUM, the total Dions relative energy density ρ_{Dion} in terms of ρ_p equals to [11]:

$$\rho_{Dion} = \frac{45}{\pi}\rho_p = 0.68775927\rho_{cr}$$

Our Model holds that the energy density of all types of self-annihilating DMPs is proportional to the proton energy density ρ_p in the World's Medium. In all, there are 5 different types of self-annihilating DMPs: DMF1, DMF2, DIRAC, ELOP, and DMF3. Then the total energy density of DM ρ_{DM} is

$$\rho_{DM} = 5\rho_p = 0.24007327\rho_{cr}$$

The total baryonic energy density ρ_B is:

$$\rho_B = 1.5\rho_p$$

The sum of electron and MBR energy densities ρ_{eMBR} equals to:

$$\rho_{eMBR} = \rho_e + \rho_{MBR} = 1.5\frac{m_e}{m_p}\rho_p + 2\frac{m_e}{m_p}\rho_p = 3.5\frac{m_e}{m_p}\rho_p$$

We take energy density of neutrinos ρ_ν to equal:

$$\rho_\nu = \rho_{MBR}$$

For FIRB radiation energy density ρ_{FIRB} we take

$$\rho_{FIRB} = \frac{1}{5\pi}\frac{m_e}{m_p}\rho_p \approx 0.032\rho_{MBR}$$

which corresponds to the value of $0.034\rho_{MBR}$ calculated by E. L. Wright [70]. Then the energy density of the World ρ_W in Luminous Epoch equals to the theoretical critical energy density ρ_{cr}

$$\rho_W = \left[\frac{45}{\pi} + 6.5 + \left(5.5 + \frac{1}{5\pi}\right)\frac{m_e}{m_p}\right]\rho_p = \rho_{cr}$$

Considering the equation (3.1.2) for ρ_p , from this equation we can calculate the value of $1/\alpha$ using electron-to-proton mass ratio m_e/m_p

$$\frac{1}{\alpha} = \frac{\pi}{15}\left[450 + 65\pi + (55\pi + 2)\frac{m_e}{m_p}\right] = 137.03600$$

which is in excellent agreement with the commonly adopted value of 137.035999. It follows that there is a direct correlation between constants α and m_e/m_p expressed by the obtained equation. As shown, m_e/m_p is not an independent constant but is instead derived from α [11].
As the conclusion, according to WUM:

- The World's energy density is inversely proportional to Fundamental parameter Q in all cosmological times;
- The particles relative energy densities are proportional to Fundamental constant α in Luminous Epoch.

6. Dark Matter Astrophysics

6.1. Macroobject Shell Model

In our view, Macroobjects of the World possess the following properties [8]:

- Nuclei are made up of DMPs. Surrounding shells contain DM and baryonic matter;
- Nuclei and shells are growing in time proportionally to square root of cosmological time $\propto \tau^{1/2}$ until one of them reaches the critical point of its local stability, at which it detonates. The energy released during detonation is produced by the annihilation of DMPs. The detonation process does not destroy the Macroobject; instead, Hyper-flares occur in active regions of the shells, analogous to Solar flares;
- All other DMPs in different shells can start annihilation process as the result of the first detonation;
- Different emission lines in spectra of bursts are connected to the Macroobjects' structure which depends on the composition of the Nuclei and surrounding shells made up of DMPs. Consequently, the diversity of Very High Energy Bursts has a clear explanation;
- Afterglow is a result of processes developing in Nuclei and shells after detonation.

6.2. Multiwavelength Pulsars

According to WUM, Macroobjects Cores made up of self-annihilating DMF1 and DMF2 have maximum mass and minimum size which are equal to parameters of neutron stars [8]. It follows that Gamma-Ray Pulsars might be, in fact, rotating DMF1 or DMF2 star. The nuclei of such pulsars may also be made up of their mixture surrounded by shells composed of other DMPs. Gamma-Ray Pulsar multiwavelength radiation depends on the composition of Nucleus and shells [8].

S. Ansoldi, *et al.* report the most energetic pulsed emission ever detected from the Crab pulsar reaching up to 1.5 TeV. Such TeV pulsed quants require a parent population of electrons with a Lorentz factor of at least 5×10^6. These results strongly suggest Inverse Compton scattering of low energy photons as the emission mechanism [71].

Ge Chen, *et al.* report hard X-ray observations of the young rotation-powered radio pulsar PSR B1509 in the range spanning from 3 keV through 500 MeV. Astronomers hypothesize that the pulsar's lack of GeV emission is due to viewing geometry, with the X-rays originating from synchrotron emission from secondary pairs in the magnetosphere [72].

WUM: Very High Energy pulsed emission from the Crab pulsar can be explained by active area of rotating Star composed of a mixture of annihilating DMF1 (1.3 TeV) and DMF2 (9.6 GeV). Multiwavelength emission from pulsar PSR B1509 can be explained by rotating DMF2 star with an active area irradiating gamma quants with energy 9.6 GeV, which interact with surrounding shells, causing them to glow in X-ray spectrum [8].

6.3. Binary Millisecond Pulsars

The properties of the growing class of radio pulsars with low-mass companions are discussed in literature. S. Johnston, *et al.* have discovered pulsar PSR J0437–4715 with by far the greatest flux density of any known millisecond pulsar [73]. M. Bailes, *et al.* report the discovery of millisecond pulsar PSR J2145-0750 that has a spin-down age of approximately greater than 12 Gyr [74]. Binary millisecond pulsar PSR J1311–3430 was explained by a model where mass from a low mass companion is transferred onto the pulsar, increasing the mass of the pulsar and decreasing its period. The averaged gamma-ray spectral energy distribution for the pulsar has cut-off about 10 GeV [75].

WUM: These experimental results can be explained by rotating DMF2 star made up of annihilating DMF2 (9.6 GeV) with mass that is growing in time proportionally to $\propto \tau^{3/2}$. DMF2 star is receiving mass and energy at the rate $W_r \propto \tau^{1/2}$. When the received power W_r is greater than the gamma-ray power irradiated by the active area of the rotating DMF2 star, the decreasing of its period will be observed. Then there is no need to introduce a low-mass companion [8].

6.4. Gamma-Ray Bursts

Gamma-Ray Bursts (GRBs) status after 50 years of investigations looks as follows [6]:

- The intense radiation of most observed GRBs is believed to be released when a rapidly rotating, high-mass star collapses to form a neutron star, quark star, or black hole;
- Short GRBs appear to originate from merger of binary neutron stars;
- There are seven known soft gamma repeaters. It means that some GRBs are not catastrophic events.

WUM: The experimental results for GRBs have the following explanation [6]:

- Nuclei and shells of galaxies made up of DMPs are responsible for GRBs;
- GRBs convert energy into radiation through annihilation of DMPs;
- Spectrum of GRBs depends on composition of Nuclei and shells;
- Afterglow is a result of processes developing in the Nuclei and shells after detonation.

6.5. Young Stellar Object Dippers

The Mysterious Star **KIC 8462852** with its large irregular dimmings is a main-sequence star with a rotation period ~ 0.88 day that exhibits no significant Infrared excess. A stellar mass is $M = 1.43\ M_{\odot}$,

luminosity $L = 4.68\ L_{\odot}$, and radius $R = 1.58\ R_{\odot}$. While KIC 8462852's age was initially estimated to be hundreds of millions of years, a number of astronomers have argued that it could be much younger – just like EPIC 204278916. Young stars with protoplanetary disks should emit light in the infrared, but observations show no evidence for warm dust, which would exist if a planetary collision debris were at play.

Results obtained by T. S. Boyajian, *et al.* [76] show that the 0.88-day signal is present in most of the Kepler time series, with the strongest presence occurring around day 1200. Interestingly however, around day 400 and day 1400, T. S. Boyajian, *et al.* observed major contributions at different frequencies, corresponding to 0.96 days and 0.90 days, respectively. A prominent hypothesis, based on a lack of observed infrared light, posits a swarm of cold, dusty comet fragments in a highly eccentric orbit. However, the notion that disturbed comets from such a cloud could exist in high enough numbers to obscure 22% of the star's observed luminosity has been doubted [76].

EPIC 204278916 had irregular dimmings of up to 65% for ≈25 consecutive days out of 78.8 days of observations. For the remaining duration of the observations, the variability is highly periodic and attributed to stellar rotation. The star is about five million years old with radius $R = 0.97\ R_{\odot}$ and mass $M \sim 0.5\ M_{\odot}$ [77]. S. Scaringi, *et al.* hypothesize that the irregular dimmings are caused by either a warped inner-disk edge or transiting cometary-like objects in either circular or eccentric orbits. Most of the proposed mechanisms assume nearly edge-on viewing geometries. However, an analysis of the known dippers by M. Ansdell, *et al.* shows that nearly edge-on viewing geometries are not a defining characteristic of the dippers and that additional models should be explored [78], [79].

EPIC 204376071 is a young M star of mass $0.16\ M_{\odot}$ and radius $0.63\ R_{\odot}$ that exhibits only a single 80 percent deep occultation of 1-d duration. The star has frequent flares and a low-amplitude rotational modulation but is otherwise quiet over 160 days of cumulative observation. S. Rappaport, *et al.* give two possible explanations: orbiting dust or small particles (e.g. a disc bound to a smaller orbiting body, or unbound dust that emanates from such a body) or a transient accretion event of dusty material near the corotation radius of the star [80].

WUM: The experimental results above can be explained as follows [8]:

- The average density of the Dippers is 1.5-3 times smaller than the average density of the Sun;
- Consequently, the density of these stars' Nuclei (made of DMF1 or DMF2) is smaller than nuclear density. This relatively low density makes density fluctuations inside of the Nucleus possible;
- An annihilation of DMF1 or DMF2 depends on a concentration of DMPs squared;
- As the result of the huge density fluctuation, some bulk of the Nucleus can arise in which the annihilation process ceases. It will cause a drop of the star luminosity in this area;
- The Nucleus is rotating ($\sim$ 0.88 days in case of KIC 8462852), and consequently the regular dimming events are observed;
- Change in the position of the huge density fluctuation inside of the Nucleus is responsible for the change of the regular dimming event frequency from $\sim$ 0.88 days (around day 1200) to $\sim$ 0.96 and $\sim$ 0.90 days (around day 400 and day 1400) respectively [76];
- Irregular dimming events are the result of random density fluctuations in the bulk of Nucleus.

6.6. Multiworld

In Section 4.3 we introduced Weak interaction with the parameter $G_W = G_O \times Q^{-1/4}$, which is about 30 orders of magnitude greater than G. According to Multiworld proposed in WUM [11], Weak interaction defines a Micro-World and its objects with mass about Planck mass are the building blocks of Macroobjects.

Below we discuss the main characteristics of a Large-World and Small-World in the Multiworld based on the proposed Extremely-Weak and Super-Weak interaction respectively. Large-World is characterized by the parameter $G_{EW} = G_O \times Q^{-3/4}$, which is about 10 orders of magnitude greater than G. The range of the extremely-weak interaction R_{EW} in the present epoch equals to [12]:

$$R_{EW} = a \times Q^{3/4} = 1.44115 \times 10^{16}\ m = 1.5233\ ly$$

According to WUM, Extrasolar Systems (ESS) are Large-Worlds with a boundary between ESS and Intergalactic Medium that has a surface energy density σ_0. This vast, bubble-like region of space, which surrounds Sun, is named Heliosphere. The bubble of the heliosphere is continuously inflated by solar jets, known as the solar wind [81]. The outside radius of the solar heliosphere R_{HS} equals to:

$$R_{HS} = (\frac{3M_\odot c^2}{4\pi\sigma_0})^{1/2} \cong 1.1 \times 10^{15} m \cong 0.12\ ly$$

where $M_\odot$ is the mass of the Sun. The value of 3 above follows from the ratio for all Macroobjects of the World: $1/3$ of the total mass is in the central macroobject and $2/3$ of the total mass is in the structure around it (see Section 7.5). In WUM, ESS have Cores made up of DMPs surrounded by shells composed of DM and baryonic matter. Extremely-weak interaction between DM Cores and all particles around them provide integrity of ESS.

Let's calculate parameters of Large Objects (LOs) made up of self-annihilating DMF1 and DMF2 particles, considering extremely-weak interaction between them. WUM develops the mathematical framework that allows for the calculation of these parameters [7]. According to WUM, the maximum mass of Macroobjects (MOs) M_{MO}^{max} composed of self-annihilating particles DMF1 and DMF2 in the Macro-World can be found by the following equation [7]:

$$M_{MO}^{max} = \frac{\pi}{6}\frac{M_P^3}{m_p^2}$$

where Planck mass M_P squared equals to:

$$M_P^2 = \frac{hc}{2\pi G} = 2m_0^2 \times Q$$

and m_p is proton mass. The minimum radius of these MOs R_{MO}^{min} equals to:

$$R_{MO}^{min} = \frac{M_P m_0}{2m_p^2} a$$

The maximum density of these MOs ρ_{MO}^{max} equals to the nuclear density ρ_{max}:

$$\rho_{max} = (\frac{m_p}{m_0})^4 \rho_0 \qquad 6.6.1$$

In the Large-World, the maximum mass of Large Objects M_{LO}^{max} made up of self-annihilating particles DMF1 and DMF2 equals to:

$$M_{LO}^{max} = \frac{\pi}{6}\frac{M_{EW}^3}{m_p^2} \quad 6.6.2$$

where mass M_{EW} squared equals to:

$$M_{EW}^2 = \frac{hc}{2\pi G_{EW}} = 2m_0^2 \times Q^{3/4} \quad 6.6.3$$

The minimum radius of these LOs R_{LO}^{min} equals to:

$$R_{LO}^{min} = \frac{M_{EW} m_0}{2m_p^2} a \quad 6.6.4$$

with the maximum density ρ_{LO}^{max} equals to the nuclear density (6.6.1).

Considering the constancy of the product of a mass of MO and cube of its radius: $M_{MO} \times R_{MO}^3 = const$ [7] and the minimum density of LO ρ_{min} that is enough for the self-annihilation of DMPs we can estimate the minimum mass M_{LO}^{min} and maximum radius R_{LO}^{max} of LOs:

$$M_{LO}^{min} = (\frac{\rho_{min}}{\rho_{max}})^{1/2} M_{LO}^{max} \quad 6.6.5$$

$$R_{LO}^{max} = (\frac{\rho_{max}}{\rho_{min}})^{1/6} R_{LO}^{min} \quad 6.6.6$$

In our opinion, Fermi Bubbles contain Large Objects built up from self-annihilating particles DMF1 and DMF2 (see Section 6.7).

Small-World is characterized by the parameter $G_{SW} = G_O \times Q^{-1/2}$, which is about 20 orders of magnitude greater than G. The range of the super-weak interaction R_{SW} in the present epoch equals

$$R_{SW} = a \times Q^{1/2} = 1.54351 \times 10^6\ m$$

In WUM, Ball Lightnings are the objects of the Small-Worlds that have cores made up of DMPs surrounded by shells composed of electron-positron plasma. Super-weak interaction between DM cores and all particles around them provide integrity of Ball Lightnings (see Section 7.8).

Parameters of Small Objects made up of self-annihilating particles DMF1 and DMF2 considering super-weak interaction between them can be calculated by the same equations (6.6.1)-(6.6.6) with the replacement of the mass M_{EW} for the mass M_{SW} that equals to:

$$M_{SW}^2 = \frac{hc}{2\pi G_{SW}} = 2m_0^2 \times Q^{1/2} \quad 6.6.7$$

In our view, Fermi Bubbles also contain Small Objects made up of self-annihilating particles DMF1 and DMF2 (see Section 6.7).

6.7. Dark Matter Fermi Bubbles

In November 2010, the discovery of two Fermi Bubbles (FBs) emitting gamma- and X-rays was announced. FBs extend for about 25 thousand light years above and below the center of the galaxy [82]. The outlines of the bubbles are quite sharp, and the bubbles themselves glow in nearly uniform gamma rays over their colossal surfaces. Gamma-ray spectrum measured by the Fermi Large Area Telescope at Galactic latitude $\geq 10^\circ$ has an exponential cutoff at energies $\sim$ 100 GeV. However, the

FBs gamma-ray spectrum at latitude $\leq 10^{\circ}$, without showing any sign of cutoff up to around 1 TeV in the latest tentative results, remains unconstrained [83]. Years after the discovery of FBs, their origin and the nature of the gamma-ray emission remain unresolved.

M. Su and D. P. Finkbeiner identify a gamma-ray cocoon feature in the southern Fermi bubble, a jet-like feature along the cocoon's axis of symmetry, and another directly opposite the Galactic center in the north. Both the cocoon and jet-like feature have a hard spectrum from 1 to 100 GeV. If confirmed, these jets are the first resolved gamma-ray jets ever seen [84].

G. Ponti, *et al.* report prominent X-ray structures on intermediate scales (hundreds of parsecs) above and below the plane, which appear to connect the Galactic Centre region to the Fermi bubbles. They propose that these structures, which they term the Galactic Centre 'chimneys', constitute exhaust channels through which energy and mass, injected by a quasi-continuous train of episodic events at the Galactic Centre, are transported from the central few parsecs to the base of the FBs [85].

D. Hooper and T. R. Slatyer discuss two emission mechanisms in the FBs: inverse Compton scattering and annihilating DM [86]. In their opinion, the second emission mechanism must be responsible for the bulk of the low-energy, low-latitude emission. The spectrum and angular distribution of the signal is consistent with that predicted from ~10 GeV DMPs annihilating to leptons. This component is similar to the excess GeV emission previously reported by D. Hooper from the Galactic Center [87].

It is worth to note that a similar excess of gamma-rays was observed in the central region of the Andromeda galaxy (M31). A. McDaniel, T. Jeltema, and S. Profumo calculated the expected emission across the electromagnetic spectrum in comparison with available observational data from M31 and found that the best fitting models are with the DMP mass 11 GeV [88].

According to H.-Y. Karen Yang, M. Ruszkowski, and E. G. Zweibel, for understanding the physical origin of the FBs, three major questions need to be answered:

- First, what is the emission mechanism? The bubbles can either be hadronic, where the gamma rays are produced by inelastic collisions between cosmic-ray protons and the thermal nuclei via decay of neutral pions, or leptonic, where the gamma rays are generated by inverse-Compton scattering of the interstellar radiation field by cosmic-ray electrons;
- Second, what activity at the Galactic Center triggered the event – are the bubble associated with nuclear star formation or active galactic nucleus activity?
- Third, where are the Cosmic rays accelerated? They could either be accelerated at the Galactic Center and transported to the surface of the bubbles or accelerated in-situ by shocks or turbulence. Note however that not all combinations of the above three considerations would make a successful model because of constraints given by the hard spectrum of the observed bubbles [89].

WUM explains FBs the following way:

- Core of Milky Way galaxy is made up of DM particles: DMF1 (1.3 TeV), DMF2 (9.6 GeV), and DMF3(3.7 keV). The second component (DMF2) explains the excess GeV emission reported by Dan Hooper from the Galactic Center [87]. Core rotates with surface speed at equator close to the escape velocity between Gravitational Bursts (GBs), and over the escape velocity at the moments of GBs;

- Bipolar astrophysical jets (which are astronomical phenomena where outflows of matter are emitted as an extended beams along the axis of rotation [90]) of DMPs are ejected from the rotating Core into the Galactic halo along the rotation axis of the Galaxy;
- Due to self-annihilation of DMF1 and DMF2, these beams are gamma-ray jets [84]. The prominent X-ray structures on intermediate scales (hundreds of parsecs) above and below the plane (named the Galactic Centre 'chimneys' [85]) are the result of the self-annihilation of DMF3;
- FBs are bubbles with boundary between them and Intergalactic Medium that has a surface energy density σ_0 . These bubbles are filled with DM particles: DMF1, DMF2, and DMF3. In our Model, FBs are Macroobjects with a mass M_{FB} and diameter D_{FB} , which are proportional to: $M_{FB} \propto Q^{3/2}$ and $D_{FB} \propto Q^{3/4}$ respectively. According to WUM, diameter of FBs equals to:

$$D_{FB} = L_{DMF3} \times Q^{3/4} = \frac{a}{\alpha^2} \times Q^{3/4} = 28.6\ kly$$

  where L_{DMF3} is Compton length of particles DMF3 with mass $m_{DMF3} = \alpha^2 m_0$. The calculated diameter is in good agreement with the measured size of the FBs 25 kly [82] and 32.6 kly [84]. With Nikola Tesla's principle at heart – *There is no energy in matter other than that received from the environment* – we calculate mass M_{FB} and average density ρ_{FB} :

$$M_{FB} = \frac{\pi D_{FB}^2 \sigma_0}{c^2} = \frac{\pi m_0}{\alpha^4} \times Q^{3/2} \cong 3.6 \times 10^{41} kg$$

$$\rho_{FB} = \frac{6\sigma_0}{D_{FB} c^2} = 6\alpha^2 \rho_0 \times Q^{-3/4} \cong 4.4 \times 10^{-21} kg/m^3 \qquad 6.7.1$$

  Recall that the mass of Milky Way galaxy M_{MW} is about: $M_{MW} \cong 3.2 \times 10^{42} kg$ [11];
- DMF3 (3.7 keV) particles have the smallest mass and hence the largest particle concentration. When the distance between them is less than R_W (4.3), weak interaction will provide the integrity of FBs. Let's compare average density of FBs (6.7.1) with the minimum density of the DMF3 ρ_{DMF3} providing weak interaction:

$$\rho_{DMF3} = \frac{m_{DMF3}}{R_W^3} = \frac{\alpha^2 m_0}{\alpha^3 Q^{3/4}} = \alpha^2 \rho_0 \times Q^{-3/4} \qquad 6.7.2$$

  Comparison of (6.7.1) with (6.7.2) shows that if the density of the DMF3 particles in FBs is larger than $\frac{1}{6}\rho_{FB}$, then the distance between them is less than R_W . It is a reasonable assumption considering that the shell of DMF3 particles in the Core of galaxy is the biggest in size and the largest in mass. As the result:

  - Weak interaction between DMF3 particles provides integrity of Fermi Bubbles;
  - FBs made up of DMF3 particles resembles a honeycomb filled with DMF1 and DMF2;
- FBs radiate X-rays due to the annihilation of DMF3 particles with concentration $n_{DMF3} \geq R_W^{-3}$. Concentrations of DMF1 and DMF2 in FBs are very small: about α^3 and α^4 smaller than n_{DMF3} , respectively. In our view, gamma rays up to 1 TeV [80] are the result of annihilation of DMF1 (1.3 TeV) and DMF2 (9.6 GeV) in Dark Matter Objects (DMOs). DMOs are macroobjects whose density is sufficient for the annihilation of DMPs to occur. On the other hand, DMOs are much smaller than stars in the World, and have a high concentration in FBs to provide nearly uniform gamma ray glow over their colossal surfaces;

- Considering the value of the nuclear density $\rho_{max} = 7.2 \times 10^{17} kg/m^3$ [7] and the minimum density of DMOs $\rho_{min} \cong 10^3 kg/m^3$ [11] we can calculate the parameters of Large Objects (LOs) according to equations (6.6.1)-(6.6.6):

$$M_{LO}^{max} \cong 2.1 \times 10^{15} kg$$

$$M_{LO}^{min} \cong 7.8 \times 10^{7} kg$$

$$R_{LO}^{min} \cong 8.9 \times 10^{-2} m$$

$$R_{LO}^{max} \cong 27\ m$$

- Following equations (6.6.1)-(6.6.7), we can calculate parameters of Small Objects (SOs):

$$M_{SO}^{max} \cong 2.3\ kg$$

$$M_{SO}^{min} \cong 8.5 \times 10^{-8} kg$$

$$R_{SO}^{min} \cong 9.2 \times 10^{-7} m$$

$$R_{SO}^{max} \cong 2.7 \times 10^{-4}\ m$$

It is worth to note that in WUM SOs are macroobjects with mass larger than Planck mass [5].

- The total flux of the gamma radiation from FBs is the sum of the contributions of all individual LOs and SOs. Their abundance: $(10^{26} - 10^{33})$ LOs and $(10^{34} - 10^{41})$ SOs) and uniform distribution explain the nearly uniform gamma ray glow of Fermi Bubbles over their colossal surfaces [80]. The LOs and SOs irradiate gamma quants with different energies and attract new DMF1 and DMF2 from BFs due to super-weak interaction. The Core of the Milky Way supplies FBs with new DMPs through the galactic wind, explaining the brightness of FBs remaining fairly constant during the time of observations. In our opinion, FBs are built continuously throughout the lifetime of Milky Way (13.8 By).

In our view, FBs are DMP clouds containing uniformly distributed clumps of Small Objects and Large Objects, in which DMPs annihilate and radiate X-rays and gamma rays. Dark Matter Fermi Bubbles constitute a principal proof of the World-Universe Model.

7. Solar System

The most widely accepted model of Solar System formation, known as the **Nebular hypothesis**, was first proposed in 1734 by Emanuel Swedenborg [91] and later elaborated and expanded upon by Immanuel Kant in 1755 in his "Universal Natural History and Theory of the Heavens" [92].

Lunar origin fission hypothesis was proposed by George Darwin in 1879 to explain the origin of the Moon by rapidly spinning Earth, on which equatorial gravitative attraction was nearly overcome by centrifugal force [93]. Donald U. Wise made a detailed analysis of this hypothesis in 1966 and concluded that "*it might seem prudent to include some modified form of rotational fission among our working hypothesis*" [94].

Solar fission theory was proposed by Louis Jacot in 1951 [95]. Tom Van Flandern further extended this theory in 1993 [96]. Neither L. Jacot nor T. Van Flandern proposed an origin for the Sun itself. It seems that they followed the standard Nebular hypothesis of formation of the Sun. In WUM we concentrate on furthering the Solar Fission theory [11].

Not one of existing models solves the Angular Momentum problem – why is the orbital momentum of Jupiter larger than rotational momentum of the Sun?

7.1. Angular momentum

Considering rotational and orbital angular momentum of all gravitationally-rounded objects in the Solar system, from Mimas, a small moon of Saturn ($\mathbf{3.75 \times 10^{19} kg}$), to the Sun itself ($\mathbf{2 \times 10^{30} kg}$) [11] , we find that

- The rotational momentum of the Sun is smaller than Jupiter's, Saturn's, Uranus's, and Neptune's orbital momentum;
- The rotational momentum of the Earth is substantially smaller than Moon's orbital momentum.

From the point of view of Fission model, the prime object is transferring some of its rotational momentum to orbital momentum of the satellite. It follows that at the moment of creation **the rotational momentum of the prime object should exceed the orbital momentum of its satellite**.

As we pointed out in Section 5.2, Extrasolar system Cores made up of DMFs can give birth to planetary cores, and they can generate cores of moons through the same Rotational Fission mechanism. Let's analyze this possibility for the Solar System.

The Solar system was born 4.6 billion years ago as the result of a Gravitational burst of Milky Way's Core. At that time, Age parameter $\theta_{9.6}$ equaled about $\cong 2/3$, and the rotational angular momentum of the Core L_{rot}^{MWC} was (see equation (5.2)):

$$L_{rot}^{MWC} = 1.4 \times 10^{63}\ J\ s$$

At that time, the Galactic Core could generate approximately $\sim 10^7$ Extrasolar systems like the Solar system. Considering that Jupiter's orbital momentum is about 60% of the total angular momentum of Solar System L_{tot}^{SS} , we obtain for L_{tot}^{SS} :

$$L_{tot}^{SS} \cong 3.2 \times 10^{43}\ J\ s$$

Let's calculate parameters of the Sun's Core necessary to provide this angular momentum. Substituting mass $M_{\odot} = 2 \times 10^{30}\ kg$ and radius $R_{\odot} = 7 \times 10^{8}\ m$ and using equation (5.2) we obtain

$$L_{rot}^{Sun} = 1.1 \times 10^{44}\ J\ s$$

which is 3.3 times greater than L_{tot}^{SS} . It follows that the Sun's Core can be smaller.

Let's consider the structure of the Sun. According to the standard Solar model it has:

- Nucleus that extends from the center to about 20-25% of the solar radius, contains 34% of the Sun's mass with density $\rho_{max} = 1.5 \times 10^5\ kg/m^3$ and $\rho_{min} = 2 \times 10^4\ kg/m^3$. It produces all Sun's energy;
- Radiative zone from the center to about 70% of the solar radius with density $\rho_{max} = 2 \times 10^4\ kg/m^3$ and $\rho_{min} = 2 \times 10^2\ kg/m^3$ in which convection does not occur and energy transfer occurs by means of radiation;
- Nucleus and Radiative zone contain practically all Sun's mass [97].

In our opinion, the Sun has an Inner Core (Nucleus made up of DMF1) whose radius is 20-25% of the

solar radius, and an Outer Core – the Radiative zone. We then calculate the Solar Core rotational angular momentum L_{rot}^{SC} :

$$L_{rot}^{SC} \cong 8.9 \times 10^{43}\ J\ s$$

which is 2.8 times larger than the overall angular momentum of the Solar System.

Let's follow the same procedure for the Earth – Moon pair. Considering the mass of Earth $M_{\oplus} = 6 \times 10^{24} kg$, radius $R_{\oplus} = 6.4 \times 10^{6} m$, $\theta_{9.6} \cong 2/3,\ \delta = 2.9/13.1$, we calculate

$$L_{rot}^{Earth} = 6.6 \times 10^{34}\ J\ s$$

that is 2.3 times larger than the Moon's orbital momentum $L_{orb}^{Moon} = 2.9 \times 10^{34}$ J s [11].

Let's contemplate the structure of the Earth. According to the standard model, it is composed of:

- An inner core and an outer core that extend from the center to about 45% of the Earth radius with density $\rho_{max} = 1.3 \times 10^{4}\ kg/m^3$and $\rho_{min} = 9.9 \times 10^{3}\ kg/m^3$;
- Lower mantle, spanning from the outer core to about 90% of the Earth radius (below 660 km) with density $\rho_{max} = 5.6 \times 10^{3}\ kg/m^3$ and $\rho_{min} = 4.4 \times 10^{3}\ kg/m^3$.
- Inner core, outer core, and lower mantle contain practically all of the Earth's mass [98].

Very little is known about the lower mantle apart from that it appears to be relatively seismically homogeneous. Outer core-lower mantle boundary has a sharp drop of density $(9.9 \rightarrow 5.6) \times 10^{3}\ kg/m^3$ [98].

In our opinion, lower mantle is a part of the Earth's core. It could be significantly different 4.6 billion years ago, since during this time it was gradually filled with all chemical elements produced by Earth's core due to DMF1 annihilation. Considering the Earth's core with radius $R_{core}^{Earth} = 5.7 \times 10^{6}\ m$ ($\theta_{9.6} \cong 2/3$ and $\delta = 4.4/13.1$), the rotational angular momentum equals to:

$$L_{rot}^{EC} = 6.5 \times 10^{34}\ J\ s$$

which is 2.2 times larger than the orbital momentum of the Moon.

As the conclusion, the overspinning Core of the Sun can give birth to planetary cores, and they can generate cores of moons through the Rotational Fission mechanism [11].

7.2. Dark Matter Cores of Macroobjects

The following facts support the existence of DM Cores in Macroobjects [11]:

- Fossat, *et al.* found that Solar Core rotates 3.8 ± 0.1 faster than the surrounding envelope [99];
- By analyzing the earthquake doublets, Zhang, *et al.* concluded that the Earth's inner core is rotating faster than its surface by about 0.3-0.5 degrees per year [100].

The fact that Macroobject Cores rotate faster than surrounding envelopes, despite high viscosity of the internal medium, is intriguing. WUM explains this phenomenon through absorption of DMPs by Cores. Dark Matter particles supply not only additional mass ($\propto \tau^{3/2}$), but also additional angular momentum ($\propto \tau^{2}$). Cores irradiate products of annihilation, which carry away excessive angular momentum. The Solar wind is the result of this mechanism.

7.3. Gravitationally-Rounded Objects Internal Heat

Earth. The analysis of Sun's heat for planets in Solar system yields the effective temperature of Earth of 255 K [101]. The actual mean surface temperature of Earth is 288 K [102]. The higher actual temperature of Earth is due to energy generated internally by the planet itself. According to the standard model, the Earth's internal heat is produced mostly through radioactive decay. The major heat-producing isotopes within Earth are K-40, U-238, and Th-232. The mean global heat loss from Earth is 44.2 *TW* [103]. The Earth's Uranium has been thought to be produced in one or more supernovae over 6 billion years ago [104].

Radiogenic decay can be estimated from the flux of geoneutrinos that are emitted during radioactive decay. The KamLAND Collaboration combined precise measurements of the geoneutrino flux from the Kamioka Liquid-Scintillator Antineutrino Detector, Japan, with existing measurements from the Borexino detector, Italy. They found that decay of U-238 and Th-232 together contribute about 20 TW to the total heat flux from the Earth to space. The neutrinos emitted from the decay of K-40 contribute 4 TW. Based on the observations the KamLAND Collaboration made a conclusion that *heat from radioactive decay contributes about half of Earth's total heat flux* [105].

Plutonium-244 with half-life of 80 million years is not produced in significant quantities by the nuclear fuel cycle, because it needs very high neutron flux environments. Any Plutonium-244 present in the Earth's crust should have decayed by now. Nevertheless, D. C. Hoffman, *et al.* in 1971 obtained the first indication of Pu-244 present existence in Nature [106].

In our opinion, all chemical products of the Earth including isotopes K-40, U-238, Th-232, and Pu-244, are produced within the Earth as the result of DMF1 annihilation [11]. They arrive in the Crust of the Earth due to convection currents in the mantle carrying heat and isotopes from the interior to the planet's surface [107].

Jupiter radiates more heat than it receives from the Sun [108]. Giant planets like Jupiter are hundreds of degrees warmer than current temperature models predict. Until now, the extremely warm temperatures observed in Jupiter's atmosphere (about 970 degrees C [109]) have been difficult to explain, due to lack of a known heat source [12]. **Saturn** radiates 2.5 times more energy than it receives from the Sun [110]; **Uranus** – 1.1 times [111]; **Neptune** – 2.6 times [112].

S. Kamata, *et al.* report that "*many icy Solar System bodies possess subsurface oceans. To maintain an ocean, **Pluto** needs to retain heat inside*". Kamata, *et al.* show that "*the presence of a thin layer of gas hydrates at the base of the ice shell can explain both the long-term survival of the ocean and the maintenance of shell thickness contrasts. Gas hydrates act as a thermal insulator, preventing the ocean from completely freezing while keeping the ice shell cold and immobile. The most likely guest gas is methane*" [113].

According to WUM, the internal heating of all gravitationally-rounded objects of the Solar system is due to DMPs annihilation in their cores made up of DMF1 (1.3 TeV). The amount of energy produced due to this process is sufficiently high to heat up the objects. New DMF1 freely penetrate through the entire objects' envelope, get absorbed into the cores, and continuously support DMF1 annihilation. Objects' cores are essentially Dark Matter Reactors fueled by DMF1 [11].

In our opinion, all chemical elements are produced by Macroobjects themselves as the result of DMPs

annihilation. The diversity of all gravitationally-rounded objects of the Solar System is explained by the differences in their cores (mass, size, composition). The DM Reactors inside of all gravitationally-rounded objects (including Earth) provide sufficient energy for all geological processes on planets and moons. All gravitationally-rounded objects in hydrostatic equilibrium, down to Mimas in Solar system, prove the validity of WUM [11].

7.4. The evolution of the Sun

By 1950s, stellar astrophysicists had worked out the physical principles governing the structure and evolution of stars [114]. According to these principles, the Sun's luminosity had to change over time, with the young Sun being about 30% less luminous than today. The long-term evolution of the bolometric solar luminosity $L(\tau)$ as a function of cosmological time τ can be approximated by simple linear law: $L(\tau) \propto \tau$ [114]-[118].

One of the consequences of WUM holds that all stars were fainter in the past. As their Cores absorb new DM, size of MO Cores R_{MO} and their luminosity L_{MO} are increasing in time: $R_{MO} \propto \tau^{1/2}$ and $L_{MO} \propto R_{MO}^2 \propto \tau$ respectively. Taking the age of the World $A_W \cong 14.2\ Byr$ and the age of the solar system $A_{SS} \cong 4.6\ Byr$, it is easy to find that the young Sun's output was 67% of what it is today [12]. Literature commonly refers to the value of 70% [117], [118]. This result supports the developed model of the structure and evolution of the Sun [114].

7.5. Pioneer anomaly

According to Fractal Cosmology, Macroobjects are surrounded by transitional regions, in which the density decreases rapidly to the point of the zero level of the fractal structure [119] characterized by radius R_f and density ρ_f, that satisfy the following equation for $r \geq R_f$:

$$\rho(r) = \frac{\rho_f R_f}{r} \qquad 7.5.1$$

According to Yu. Baryshev: *For a structure with fractal dimension D = 2 the constant $\rho_f R_f$ may be actually viewed as a new fundamental physical constant* [119]. In WUM, it is natural to connect this constant with a basic unit of energy density σ_0 [11]:

$$\rho_f R_f = 4\sigma_0/c^2 \qquad 7.5.2$$

Pioneer anomaly is an observed deviation from predicted acceleration of Pioneer 10 and Pioneer 11 spacecrafts, after they passed about 20 astronomical units on their trajectories out of the Solar System. An unexplained force appeared to cause an approximately constant sunward acceleration of $a_P = (8.74 \pm 1.33) \times 10^{-10}$ m/s^2 for both spacecrafts.

Let us calculate deceleration a_P at the distance $r_P \gg R_f$ due to additional mass of the structure $M_{FS} \propto r_P^2$:

$$a_P = \frac{GM_{FS}}{r_P^2} = cH_0 = 6.68 \times 10^{-10}\ m/s^2$$

which is in good agreement with the experimentally measured value (R_0 and H_0 are the values of the World's size R and Hubble's parameter H at the present Epoch). It is important to notice that the calculated deceleration does not depend on r_P and equals to cH_0 for all objects around the Macroobject at the distance $r \gg R_f$. Mass of the structure around Sun M_V at distance to Voyager 1 $R_V \cong 1.8 \times 10^{13}\ m$ [120] is $\sim 0.15\%\ M_{Sun}$ [11].

7.6. Solar Corona

According to the standard model, the visible surface of the Sun, the **photosphere**, is the layer below which the Sun becomes opaque to visible light. Above the photosphere visible sunlight is free to propagate into space, and almost all of its energy escapes the Sun entirely. Above the photosphere lies the **chromosphere** that is about 2500 km thick with temperature that increases gradually with altitude to around $2 \times 10^4 K$ near the top [121]. The particle density decreases rapidly from 10^{22} to $10^{17} m^{-3}$. Above the chromosphere, in a thin (about 200 km) **transition region**, the temperature rises rapidly from around $2 \times 10^4 K$ in the upper chromosphere to coronal temperatures closer to $10^6 K$. The particle density decreases from 10^{17} up to $10^{16}-10^{15}\ m^{-3}$ in the low corona. In our opinion, this is a zero level of the fractal structure. The calculated density according to equation (7.5.2) is:

$$\rho_f \cong 2.3 \times 10^{-9}\ kg/m^3 \qquad 7.6.1$$

Corona is an aura of plasma that surrounds the Sun and other stars. The Sun's corona extends at least 8 million kilometers into outer space [122] and is most easily seen during a total solar eclipse. Spectroscopy measurements indicate strong ionization and plasma temperature in excess of $10^6 K$ [123]. The corona emits radiation mainly in the X-rays, observable only from space. The plasma is transparent to its own radiation and to solar radiation passing through it, therefore we say that it is optically-thin. The gas, in fact, is very rarefied, and the photon mean free-path by far overcomes all other length-scales, including the typical sizes of the coronal features.

J. T. Schmelz made the following comment on the composition of Solar corona: *Along with temperature and density, the elemental abundance is a basic parameter required by astronomers to understand and model any physical system. The abundances of the solar corona are known to differ from those of the solar photosphere* [124].

Coronal heating problem in solar physics relates to the question of why the temperature of the Solar corona is millions of degrees higher than that of the photosphere. The high temperatures require energy to be carried from the solar interior to the corona by non-thermal processes.

In our opinion, the origin of the Solar corona plasma is not the coronal heating. Plasma particles (electrons, protons, multicharged ions) are so far apart that plasma temperature in the usual sense is not very meaningful. The plasma is the result of annihilation of DMF1 (1.3 TeV), DMF2 (9.6 GeV), and DMF3 (3.7 keV) particles. The Solar corona made up of DMPs resembles a honeycomb filled with plasma [11].

The following experimental results speak in favor of this model [11]:

- The corona emits radiation mainly in the X-rays due to the annihilation of DMF3;
- The plasma is transparent to its own radiation and to the radiation coming from below;
- The elemental composition of the Solar corona and the Solar photosphere are known to differ;
- During the impulsive stage of Solar flares, radio waves, hard x-rays, and gamma rays with energy above 100 GeV are emitted [125]. In our view, it is the result of enormous density fluctuations of DMF1 and DMF2 in the Solar corona and their annihilation;
- Assuming the particle density in the low corona $10^{15}\ m^{-3}$ and mass of DMF1: $m_{DMF1} =$

$2.3 \times 10^{-24}\ kg$ we can find mass density $\rho_{DMF1}^{in} = 2.3 \times 10^{-9}\ kg/m^3$ that is equal to the density of the fractal structure (7.6.1);

- A distance between DMF1 is about $10^{-5}\ m$ that is much smaller than the range of the weak interaction of DMPs R_W (4.3);
- At the same density of the fractal structure, distance between DMF2 with mass $m_{DMF2} = 1.7 \times 10^{-26}\ kg$ is about $10^{-6}\ m$, and DMF3 with mass $m_{DMF3} = 6.7 \times 10^{-33}\ kg$ is about $10^{-8}\ m$. The smallest distance between DMF3 particles explains the fact that corona emits radiation mainly in the X-rays;
- The Solar corona is a stable Shell around the Sun with density decreasing according to equation (7.5.1) with inner radius $R_{in} \cong 7 \times 10^8\ m$, and outer radius R_{out}: $R_{out} = 4\alpha^2 a \times Q^{3/4} \cong 3 \times 10^{12}\ m$;
- The total mass of the Solar Corona M_{SC}: $M_{SC} = \frac{8\pi\sigma_0}{c^2} R_{out}^2 \cong 9 \times 10^{25}\ kg$.

7.7. Geocorona and Planetary Coronas

The geocorona is the luminous part of the outermost region of the Earth's atmosphere that extends to at least 640,000 km from the Earth [126]. It is seen primarily via far-ultraviolet light (Lyman-alpha) from the Sun that is scattered by neutral hydrogen.

Far-ultraviolet photons in the Geocorona have been observed out to a distance of approximately 100,000 km from the Earth [127]. The first high-quality and wide-field-of-view image of Earth's corona of 243,000 km was obtained by Hisaki, the first interplanetary microspacecraft [128]. Hisaki with its extreme ultraviolet spectrometer EXCEED acquires spectral images (52-148 nm) of the atmospheres of planets from Earth orbit and has provided quasi-continuous remote sensing observations of the geocorona since 2013 [129]. The most popular explanation of this geocoronal emission is the scattering of Solar Far-Ultraviolet (FUV) photons by exospheric hydrogen.

X-rays from Earth's geocorona were first detected by Chandra X-ray Observatory in 1999 [130]. X-rays were observed in the range of energies $0.08 - 10\ keV$ [129]. The main mechanism explaining the geocoronal X-rays is that they are caused by collisions between neutral atoms in the geocorona with carbon, oxygen and nitrogen ions that are streaming away from the Sun in the solar wind [130], [131], [132]. This process is called "charge exchange", since an electron is exchanged between neutral atoms in geocorona and ions in the solar wind.

X-rays from Planets were also observed by Chandra [130]. According to NASA:

- The X-rays from Venus and, to some extent, the Earth, are due to the fluorescence of solar X-rays striking the atmosphere;
- Fluorescent X-rays from oxygen atoms in the Martian atmosphere probe heights similar to those on Venus. A huge Martian dust storm was in progress when the Chandra observations were made. The intensity of the X-rays did not change during the dust storm;
- Jupiter has an environment capable of producing X-rays in a different manner because of its substantial magnetic field. X-rays are produced when high-energy particles from the Sun get trapped in its magnetic field and accelerated toward the polar regions where they collide with atoms in Jupiter's atmosphere;
- Like Jupiter, Saturn has a strong magnetic field, so it was expected that Saturn would also

show a concentration of X-rays toward the poles. However, Chandra's observation revealed instead an increased X-ray brightness in the equatorial region. Furthermore, Saturn's X-ray spectrum was found to be similar to that of X-rays from the Sun.

V. I. Shematovich and D. V. Bisikalo gave the following explanation of the planetary coronas [133]: *The measurements reveal that planetary coronas contain both a fraction of thermal neutral particles with a mean kinetic energy corresponding to the exospheric temperature and a fraction of hot neutral particles with mean kinetic energy much higher than the exospheric temperature. These suprathermal (hot) atoms and molecules are a direct manifestation of the non-thermal processes taking place in the atmospheres.*

In our opinion, the Planetary Coronas are similar to the Solar Corona [11]:

- At the distance of 640,000 km from the Earth [126], atoms and molecules are so far apart that they can travel hundreds of kilometers without colliding with one another. Thus, the exosphere no longer behaves like a gas, and the particles constantly escape into space. In our view, FUV radiation and X-rays are the consequence of DMF3 annihilation;
- All planets and some observed moons (Europa, Io, Io Plasma Torus, Titan) have X-rays in upper atmosphere of the planets, similar to the Solar Corona;
- The calculated density of the Earth's fractal structure $\rho_f \cong 2.5 \times 10^{-7}\ kg/m^3$ is in good agreement with experimental results for atmosphere density at 100 km altitude [12];
- The Geocorona is a stable Shell around the Earth with inner radius $R_{in} \cong 6.5 \times 10^6\ m$ and observed outer radius $R_{out} \cong 6.4 \times 10^8\ m$. The total mass of this Shell $\cong 4.1 \times 10^{18}\ kg$;
- Suprathermal atoms and molecules proposed by V. I. Shematovich and D. V. Bisikalo are the result of DMPs annihilation in Geocorona, similar to that of Solar corona.

7.8. High-Energy Atmospheric Physics. Ball Lightning

Lightning initiation problem. Years of balloon, aircraft, and rocket observations have never found large enough electric fields inside thunderstorms to make a spark. And yet lightnings strike the Earth about 4 million times per day. This has led to the cosmic-ray model of lightning initiation [134], [135].
Terrestrial Gamma-Ray Flashes (TGFs) were first detected by chance by NASA's Earth-orbiting Compton gamma ray telescope. Compton was searching for GRBs from exploding stars, when it unexpectedly began detecting very strong bursts of high energy x-rays and gamma rays, coming from Earth [130].

There are two leading models of TGF formation: Lightning leader emission and Dark Lightning [134], but they still don't account for

- A bright TGF observed by a spacecraft in the middle of Sahara Desert on a nice day. The nearest thunderstorms were ~ 1000 miles away [136];
- An ultraviolet telescope installed on the Russian satellite Lomonosov has registered several powerful explosions of light in the Earth's atmosphere at an altitude of several dozen kilometers in clear weather [137].

Additionally, in frames of existing models it is difficult to explain the following results [12]:

- Unusual surges of radiation at 511 keV when there were no thunderstorms;
- Beams of antimatter (positrons) produced above thunderstorms on Earth;

- A gamma-ray flash coming down from the overhead thundercloud;
- Some lightnings produce X-rays and others do not;
- Explosive production of energetic particles observed from space;
- The spectra of TGFs at very high energies (40–100 MeV).

According to WUM, the characteristics of Geocorona are similar to the characteristics of the Solar Corona (see Section 7.6). As the result of a large fluctuation of DMPs in Geocorona and their annihilation, X-rays and gamma-rays are going not only up and out of the Earth, but also down to the Earth's surface. In our view, TGFs are, in fact, well-known GRBs [7]. The spectra of TGFs at very high energies can be explained by DMF1 and DMF2 annihilation. Lightning initiation problem can be solved by X-rays and gamma-rays, which slam into the thunderclouds and carve a conductive path through a thunderstorm. From this point of view, it is easy to explain all experimental results summarized above.

Short History of Ball Lightning Hypothesis. Ball lightning (BL) is an unexplained atmospheric phenomenon that is usually associated with thunderstorms and lasts considerably longer than the split-second flash of a lightning bolt. BL usually appears during thunderstorms, sometimes within a few seconds of lightning, but sometimes without apparent connection to a lightning bolt. Different hypothesis were proposed to explain BL, but no one explanation is widely accepted at present:

- Vacuum hypothesis by Nikola Tesla [138], [139];
- Microwave cavity hypothesis by Peter Kapitsa [140];
- Maser-Soliton hypothesis by Peter H. Handel [141];
- Antimatter hypothesis by David Ashby and Colin Whitehead [142];
- Black hole hypothesis by Mario Rabinowitz [143];
- Extreme Ball Lightning hypothesis by Van Devender [144], [145];
- Microwave Bubble hypothesis by H.-C. Wu [146].

According to A. G. Oreshko, "*P. L. Kapitsa supposed that a ball lightning is a window in another world*" [147]. In WUM, it was suggested that BL is an object of the Small-World [12].

Observation of the Optical and Spectral Characteristics of BL was conducted by Jianyong Cen, *et al.* in 2012 [148]. At a distance of 900 m a total of 1.64 seconds of digital video of the BL and its spectrum was obtained, from the formation of the BL after the ordinary lightning struck the ground, up to the optical decay of the phenomenon. The BL traveled horizontally across the video frame at an average speed of 8.6 m/s . It had a diameter of 5 m.

Ball Lightning Formation. The clue of our model comes from the observed ability of BLs to penetrate solid materials. It means that the core of BL should be composed of DMPs. In WUM, they are DMF1 and DMF2. Small Objects made up of self-annihilating particles DMF1 or DMF2 can form cores of BLs in Small-Worlds characterized by super-weak interaction (see Section 6.6).

Following Tesla vacuum hypothesis [138], [139], we suppose that when sudden and very powerful TGF passes through the air and strike the surface of the Earth, "*the tremendous expansion of some portions of the air and subsequent rapid cooling and condensation gives rise to the creation of partial vacua in the places of greatest development of heat. These vacuous spaces, owing to the properties*

of the gas, are most likely to assume the shape of hollow spheres when, upon cooling, the air from all around rushes in to fill the cavity created by the explosive dilatation and subsequent contraction".

In our Model, the places of greatest development of heat are the spots on the Earth's surface struck by TGFs. As the result, the ablation of the soil takes place and vaporized chemical elements of soil and air can be absorbed by BLs and observed experimentally [148].

Very powerful gamma quants with energy of at least 1.02 MeV in the vicinity of atomic nuclei of the ground can produce electron-positron pairs with high concentration. This electron-positron plasma composes a shell around DM core of BL made up of DMF1 or DMF2 and provides their affinity for metal objects such as wires [148].

The most important part of the BL formation is a DM core. The calculated density of the Geocorona composed of DMF1 ρ_{DMF1} near the surface of the Earth is [12]:

$$\rho_{DMF1} \cong 2.5 \times 10^{-7}\ kg/m^3$$

When powerful TGF strikes the surface of the Earth, the explosive dilatation of some portion of Geocorona gives rise to the creation of hollow sphere with partial vacua and all DMPs outside of the sphere. The subsequent rapid contraction induces DMPs rush in to fill the cavity. As the result, at the center of the sphere arises microobject with density high enough for the beginning of the DMPs annihilation. The described microobject attracts new DMPs from Geocorona due to super-weak interaction and grows up to the macroobject with a mass about $\sim 10^{-6} kg$ that will start attracting electron-positron pairs produced by TGF [12].

According to WUM, mass of BL's core can grow up to 2.3 kg, and the radius of plasma shell can reach a few meters [12]. Mass of a small BL is mostly concentrated in its DM core. A small BL can thus easily penetrate through walls, glass and metal, generally without leaving a hole. Practically all mass of large BLs is in the plasma. The BL with diameter 5 m observed by J. Cen, *et al.* [148] had the mass of about 83 kg [12].
As the conclusion:

- BL has a core made up of DMF1 or DMF2 surrounded by the electron-positron plasma contaminated by chemical elements of soil and air as the result of TGF strike of the ground;
- Super-weak interaction between DM core and all particles around it provides integrity of BL;
- The core of BL irradiates quants with different energies and attracts new DMPs from Geocorona due to super-weak interaction. It explains the observed result that the brightness of BL remains fairly constant during its lifetime.

It is important to emphasize that the initial energy required for a BL creation is insufficient for its sustenance of up to 1200 seconds. Additional energy, therefore, must be consumed by a BL once it had been formed. Once we master the creation of BLs in a controlled environment, we can concentrate our efforts on harvesting that energy. World – Universe Model can serve as a basis for High-Energy Atmospheric Physics.

8. Conclusion

Dark Matter is abundant:

- 2.4 % of Luminous Matter is in Superclusters, Galaxies, Stars, Planets, etc.

- 4.8 % of Luminous Matter is in the Medium of the World;
- The remaining 92.8 % of mass is Dark Matter.

Dark Matter is omnipresent:

- Cores of all Macroobjects;
- Coronas of all Macroobjects of the World;
- Fermi Bubbles;
- The Medium of the World;
- Dark Matter Reactors in Cores of all gravitationally-rounded Macroobjects.

Based on the totality of the results obtained by WUM, we suggest adopting existence of Dark Matter in the World from the Classical Physics point of view. While WUM needs significant further elaboration, it can already serve as a basis for a New Physics proposed by Paul Dirac in 1937.

Acknowledgements

I am a Doctor of Sciences in Physics. I belong to the school of physicists established by Alexander Prokhorov – Nobel Prize Laureate in Physics. I am an author of more than 150 published papers, mostly in the area of Laser Physics. I am eternally grateful to Prof. A. M. Prokhorov and Prof. A. A. Manenkov, whose influence on my scientific life has been decisive.

For 17 years I have developed a model I dubbed the World-Universe Model and published a serious of papers in the Journal of High Energy Physics, Gravitation and Cosmology (JHEPGC). I am much obliged to Prof. C. Corda for publishing my manuscripts in JHEPGC.

Many thanks to my long-term friend Felix Lev for stimulating discussions of history and philosophy of Physics and important comments on the Model. Special thanks to my son Ilya Netchitailo who questioned every aspect of the Model, gave valuable suggestions and helped shape it to its present form.

References

[1] Netchitailo, V. (2015) 5D World-Universe Model Space-Time-Energy. *Journal of High Energy Physics, Gravitation and Cosmology*, **1**, 25-34. doi: 10.4236/jhepgc.2015.11003.

[2] Netchitailo, V. (2015) 5D World-Universe Model. Multicomponent Dark Matter. *Journal of High Energy Physics, Gravitation and Cosmology*, **1**, 55-71. doi: 10.4236/jhepgc.2015.12006.

[3] Netchitailo, V. (2016) 5D World-Universe Model. Neutrinos. The World. *Journal of High Energy Physics, Gravitation and Cosmology*, **2**, 1-18. doi: 10.4236/jhepgc.2016.21001.

[4] Netchitailo, V. (2016) 5D World-Universe Model. Gravitation. *Journal of High Energy Physics, Gravitation and Cosmology*, **2**, 328-343. doi: 10.4236/jhepgc.2016.23031.

[5] Netchitailo, V. (2016) Overview of Hypersphere World-Universe Model. *Journal of High Energy Physics, Gravitation and Cosmology*, **2**, 593-632. doi: 10.4236/jhepgc.2016.24052.

[6] Netchitailo, V. (2017) Burst Astrophysics. *Journal of High Energy Physics, Gravitation and Cosmology*, **3**, 157-166. doi: 10.4236/jhepgc.2017.32016.

[7] Netchitailo, V. (2017) Mathematical Overview of Hypersphere World-Universe Model. *Journal of High Energy Physics, Gravitation and Cosmology*, **3**, 415-437. doi: 10.4236/jhepgc.2017.33033.

[8] Netchitailo, V. (2017) Astrophysics: Macroobject Shell Model. *Journal of High Energy Physics, Gravitation and Cosmology*, **3**, 776-790. doi: 10.4236/jhepgc.2017.34057.

[9] Netchitailo, V. (2018) Analysis of Maxwell's Equations. Cosmic Magnetism. *Journal of High Energy Physics, Gravitation and Cosmology*, **4**, 1-7. doi: 10.4236/jhepgc.2018.41001.
[10] Netchitailo, V. (2018) Hypersphere World-Universe Model. Tribute to Classical Physics. *Journal of High Energy Physics, Gravitation and Cosmology*, **4**, 441-470. doi: 10.4236/jhepgc.2018.43024.
[11] Netchitailo, V. (2019) Solar System. Angular Momentum. New Physics. *Journal of High Energy Physics, Gravitation and Cosmology*, **5**, 112-139. doi: 10.4236/jhepgc.2019.51005.
[12] Netchitailo, V. (2019) High-Energy Atmospheric Physics: Ball Lightning. *Journal of High Energy Physics, Gravitation and Cosmology*, **5**, 360-374. doi: 10.4236/jhepgc.2019.52020.
[13] Riemann, B. (1854) On the Hypotheses which lie at the Bases of Geometry. Translated by William Kingdon Clifford .Nature, Vol. VIII. Nos. 183, 184, pp. 14–17, 36, 37.
[14] Heaviside, O. (1893) A gravitational and electromagnetic analogy. The Electrician, **31**, 81.
[15] Tesla, N. (1937) Prepared Statement on the 81st Birthday Observance. http://www.institutotesla.org/tech/TeslaGravity.html .
[16] Dirac, P.M. (1951). "Is there an Aether?" Nature, **168**, 906. Bibcode:1951Natur.168..906D. doi:10.1038/168906a0.
[17] Dirac, P.A.M. (1937) Nature, **139**, 323.
[18] Hoyle, F. and Narlikar, J.V. (1964) A New Theory of Gravitation. Proc. R. Soc. Lond., **A282**, 178.
[19] Dirac, P.A.M. (1974) Cosmological Models and the Large Numbers Hypothesis. Proc. R. Soc. Lond. **A338**, 439.
[20] McCullagh, J. (1846) An Essay towards a Dynamical Theory of Crystalline Reflexion and Refraction. Transactions of the Royal Irish Academy, **21**, 17.
[21] Burbidge, E.M., Burbidge, G.R., Fowler, W.A. and Hoyle, F. (1957) Synthesis of the Elements in Stars. Reviews of Modern Physics, **29**, 547.
[22] Kohlrausch, R. and Weber, W. (1857) Elektrodynamische Maaßbestimmungen : insbesondere Zurückführung der Stromintensitäts-Messungen auf mechanisches Maass. On the Amount of Electricity which Flows through the Cross-Section of the Circuit in Galvanic Currents (Translated by Susan P. Johnson and edited by Laurence Hecht). http://ppp.unipv.it/Collana/Pages/Libri/Saggi/Volta%20and%20the%20History%20of%20Electricity/V%26H%20Sect3/V%26H%20287-297.pdf.
[23] Heüman, G.D. (1888) The Rydberg formula as presented to Matematiskt-Fysiska förening. https://commons.wikimedia.org/wiki/File:Rydbergformula.jpg .
[24] Thomson, J.J. (1897) Cathode Rays. Philosophical Magazine, **44**, 293. http://web.lemoyne.edu/~giunta/thomson1897.html .
[25] Plank, M. (1901) On the Law of Distribution of Energy in the Normal Spectrum. Annalen der Physik, **4**, 553. https://web.archive.org/web/20081217042934/http://dbhs.wvusd.k12.ca.us/webdocs/Chem-History/Planck-1901/Planck-1901.html .
[26] Bennett, C.L., *et al.* (2013) Nine-Year Wilkinson Microwave Anisotropy Probe (WMAP) Observations: Final Maps and Results. arXiv:1212.5225.
[27] Zuckerman, B. and Malkan, M.A. (1996) The Origin and Evolution of the Universe. Jones and Bartlet Publishers.https://books.google.com/books?id=G0iR4jpWKN4C&pg=PA4&lpg=PA4&dq=%22critical+density+universe%22+%22escape+velocity%22&source=bl&ots=ym46gfQUpI&sig=ACfU3U0-2_bRxgpJURIP0Kj44xTq7JHK7w&hl=en&sa=X&ved=2ahUKEwiO-aK4lZXhAhUDHDQIHW7_BmYQ6AEwBHoECAkQAQ#v=onepage&q=%22critical%20density%20universe%22%20%22escape%20velocity%22&f=false
[28] Mirizzi, A., Raffelt, G.G. and Serpico, P.D. (2006) Photon-Axion Conversion in Intergalactic Magnetic Fields and Cosmological Consequences. arXiv:0607415.
[29] Keane, E.F., *et al.* (2016) A Fast Radio Burst Host Galaxy. https://doi.org/10.1038/nature17140
[30] Fixsen, D.J. (2009) The Temperature of the Cosmic Microwave Background. arXiv: astro-ph/ 0911.1955.

[31] Bonetti, L., *et al.* (2017) FRB 121102 Casts New Light on the Photon Mass. arXiv:1701.03097.
[32] Sanchez, M. (2003) Oscillation Analysis of Atmospheric Neutrinos in Soudan 2. PhD Thesis, Tufts University. http://nu.physics.iastate.edu/Site/Bio_files/thesis.pdf.
[33] Kaus, P. and Meshkov, S. (2003) Neutrino Mass Matrix and Hierarchy. AIP Conf. Proc., **672**, 117.
[34] Battye, R.A. and Moss, A. (2014) Evidence for Massive Neutrinos from CMB and Lensing Observations. arXiv: 1308.5870.
[35] Maurette, M., Cragin, J. and Taylor, S. (1992) Cosmic Dust in ~50 KG Blocks of Blue Ice from Cap-Prudhomme and Queen Alexandra Range, Antarctica. Meteoritics, **27**, 257.
[36] Saxton, J.M., Knotts, S.F., Turner, G. and Maurette, M. (1992) 40Ar/39Ar Studies of Antarctic Micrometeorites. Meteoritics, **27**, 285.
[37] Jackson, A.A. and Zook, H.A. (1991) Dust Particles from Comets and Asteroids: Parent-Daughter Relationships. Abstracts of the Lunar and Planetary Science Conference, **22**, 629.
[38] Lagache, G., *et al.* (1999) First detection of the Warm Ionized Medium Dust Emission. Implication for the Cosmic Far-Infrared Background. arXiv: 9901059.
[39] Finkbeiner, D.P., Davis, M. and Schlegel, D.J. (2000) Detection of a Far IR Excess with DIRBE at 60 and 100 Microns. arXiv: 0004175.
[40] Siegel, P.H. (2002) Terahertz Technology. IEEE Transactions on Microwave Theory and Techniques, **50**, No. 3, 910.
[41] Phillips, T.G. and Keene, J. (1992) Submillimeter Astronomy [Heterodyne Spectroscopy]. Proc. IEEE, **80**, 1662.
[42] Dupac, X., *et al.* (2003) The Complete Submillimeter Spectrum of NGC 891. arXiv: 0305230.
[43] Aguirre, J.E., *et al.* (2003) The Spectrum of Integrated Millimeter Flux of the Magellanic Clouds and 30-Doradus from TopHat and DIRBE Data. arXiv: 0306425.
[44] Pope, A., *et al.* (2006) Using Spitzer to Probe the Nature of Submillimetre Galaxies in GOODS-N. arXiv: 0603409.
[45] Marshall, J.A., *et al.* (2007) Decomposing Dusty Galaxies. I. Multi-Component Spectral Energy Distribution Fitting. arXiv: 0707.2962.
[46] Devlin, M.J., *et al.* (2009) Over Half of the Far-Infrared Background Light Comes from Galaxies at z >= 1.2. arXiv: 0904.1201.
[47] Chapin, E.L., *et al.* (2010) A Joint Analysis of BLAST 250--500um and LABOCA 870um Observations in the Extended Chandra Deep Field South. arXiv: 1003.2647.
[48] Mackenzie, T., *et al.* (2010) A Pilot Study for the SCUBA-2 'All-Sky' Survey. arXiv: 1012.1655.
[49] Serra, P., *et al.* (2014) Cross-Correlation of Cosmic Infrared Background Anisotropies with Large Scale Structures. arXiv: 1404.1933.
[50] Lee, B.W. and Weinberg, S. (1977) Cosmological lower bound on heavy-neutrino masses. Phys. Rev. Lett. **39**, 165.
[51] Dicus, D.A., Kolb, E.W., and Teplitz, V.L. (1977) Cosmological upper bound on heavy-neutrino lifetimes. Phys. Rev. Lett. **39**, 168.
[52] Dicus, D.A., Kolb, E.W., and Teplitz, V.L. (1978) Cosmological implications of massive, unstable neutrinos. Astrophys. J. **221**, 327.
[53] Gunn, J.E., *et al.* (1978) Some astrophysical consequences of the existence of a heavy stable neutral lepton. Astrophys. J. **223**, 1015.
[54] Stecker, F.W. (1978) The cosmic gamma-ray background from the annihilation of primordial stable neutral heavy leptons. Astrophys. J. **223**, 1032.
[55] Zeldovich, Ya.B., Klypin, A.A., Khlopov, M.Yu., and Chechetkin, V.M. (1980) Astrophysical constraints on the mass of heavy stable neutral leptons. Sov. J. Nucl. Phys. **31**, 664.
[56] Spolyar, D., Freese, K., Gondolo, P. (2007) Dark matter and the first stars: a new phase of stellar evolution. arXiv:0705.0521.

[57] Freese, K., Rindler-Daller, T., Spolyar, D., and Valluri, M. (2015) Dark Stars: A Review. arXiv:1501.02394.
[58] Corda, C. (2009) Interferometric detection of gravitational waves: the definitive test for General Relativity. Int. J. Mod. Phys. **18**, 2275.
[59] Boehm, C., Fayet, P., and Silk, J. (2003) Light and Heavy Dark Matter Particles. arXiv:0311143.
[60] Mehrgan, K., *et al.* (2019) A 40-billion solar mass black hole in the extreme core of Holm 15A, the central galaxy of Abell 85. arXiv:1907.10608.
[61] NASA (2015) The Cosmic Distance Scale. https://imagine.gsfc.nasa.gov/features/cosmic/local_supercluster_info.html.
[62] Tully, R.B. (1982) The Local Supercluster. Astrophysical Journal, **257**, 389. Bibcode:1982ApJ...257..389T. doi:10.1086/159999.
[63] Heymans, C., *et al.* (2008) The dark matter environment of the Abell 901/902 supercluster: a weak lensing analysis of the HST STAGES survey. arXiv:0801.1156.
[64] Zwicky, F. (1933) Die Rotverschiebung von extragalaktischen Nebeln. Helvetica Physica Acta, **6**, 110.
[65] Ness, M., *et al.* (2015) The Cannon: A data-driven approach to Stellar Label Determination. The Astrophysical Journal, **808**, 1. doi:10.1088/0004-637X/808/1/16.
[66] Bond, H. E., *et al.* (2013) HD 140283: A Star in the Solar Neighborhood that Formed Shortly After the Big Bang. arXiv:1302.3180.
[67] Marchetti, T., Rossi, E.M., Brown. A.G.A. (2018) Gaia DR2 in 6D: Searching for the fastest stars in the Galaxy. *Monthly Notices of the Royal Astronomical Society*, sty2592,https://doi.org/10.1093/mnras/sty2592.
[68] Koposov, S. E., *et al.* (2019) The Great Escape: Discovery of a nearby 1700 km/s star ejected from the Milky Way by Sgr A*. arXiv:1907.11725.
[69] Clarke, C.J., *et al.* (2018) High-resolution Millimeter Imaging of the CI Tau Protoplanetary Disk: A Massive Ensemble of Protoplanets from 0.1 to 100 au. The Astrophysical Journal Letters, **866**, L6.
[70] Wright, E.L. (2001) Cosmic InfraRed Background Radiation. http://www.astro.ucla.edu/~wright/CIBR/.
[71] Ansoldi, S., *et al.* (2015) Teraelectronvolt pulsed emission from the Crab pulsar detected by MAGIC. arXiv:1510.07048.
[72] Chen, G., *et al.* (2015) NuSTAR observations of the young, energetic radio pulsar PSR B1509-58. arXiv:1507.08977.
[73] Johnston, S., *et al.* (1993) Discovery of a very bright, nearby binary millisecond pulsar. Nature **361**, 613.
[74] Bailes, M., *et al.* (1994) Discovery of three binary millisecond pulsars. The Astrophysical Journal, **425**, L41.
[75] Pletsch, H.J., *et al.* (2012) Binary Millisecond Pulsar Discovery via Gamma-Ray Pulsations. arXiv:1211.1385.
[76] Boyajian, T.S., *et al.* (2015) Planet Hunters X. KIC 8462852-Where's the Flux? arXiv:1509.03622.
[77] Scaringi, S., *et al.* (2016) The peculiar dipping events in the disk-bearing young-stellar object EPIC 204278916. arXiv:1608.07291.
[78] Ansdell, M., *et al.* (2015) Young "Dipper" Stars in Upper Sco and ρ Oph Observed by K2. arXiv:1510.08853.
[79] Ansdell, M., *et al.* (2016) Dipper disks not inclined towards edge-on orbits. arXiv:1607.03115.
[80] Rappaport, S., *et al.* (2019) Deep long asymmetric occultation in EPIC 204376071. Monthly Notices of the Royal Astronomical Society, **485**, 2681. https://doi.org/10.1093/mnras/stz537 .
[81] Opher, M., *et al.* (2015) Magnetized jets driven by the sun: the structure of the heliosphere revisited. arXiv:1412.7687v2.
[82] Aguilar, D.A. and Pulliam, C. (2010) Astronomers Find Giant, Previously Unseen Structure in our Galaxy. Harvard-Smithsonian Center for Astrophysics. Release No. 2010-22.
[83] Yang, L. and Razzaque, S. (2019) Constraints on very high energy gamma-ray emission from the Fermi Bubbles with future ground-based experiments. arXiv:1811.10970v1.
[84] Su, M. and Finkbeiner, D.P. (2012) Evidence for Gamma-Ray Jets in the Milky Way. arXiv:1205.5852.
[85] Ponti, G., *et al.* (2019) An X-ray chimney extending hundreds of parsecs above and below the Galactic Centre. Nature **567**, 347–350.

[86] Hooper, D. and Slatyer, T.R. (2013) Two Emission Mechanisms in the Fermi Bubbles: A Possible Signal of Annihilating Dark Matter. arXiv:1302.6589.
[87] Hooper, D. and Goodenough, L. (2011) Dark matter annihilation in the Galactic Center as seen by the Fermi Gamma Ray Space Telescope. Physics Letters B, **697**, 412. doi:10.1016/j.physletb.2011.02.029.
[88] McDaniel, A., Jeltema, T. and Profumo, S. (2018) A Multi-Wavelength Analysis of Annihilating Dark Matter as the Origin of the Gamma-Ray Emission from M31. arXiv:1802.05258.
[89] Yang, H.Y.K., Ruszkowski, M. and Zweibel, E.G. (2018) Unveiling the Origin of the Fermi Bubbles. arxiv1802.03890.
[90] Beall, J.H. (2015) A Review of Astrophysical Jets. Proceedings of Science: 58. Bibcode: 2015mbhe.confE..58B . Retrieved 19 February 2017.
[91] Swedenborg, E. (1734) Latin: Opera Philosophica et Mineralia (English: Philosophical and Mineralogical Works). Principia, 1. https://www.milestone-books.de/pages/books/002966/emanuel-swedenborg/opera-philosophica-et-mineralia-volumes-i-iii-all-published.
[92] Brush, S.G. (2014) A History of Modern Planetary Physics: Nebulous Earth. p. 7. ISBN 0521441714.
[93] Darwin, G.H. (1879) On the Bodily Tides of Viscous and Semi-Elastic Spheroids, and on the Ocean Tides upon a Yielding Nucleus. Phil. Trans. Roy. Soc., **170**, 1.
[94] Wise, D.U. (1966) Origin of the Moon by Fission. http://adsabs.harvard.edu/full/1966ems..conf..213W .
[95] Jacot, L. (1986) Heretical Cosmology (transl. of Science et bon sense, 1981). Exposition-Banner.
[96] Van Flandern, T. (1999) Dark Matter, Missing Planets, and New Comets. North Atlantic.
[97] Djorgovski, S.G. (2016) Stellar Structure and the Sun.
http://www.astro.caltech.edu/~george/ay1/lec_pdf/Ay1_Lec08.pdf.
[98] Dziewonski, A.M., Anderson, D.L. (1981) Preliminary Reference Earth Model. Physics of the Earth and Planetary Interiors, **25**, 297. Bibcode:1981PEPI...25..297D. doi:10.1016/0031-9201(81)90046-7. ISSN 0031-9201.
[99] Fossat, E., *et al.* (2017) Asymptotic g modes: Evidence for a rapid rotation of the solar core. arXiv:1708.00259.
[100] Zhang, J., *et al*. (2005) Inner Core Differential Motion Confirmed by Earthquake Waveform Doublets. Science , **309**, 1357-1360. https://doi.org/10.1126/science.1113193.
[101] Cole, G.H.A. and Woolfson, M.M. (2002) Planetary Science: The Science of Planets around Stars. Institute of Physics Publishing, 36-37, 380-382. https://doi.org/10.1887/075030815X.
[102] Kinver, M. (2009) Global Average Temperature May Hit Record Level in 2010. BBC. Retrieved 22 April 2010.
[103] Pollack, H.N., Hurter, S.J., Johnson, J.R. (1993) Heat flow from the Earth's interior: Analysis of the global data set. *Reviews of Geophysics*, **31** (3): 267–80. Bibcode:1993RvGeo..31..267P. doi:10.1029/93RG01249.
[104] Arculus, R. (2016) The Cosmic Origins of Uranium. http://www.world-nuclear.org/information-library/nuclear-fuel-cycle/uranium-resources/the-cosmic-origins-of-uranium.aspx.
[105] Gando, A., *et al.* (2011) Partial radiogenic heat model for Earth revealed by geoneutrino measurements. Nature Geoscience, **4**, 647.
[106] Hoffman, D.C., *et al.* (1971) Detection of Plutonium-244 in Nature. Nature, **234**, 132.
[107] Ricard, Y. (2009) 2. Physics of Mantle Convection. In David Bercovici and Gerald Schubert. Treatise on Geophysics: Mantle Dynamics, **7**. Elsevier Science. ISBN 9780444535801.
[108] Elkins-Tanton, Linda T. (2006). *Jupiter and Saturn*. New York: Chelsea House. ISBN 978-0-8160-5196-0.
[109] O'Donoghue, J., Moore, L., Stallard, T.S., and Melin, H. (2016) Heating of Jupiter's upper atmosphere above the Great Red Spot. Nature, 18940.
[110] de Pater, I., Lissauer, J.J. (2010) Planetary Sciences (2nd ed.). Cambridge University Press. pp. 254–255. ISBN 978-0-521-85371-2.
[111] Class 12 – Giant Planets – Heat and Formation. 3750 – Planets, Moons & Rings. Colorado University, Boulder. 2004. Retrieved 13 March 2008.

[112] Pearl, J.C.; Conrath, B.J. (1991). "The albedo, effective temperature, and energy balance of Neptune, as determined from Voyager data". Journal of Geophysical Research: Space Physics. 96: 18, 921–18, 930. Bibcode:1991JGR....9618921P. doi:10.1029/91ja01087.
[113] Kamata, S., *et al.* (2019) Pluto's ocean is capped and insulated by gas hydrates. Nature Geoscience, **12**, Issue 5. DOI https://doi.org/10.1038/s41561-019-0369-8 .
[114] Feulner, G. (2012) The Faint Young Sun Problem. arXiv:1204.4449.
[115] Hoyle, F. (1958) Remarks on the Computation of Evolutionary Tracks, Ricerche Astronomiche, **5**, 223.
[116] Schwarzschild, M. (1958) Structure and evolution of the stars. Princeton University Press, New Jersey.
[117] Newman, M.J. and Rood, R.T. (1977) Implications of solar evolution for the earth's early atmosphere. Science, **198**, 1035. doi:10.1126/science.198.4321.1035.
[118] Gough, D.O. (1981) Solar interior structure and luminosity variations. Solar Physics, 74, 21.
[119] Baryshev, Yu. (2008) Field Fractal Cosmological Model as an Example of Practical Cosmology Approach. arXiv: gr-qc/0810.0162.
[120] Agle, D.C., Brown, D. (2012) Data from NASA's Voyager 1 Point to Interstellar Future. http://www.nasa.gov/mission_pages/voyager/voyager20120614.html.
[121] Abhyankar, K.D. (1977) A Survey of the Solar Atmospheric Models. Bulletin of the Astronomical Society of India, **5**, 40. Bibcode:1977BASI....5...40A.
[122] Fox, K.C. (2014) NASA's STEREO Maps Much Larger Solar Atmosphere Than Previously Observed. https://www.nasa.gov/content/goddard/nasas-stereo-maps-much-larger-solar-atmosphere-than-previously-observed/.
[123] Aschwanden, M.J. (2004) Physics of the Solar Corona. An Introduction. Praxis Publishing. ISBN 978-3-540-22321-4.
[124] Schmelz, J.T., *et al.* (2012) Composition of the Solar Corona, Solar Wind, and Solar Energetic Particles. The Astrophysical Journal, **755**, 1. http://iopscience.iop.org/article/10.1088/0004-637X/755/1/33/pdf.
[125] Grossman, L. (2018) Strange gamma rays from the sun may help decipher its magnetic fields. Science News, **194,** 9. https://www.sciencenews.org/article/strange-gamma-rays-sun-magnetic-fields.
[126] Baliukin, I.I., *et al.* (2019) SWAN/SOHO Lyman-α Mapping: The Hydrogen Geocorona Extends Well Beyond the Moon. JGR Space Physics. https://doi.org/10.1029/2018JA026136.
[127] Reyes, R. Exploring the Sun-Earth Connection. Southwest Research Institute. http://pluto.space.swri.edu/image/glossary/geocorona.html.
[128] Kameda, S., *et al.* (2017) Ecliptic North-South Symmetry of Hydrogen Geocorona. Geophysical Research Letter, **44**, 11706. https://doi.org/10.1002/2017GL075915.
[129] Kuwabara, M., *et al.* (2017) The Geocoronal Responses to the Geomagnetic Disturbances. Journal of Geophysical Research: Space Physics, **122**, 1269. https://agupubs.onlinelibrary.wiley.com/doi/pdf/10.1002/2016JA023247.
[130] NASA (2012) Solar System. http://chandra.harvard.edu/xray_sources/solar_system.html.
[131] Wargelin, B.J., *et al.* (2014) Observation and Modeling of Geocoronal Charge Exchange X-Ray Emission During Solar Wind Gusts. The Astrophysical Journal, **796**, 1. http://dx.doi.org/10.1088/0004-637X/796/1/28.
[132] Cravensa, T.E., *et al.* (2009) Solar Wind Charge Exchange Contributions to the Diffuse X-Ray Emission. AIP Conference Proceedings, **1156**, 37. https://doi.org/10.1063/1.3211832.
[133] Shematovich, V.I. and Bisikalo, D.V. (2018) Hot Planetary Coronas. Planetary Science. http://planetaryscience.oxfordre.com/view/10.1093/acrefore/9780190647926.001.0001/acrefore-9780190647926-e-104.
[134] Dwyer, J.R. (2012) The mystery of Lightning. http://www.insightcruises.com/events/sa24/PDF/The_Mysteries_of_Lightning.pdf
[135] Gurevich, A.V., Milikh, G.M., and Roussel-Dupre, R. (1992) Runaway electron mechanism of air breakdown and preconditioning during a thunderstorm. Phys. Lett. A, **165**, 463 – 468.

[136] Fishman, G.J., *et al.* (1994) Discovery of Intense Gamma-Ray Flashes of Atmospheric Origin. Science, **264** (5163), 1313-1316. DOI: 10.1126/science.264.5163.1313.
[137] Russian Satellite Registers Unknown Physical Phenomena in Earth's Atmosphere (2019) https://sputniknews.com/science/201902111072298631-russia-satellite-unknown-physical-phenomena-earth-atmosphere/.
[138] Tesla, N. (1904) The Transmission of Electrical Energy without Wires. Electrical World and Engineer. http://web.archive.org/web/20051222121927/http://tfcbooks.com/tesla/wireless01.htm.
[139] Tesla and Ball Lightning (1988).
https://www.bibliotecapleyades.net/tesla/esp_tesla_20.htm
[140] Kapitsa, P.L. (1955) The Nature of Ball Lightning. In Donald J. Ritchie. Ball Lightning: A Collection of Soviet Research in English Translation (1961 ed.). Consultants Bureau, New York. pp. 11–16.
[141] Handel, P.H. (1975) Maser Theory of Ball Lightning. Bulletin of the American Physical Society Series II, **20**, No. 26.
[142] Ashby, D.E.T.F. and Whitehead, C. (1971) Is Ball Lightning caused by Antimatter Meteorites? Nature, **230**, (5290): 180–182. Bibcode:1971Natur. **230**, 180A. doi:10.1038/230180a0.
[143] Rabinowitz, M. (2002) Little Black Holes: Dark Matter and Ball Lightning. arXiv:0212251.
[144] Thornhill, W. (2006) The IEEE, Plasma Cosmology and Extreme Ball Lightning. https://www.holoscience.com/wp/the-ieee-plasma-cosmology-and-extreme-ball-lightning/
[145] Van Devender, P. (2011) Extreme Ball Lightning: New Physics, New Energy Source, or Just Great Fun. https://www.osti.gov/biblio/1107768.
[146] Wu, H.C. (2014) Theory of ball lightning. arXiv:1411.4784.
[147] Oreshko, A.G. (2012) Observation of Dark Spherical Area after Passage of Ball Lightning through Thick Absorbers.https://www.researchgate.net/profile/Alexander_Oreshko/publication/312218738_Observation_of_Dark_Spherical_Area_After_Passage_of_Ball_Lightning_Through_Thick_Absorbers/links/5877307808ae329d6226e786/Observation-of-Dark-Spherical-Area-After-Passage-of-Ball-Lightning-Through-Thick-Absorbers.pdf .
[148] Cen, J., Yuan, P. and Xue, S. (2014) Observation of the Optical and Spectral Characteristics of Ball Lightning. Physical Review Letters, **112**, 035001.

World-Universe Model—Alternative to Big Bang Model

Abstract

This manuscript provides a comparison of the Hypersphere World-Universe Model (WUM) with the prevailing Big Bang Model (BBM) of the Standard Cosmology. The performed analysis of BBM shows that the Four Pillars of the Standard Cosmology are model-dependent and not strong enough to support the model. The angular momentum problem is one of the most critical problems in BBM. Standard Cosmology cannot explain how Galaxies and Extra Solar systems obtained their substantial orbital and rotational angular momenta, and why the orbital momentum of Jupiter is considerably larger than the rotational momentum of the Sun. WUM is the only cosmological model in existence that is consistent with the Law of Conservation of Angular Momentum. To be consistent with this Fundamental Law, WUM discusses in detail the Beginning of the World. The Model introduces Dark Epoch (spanning from the Beginning of the World for 0.4 billion years) when only Dark Matter Particles (DMPs) existed, and Luminous Epoch (ever since for 13.8 billion years). Big Bang discussed in Standard Cosmology is, in our view, transition from Dark Epoch to Luminous Epoch due to Rotational Fission of Overspinning Dark Matter (DM) Supercluster's Cores. WUM envisions Matter carried from the Universe into the World from the fourth spatial dimension by DMPs. Ordinary Matter is a byproduct of DM annihilation. WUM solves a number of physical problems in contemporary Cosmology and Astrophysics through DMPs and their interactions: Angular Momentum problem in birth and subsequent evolution of Galaxies and Extrasolar systems—how do they obtain it; Fermi Bubbles—two large structures in gamma-rays and X-rays above and below Galactic center; Diversity of Gravitationally-Rounded Objects in Solar system; some problems in Solar and Geophysics [1]. WUM reveals Inter-Connectivity of Primary Cosmological Parameters and calculates their values, which are in good agreement with the latest results of their measurements.

Keywords. Big Bang Model, Four Pillars of Standard Cosmology, Angular Momentum Problem, Black Holes, Hypersphere World-Universe Model, Multicomponent Dark Matter, Macroobjects Structure, Law of Conservation of Angular Momentum, Medium of the World, Inter-Connectivity of Primary Cosmological Parameters, The Beginning of the World, Dark Epoch, Rotational Fission, Luminous Epoch, Macroobject Shell Model, Dark Matter Core, Gravitational Burst, Intergalactic Plasma, Microwave Background Radiation, Far-Infrared Background Radiation, Emergent Phenomena, CODATA.

We can't solve problems by using the same kind of thinking we used when we created them.

Albert Einstein

1. Introduction

Hypersphere World-Universe Model (WUM) is proposed as an alternative to the prevailing Big Bang Model of Standard Cosmology. WUM is a classical model, and is described by classical notions, which define emergent phenomena. By definition, an emergent phenomenon is a property that is a result of simple interactions that work cooperatively to create a more complex interaction. Physically, simple interactions occur at a microscopic level, and the collective result can be observed at a macroscopic level. WUM introduces classical notions once the very first ensemble of particles has been created at

the cosmological time $\cong 10^{-18}\ s$ (state of the World at cosmological times $< 10^{-18}\ s$ is best described by Quantum Mechanics).

WUM is based on **two parameters**: dimensionless Rydberg constant $\alpha = (2aR_\infty)^{1/3}$, where R_∞ is Rydberg constant, a is the basic unit of size (classical electron radius equals to: $a_o = a/2\pi$); and a dimensionless time-varying parameter Q, which is a measure of the Size R and Age A_τ of the World $Q = R/a = A_\tau/t_0$, where $t_0 = a/c$ is the basic unit of time and c is the gravitodynamic constant. In the present Epoch, $Q = 0.759972 \times 10^{40}$. It is worth to note that the constant α was later named "Sommerfeld's constant," and subsequently "Fine-structure constant" [1].

The Big Bang Model (BBM) offers a comprehensive explanation for a broad range of observed phenomena. The framework for the BBM relies on General Relativity and on simplifying assumptions such as homogeneity and isotropy of space. The Lambda Cold Dark Matter (ΛCDM) model is a parametrization of the BBM in which the universe contains three major components: first, a Cosmological constant Λ associated with dark energy; second, the postulated Cold Dark Matter (CDM); and third, Ordinary matter.

The ΛCDM model is based on **six parameters**: baryon density Ω_B, dark matter density Ω_{DM}, dark energy density Ω_Λ, scalar spectral index, curvature fluctuation amplitude, and reionization optical depth. The values of these six parameters are mostly not predicted by current theory; other possible parameters are fixed at "natural" values e.g. total density equals to 1.00, neutrino masses are small enough to be negligible. The ΛCDM model can be extended by adding cosmological inflation. It is frequently referred to as the Standard Model of Big Bang (BB) cosmology, which is the classical model too.

The Four Pillars of the Standard Cosmology are as follows [2]:

- Expansion of the Universe;
- Origin of the cosmic background radiation;
- Nucleosynthesis of the light elements;
- Formation of galaxies and large-scale structures.

BBM and WUM are principally different models. Comparison of the main parameters of the models is presented in **Table 1**.

Angular momentum problem is one of the most critical problem in the Standard Cosmology that must be solved. Any theory of evolution of the Universe that is not consistent with the Law of Conservation of Angular Momentum should be promptly ruled out. To the best of our knowledge, the Hypersphere World-Universe Model is the only cosmological model in existence that is consistent with this Fundamental Law (see Sections 3.7, 3.8 and 3.9).

2. Analysis of the Big Bang Model

2.1. Expansion of the Universe

The fact that galaxies are receding from us in all directions was first discovered by Hubble. There is now excellent evidence for Hubble's law which states that the recessional velocity v of a galaxy is proportional to its distance d from us, that is, $v = Hd$ where H is Hubble's constant. Projecting galaxy trajectories backwards in time means that they converge to the cosmological Singularity at t=0 that is an infinite energy density state. This uncovers one of the shortcomings of the Standard Cosmology – the Horizon problem [3]: *Why does the universe look the same in all directions when it*

arises out of causally disconnected regions? This problem is most acute for the very smooth cosmic microwave background radiation.

Table 1. Parameters of Big Bang Model and World-Universe Model.

Parameter	Big Bang Model	World-Universe Model
Structure of the World	3+1 Spacetime	3D Hypersphere of 4D Nucleus of the World. Time is a Factor of the World
The Beginning	Singularity	4D Nucleus of the World with an extrapolated radius *a* as the result of a fluctuation in the Universe
Expansion	Inflation – extremely rapid exponential expansion of space	The radius of the Nucleus of the World is increasing with speed *c*
Content	Dark Energy, Cold Dark Matter, Ordinary matter	Multicomponent Dark Matter (DM), Ordinary matter
Origin of Matter	Singularity	DM comes from the Universe to the Nucleus along the fourth spatial dimension. Ordinary Matter is a byproduct of DM annihilation
Cosmic Microwave Background	Photons wavelength is increasing over time	Thermodynamic equilibrium of photons with Intergalactic plasma
Nucleosynthesis of light elements	Big Bang Nucleosynthesis	Nucleosynthesis of all elements (including light elements) occurs inside of DM Cores of Macroobjects
Primary Cosmological Parameters	Independent	Inter-connected
Galactic Center	Black Hole	DM Core of Galaxy
Law of Conservation of angular momentum	Inconsistent	Consistent

This problem was resolved by the cosmological Inflation, which is a theory of an extremely rapid exponential expansion of space in the early universe. This rapid expansion increased the linear dimensions of the early universe by a factor of at least 10^{26}, and so increased its volume by a factor of at least 10^{78}. The inflationary epoch lasted from 10^{-36} s after the conjectured BB singularity to some time between 10^{-33} and 10^{-32} s after the singularity. Following the inflationary period, the universe continued to expand, but at a slower rate.

"*It's a beautiful theory*, said Peebles. *Many people think it's so beautiful that it's surely right. But the evidence of it is very sparse*" [4].

According to Silk, *our best theory of the beginning of the universe, inflation, awaits a definitive and falsifiable probe, in order to satisfy most physicists that it is a trustworthy theory. Our basic problem is that we cannot prove the theory of inflation is correct, but we urgently need to understand whether it actually occurred* [5].

E. Conover in the paper "Debate over the universe's expansion rate may unravel physics. Is it a crisis?" outlined the following situation with the measurements of an expansion rate of the universe [6]:

- *Scientists with the Planck experiment have estimated that the universe is expanding at a rate of 67.4 km/s Mpc with an experimental error of 0.5 km/s Mpc;*
- *But supernova measurements have settled on a larger expansion rate of 74.0 km/s Mpc, with an error of 1.4 km/s Mpc. That leaves an inexplicable gap between the two estimates. Now "the*

community has started to take this [problem] extremely seriously," says cosmologist Daniel Scolnic of Duke University, who works on the supernova project led by Riess, called SH0ES;

- *It's unlikely that an experimental error in the Planck measurement could explain the discrepancy. That prospect is "not a possible route out of our current crisis," said cosmologist Lloyd Knox of the University of California, Davis;*
- *So, worries have centered on the possibility that the supernova measurements contain unaccounted for systematic errors - biases that push the SH0ES estimate to larger value.*

L. Verde, T. Treu, and A. G. Riess gave a brief summary of the "Workshop at Kavli Institute for Theoretical Physics, July 2019" [7]. It is not yet clear whether the discrepancy in the observations is due to systematics, or indeed constitutes a major problem for the Standard model.

2.2. Origin of the Cosmic Background Radiation

According to BBM, about 380,000 years after the Big Bang the temperature of the universe fell to the point where nuclei could combine with electrons to create neutral atoms. As a result, photons no longer interacted frequently with matter, the universe became transparent, and the Cosmic Microwave Background (CMB) radiation was created. This cosmic event is usually referred to as Decoupling. The photons that existed at the time of photon decoupling have been propagating ever since, though growing fainter and less energetic, since the expansion of space causes their wavelength to increase over time. The photons present at the time of decoupling are the same photons that we see in the CMB radiation now. But then, **why the CMB is a perfect black-body**?

According to WUM, wavelength is a classical notion. Photons, which are quantum objects, have only four-momenta. They don't have wavelengths. By definition, "*Black-body radiation is the thermal electromagnetic radiation within or surrounding a body in thermodynamic equilibrium with its environment*". In frames of WUM, the black-body spectrum of CMB is due to thermodynamic equilibrium of photons with the Intergalactic plasma [1], the existence of which is experimentally proved [8].

2.3. Nucleosynthesis of the Light Elements

Big Bang Nucleosynthesis (BBN) refers to the production of nuclei other than those of hydrogen during the early phases of the Universe. Primordial nucleosynthesis is believed to have taken place in the interval from roughly 10 seconds to 20 minutes after the Big Bang and is calculated to be responsible for the formation of most of the universe's helium as the isotope helium-4, along with small amounts of deuterium, helium-3, and a very small amount of lithium-7. Essentially all of the elements that are heavier than lithium were created much later, by stellar nucleosynthesis in evolving and exploding stars.

The history of BBN began with the calculations of R. Alpher in the 1940s. During the 1970s, there were major efforts to find processes that could produce deuterium, but those revealed ways of producing isotopes other than deuterium. The problem was that while the concentration of deuterium in the universe is consistent with the BBM as a whole, it is too high to be consistent with a model that presumes that most of the universe is composed of protons and neutrons. The standard explanation now used for the abundance of deuterium is that the universe does not consist mostly of baryons, but that **non-baryonic dark matter** makes up most of the mass of the universe [9].

According to modern cosmological theory, lithium was one of the three elements synthesized in the Big Bang. But in case of lithium, we observe a **cosmological lithium discrepancy** in the universe: older

stars seem to have less lithium than they should, and some younger stars have much more. M. Anders, *et al.* report on the results of the first measurement of the $^{2}H(\alpha,\gamma)^{6}Li$ cross section at Big Bang energies. The experiment was performed deep underground at the LUNA 400 kV accelerator in Gran Sasso, Italy. A BBN lithium abundance ratio of $^{6}Li/^{7}Li=(1.5 \pm 0.3) \times 10^{-5}$ is obtained, firmly **ruling out BBN lithium production** as a possible explanation for the reported ^{6}Li detections[10].

In frames of WUM, Nucleosynthesis of all elements (including light elements) occurs inside of DM Cores of all Macroobjects during their evolution. The theory of Stellar Nucleosynthesis is well developed, starting with the publication of a celebrated $B^{2}FH$ review paper [11]. With respect to WUM, this theory should be expanded to include annihilation of heavy Dark Matter fermions in Macroobjects Cores [1].

2.4. Formation of Galaxies and Large-Scale Structures

The formation and evolution of galaxies can be explained only in terms of gravitation within an inflation + dark matter + dark energy scenario [12]. The standard Hot Big Bang model provides a framework for understanding galaxy formation. At about 10,000 years after the Big Bang, the temperature had fallen to such an extent that the energy density of the Universe began to be dominated by massive particles, rather than the light and other radiation which had predominated earlier. This change in the form of the main matter density meant that the gravitational forces between the massive particles could begin to take effects, so that any small perturbations in their density would grow.

This brings into focus one of the shortcomings of the Standard Cosmology – the **density fluctuation problem** [3]: *The perturbations which gravitationally collapsed to form galaxies must have been primordial in origin; from whence did they arise?*

There is another problem in the Standard Cosmology – **angular momentum problem** [1]:

- The Sun, for example, only accounts for about 0.3% of the total angular momentum of the Solar System (SS) while about 60% is attributed to Jupiter. Evolutionary theory cannot account for this. This strange distribution was the primary cause of the downfall of the Nebular hypothesis;
- SS has an orbital momentum L_{orb}^{SS} calculated based on the distance of 26.4 kly from the galactic center and orbital speed of about 220 km/s : $L_{orb}^{SS} = 1.1 \times 10^{56} J\ s$, which far exceeds rotational angular momentum: $L_{rot}^{SS} = 3.2 \times 10^{43} J\ s$;
- Milky Way (MW) galaxy is gravitationally bounded with Local Supercluster (LS) and has an orbital momentum L_{orb}^{MW} calculated based on the distance of 65 million light- years from LS and orbital speed of about 400 km/s [13]: $L_{orb}^{MW} = 2.5 \times 10^{71}\ J\ s$, which far exceeds the rotational angular momentum [14]: $L_{rot}^{MW} \approx 1 \times 10^{67}\ J\ s$;
- How did MW galaxy and SS obtain their substantial orbital angular momenta?

To the best of our knowledge, the Standard Model doesn't answer these questions. The Hypersphere World-Universe model is the only cosmological model in existence that is consistent with the Law of Conservation of Angular Momentum (see Sections 3.7, 3.8 and 3.9).

As a conclusion, the performed analysis shows that the Four Pillars of the Standard Cosmology are model-dependent and not strong enough to support the Big Bang model.

2.5. Black Holes

Black hole is a **mathematical solution** of Einstein's field equations for gravity in 3+1 dimensional spacetime. The simplest black hole solution is the Schwarzschild solution, which describes the gravitational field in the spherically symmetric, static, **vacuum case**. **This solution is characterized with a single parameter, which corresponds to the mass of an object that produces the same gravitational field** [15].

The existence of supermassive objects in galactic centers is now commonly accepted. It is commonly believed that the central mass is a supermassive Black Hole (BH). There exists, however, evidence to the contrary. In late 2013, ICRAR astronomer Dr. N. Hurley-Walker spotted a previously unknown radio galaxy NGC1534 that is quite close to Earth at 248 million light-years but is much fainter than it should be if the central BH was accelerating the electrons in the jets: *"The discovery is also intriguing because at some point in its history the central black hole switched off but the radio jets have persisted. This is a very rare occurrence—this is only* ***the fifth of this type*** *to be discovered, and by far the faintest. We can only see it at low frequencies, which tells us that the electrons in the jets are not getting new energy from the black hole, so it must have been switched off for some time. The interesting thing about the object I found is that it's being hosted by a spiral galaxy, like our own"*. It's also possible there was never a BH there at all [16].

Recently a population of large, very low surface brightness, spheroidal galaxies was identified in the Coma cluster. The apparent survival of these Ultra Diffuse Galaxies (UDGs) in a rich cluster suggests that they have very high masses. P. van Dokkum, *et al*. present the stellar kinematics of Dragonfly 44, one of the largest Coma UDGs, whose mass about equals that of the Milky Way. However, the galaxy emits only 1% of the light emitted by the Milky Way. Astronomers reported that this galaxy might be made almost entirely of dark matter. The existence of **nearly-dark objects** with this mass is unexpected, as galaxy formation is thought to be maximally-efficient in this regime [17].

Candidate stellar-mass BHs in globular clusters of the Milky Way were reported in the following publications:

- R. Narayan, J. E. McClintock, and I Yi present a new model for BH soft X-ray transients A0620-00, V404 Cyg, and X-ray Nova Mus 1991 with mass 4.4; 9 and 7 solar mass respectively [18];
- K. Gebhardt, R. M. Rich, and L. Ho present the detection of a 20,000 solar mass BH in the Stellar Cluster G1, which is one of the most massive stellar clusters in M31. In their opinion, Globular clusters in our Galaxy should be searched for central BHs [19];
- L. Chomiuk, *et al*. report the discovery of a candidate stellar-mass BH in the globular cluster M62, which they term M62-VLA1. The radio, X-ray, and optical properties of M62-VLA1 are very similar to those for V404 Cyg, one of the best-studied quiescent stellar-mass BHs [20];
- B. Giesers, *et al.* performed multiple epoch observations of NGC 3201 with the aim of constraining the binary fraction. The obtained data show strong evidence that the target star is in a binary system with a **non-luminous object** having a minimum mass of (4.36 ± 0.41) solar mass. This object should be degenerate, since it is invisible, and the minimum mass is significantly higher than the Chandrasekhar limit [21];
- J. Liu, *et al*. report radial velocity measurements of a Galactic star, LB-1 and find that the motion of it requires the presence of a **dark companion** with mass of $68^{+11}_{-13} M_{\odot}$. In authors opinion, *forming such massive ones in a high-metallicity environment would be extremely challenging to current stellar evolution theories* [22].

In 2014, L. Mersini-Houghton claimed to demonstrate mathematically that, given certain assumptions about BH firewalls, current theories of BH formation are flawed. She claimed that Hawking radiation causes the star to shed mass at a rate such that it no longer has the density sufficient to create a BH [23].

R. K. Leane and T. R. Slatyer in the paper "Revival of the Dark Matter Hypothesis for the Galactic Center Gamma-Ray Excess" examine the impact of unmodeled source populations on identifying the true origin of the galactic center GeV excess (GCE). The authors discover striking behavior consistent with a mismodeling effect in the real Fermi data, finding that large artificial injected dark matter signals are completely misattributed to point sources. Consequently, they conclude that dark matter may provide a dominant contribution to the GCE after all [24].

As a conclusion, we have the observational evidences for the existence of **non-luminous objects** in centers of galaxies (for example, by the orbits of stars in the center of our galaxy), globular clusters, binary systems, and commonly accept them as BHs. But they might be "Dark Stars" composed of fermion Dark Matter Particles. A mechanism whereby Dark Matter (DM) in protostellar halos plays a role in the formation of the first stars is discussed by D. Spolyar, K. Freese, and P. Gondolo [25]. Heat from neutralino DM annihilation is shown to overwhelm any cooling mechanism, consequently impeding the star formation process. A "dark star'' powered by DM annihilation instead of nuclear fusion may result. Dark stars are in hydrostatic and thermal equilibrium, but with an unusual power source [26].

In frames of WUM, supermassive objects in galactic centers are Macroobjects with Cores made up of DM fermions (see Sections 3.1 and 3.2).

3. Hypersphere World-Universe Model

There exist a number of competing cosmological models. In our opinion, the most probable model is the one that built on the minimum number of parameters. World-Universe Model (WUM) is based on **two parameters** only: dimensionless Rydberg constant α and dimensionless quantity Q, which increases in time $Q \propto \tau$, and is, in fact, a measure of the Size and Age of the World. In WUM we often use well-known physical parameters, keeping in mind that all of them can be expressed through the Basic Units. Taking the relative values of physical parameters in terms of the Basic Units we can express all dimensionless parameters of the World through two Fundamental Parameters α and Q in various rational exponents, as well as small integer numbers and π.

Key concepts and observations of WUM are the following [1]:

- The Beginning of the World;
- Expansion and Creation of Matter;
- Content of the World;
- Structure of Macroobjects;
- Inter-Connectivity of Primary Cosmological Parameters;
- Gravity, Space and Time are all emergent phenomena.

WUM makes reasonable assumptions in each of these areas. The remarkable agreement of the calculated values of the primary cosmological parameters with the observational data gives us considerable confidence in the Model (see **Table 3**, Section 3.6).

In WUM we introduce a basic unit of mass m_0 that equals to: $m_0 = h/ac = 70.025267\ MeV$, where h is Planck constant. m_0 plays a key role when masses of DMPs are discussed below.

3.1. Multicomponent Dark Matter

Possibility of DMP observation in Centers of Macroobjects has drawn many new researchers to the field in the last forty years. Indirect effects in cosmic rays and gamma-ray background from the annihilation of cold DM in the form of heavy stable neutral leptons in Galaxies were considered in pioneer articles [27]-[32]. Important cosmological problems like Dark Matter and Dark Energy could be, in principle, solved through extended gravity. This is stressed, for example, in the famous paper of Prof. C. Corda [33]. A paper by G. Bertone and T. M. P. Tait [34] provides an excellent review of what we have learned about the nature of DM from past experiments, and the implications for planned DM searches in the next decade.

Two-component DM system consisting of bosonic and fermionic components is proposed for the explanation of emission lines from the bulge of Milky Way galaxy. C. Boehm, P. Fayet, and J. Silk analyze the possibility of two coannihilating neutral and stable DMPs: a heavy fermion (for example the lightest neutralino > 100 GeV) and a light spin-0 particle (~ 100 MeV) [35].

In WUM, the World consists of DM (about 92.8% of the total Matter) and Ordinary matter (about 7.2%). It means that DM should play the main role in any Cosmological model. It is the case in WUM, and Ordinary matter is a byproduct of DMPs annihilation [1].

WUM proposes multicomponent DM system consisting of two couples of coannihilating DMPs: a heavy DM fermion – DMF1 (1.3 TeV) and a light spin-0 boson – DIRAC (70 MeV) that is a dipole of Dirac's monopoles; a heavy fermion – DMF2 (9.6 GeV) and a light spin-0 boson – ELOP (340 keV) that is a dipole of preons; fermions – DMF3 (3.7 keV) and DMF4 (0.2 eV).

WUM postulates that masses of DMFs and bosons are proportional to m_0 multiplied by different exponents of α and can be expressed with the following formulae [1]:

DMF1 (fermion): $m_{DMF1} = \alpha^{-2} m_0 = 1.3149950\ TeV$

DMF2 (fermion): $m_{DMF2} = \alpha^{-1} m_0 = 9.5959823\ GeV$

DIRAC (boson): $m_{DIRAC} = \alpha^{0} m_0 = 70.025267\ MeV$

ELOP (boson): $m_{ELOP} = 2/3\alpha^{1} m_0 = 340.66606\ keV$

DMF3 (fermion): $m_{DMF3} = \alpha^{2} m_0 = 3.7289402\ keV$

DMF4 (fermion): $m_{DMF4} = \alpha^{4} m_0 = 0.19857111\ eV$

It is worth to note that Rydberg unit of energy Ry equals to: $Ry = 1/2\ \alpha^3 m_0 c^2 = 13.605693\ eV$.

The values of mass of DMF1, DMF2, DMF3 fall into the ranges estimated in literature for neutralinos, WIMPs, and sterile neutrinos respectively [1]. DMF1, DMF2 and DMF3 partake in the self-annihilation interaction with strength equals to α^{-2}, α^{-1} and α^{2} respectively.

WUM introduces a new **Weak Force**, providing interaction between DMPs. The strength of this force G_W is about 30 orders of magnitude greater than the strength of the gravity G: $G_W = G \times Q^{3/4}$, and its range in the present epoch $R_W = a \times Q^{1/4} = 1.65314 \times 10^{-4}\ m$ is considerably greater than that of the weak nuclear force. Proposed Weak Interaction between DMPs provides the integrity of DM Cores of all Macroobjects [1].

3.2. Macroobjects Cores Made up of Dark Matter Particles

According to WUM, Macrostructures of the World (Superclusters, Galaxies, Extrasolar Systems) have Nuclei made up of DMFs, which are surrounded by Shells composed of DM and Ordinary matter. The shells envelope one another, like a Russian doll. The lighter a particle, the greater the radius and mass of its shell. Innermost shells are the smallest and are made up of heaviest particles; outer shells are larger and consist of lighter particles [1].

Table 2 describes the parameters of Macroobjects Cores (which are Fermionic Compact Stars in WUM) in the present Epoch made up of different DM fermions: self-annihilating DMF1, DMF2, DMF3; fermion DMF4 and electron-positron plasma.

The calculated parameters of the shells show that [1]:

- Nuclei made of self-annihilating DMF1 and/or DMF2 compose Cores of stars in extrasolar systems;
- Shells of electron-positron plasma around Nuclei made up of self-annihilating DMF1 and/or DMF2 make up Cores of globular clusters. Electron-positron plasma explains radio properties of Macroobjects;
- Shells of DMF3 around Nuclei made up of self-annihilating DMF1 and/or DMF2 with shells of electron-positron plasma make up Cores of galaxies;
- Nuclei made of DMF1 and/or DMF2 surrounded by shells of DMF3 and DMF4 compose Cores of superclusters.

Macroobject Cores have the following properties [1]:

- The minimum radius of Core R_{min} made of any fermion equals to **three Schwarzschild radii**;
- Core density does not depend on M_{max} and R_{min} and does not change in time while $M_{max} \propto \tau^{3/2}$ and $R_{min} \propto \tau^{1/2}$.

K. Mehrgan, *et al.* observed a supergiant elliptical galaxy Holmberg 15A about 700 million light-years from Earth. They found an **Extreme Core** with a mass of 4×10^{10} solar masses at the center of Holm 15A [36]. The calculated maximum mass of galaxy Core of 6×10^{10} solar masses (see **Table 2**) is in good agreement with the experimentally found value [36].

3.3. The Beginning of the World

Before the Beginning of the World there was nothing but an Eternal Universe. About 14.2 billion years ago the World was started by a fluctuation in the Eternal Universe, and the **Nucleus of the World**, which is a four-dimensional ball, was born. An extrapolated Nucleus radius at the Beginning was equal to a basic unit of size a. The 3D World is a hypersphere that is the surface of a 4-ball Nucleus. All points of the hypersphere are equivalent; there are no preferred centers or boundary of the World [1]. Hypersphere World as a model of a finite universe was proposed by Georg Riemann in 1854 [37].

Table 2. Parameters of Macroobject Cores made up of different Fermions in present Epoch.

Fermion	Fermion Mass m_f, MeV	Macroobject Mass M_{max}, kg	Macroobject Radius R_{min}, m	Macroobject Density ρ_{max}, kgm^{-3}
DMF1	1.3×10^6	1.9×10^{30}	8.6×10^3	7.2×10^{17}
DMF2	9.6×10^3	1.9×10^{30}	8.6×10^3	7.2×10^{17}
Electron-Positron	0.51	6.6×10^{36}	2.9×10^{10}	6.3×10^4
DMF3	3.7×10^{-3}	1.2×10^{41}	5.4×10^{14}	1.8×10^{-4}
DMF4	2×10^{-7}	4.2×10^{49}	1.9×10^{23}	1.5×10^{-21}

3.4. Expansion and Creation of Matter

The Nucleus is expanding in the Universe, and its surface, the hypersphere, is likewise expanding. The radius of the Nucleus R is increasing with speed c (gravitodynamic constant) for the absolute cosmological time τ from the Beginning and equals to $R = c\tau$. The expansion of the Hypersphere World can be understood through the analogy with an expanding 3D balloon: imagine an ant residing on a seemingly two-dimensional surface of a balloon. As the balloon is blown up, its radius increases, and its surface grows. The distance between any two points on the surface increases. The ant sees her world expand but does not observe a preferred center.

According to WUM, the surface of the Nucleus is created in a process analogous to sublimation. Continuous creation of matter is the result of such process. Sublimation is a well-known endothermic process that happens when surfaces are intrinsically more energetically favorable than the bulk of a material, and hence there is a driving force for surfaces to be created.

Matter comes from the Universe to the Nucleus along the fourth spatial dimension, passing through the 4-ball surface, which is our World. Dark Matter Particles (DMPs) carry new Matter into the Nucleus. By analogy with three-dimensional ball, which has two-dimensional sphere surface (that has surface energy), we can imagine that our three-dimensional World (Hypersphere) has a "Surface energy" of the four-dimensional Nucleus [1].

It is important to emphasize that

- Creation of Matter is a direct consequence of expansion;
- Creation of DM occurs homogeneously in all points of the hypersphere World;
- Ordinary Matter is a byproduct of DM annihilation. Consequently, the matter-antimatter asymmetry problem discussed in literature does not arise (since antimatter does not get created by DM annihilation).

3.5. Content of the World

The existence of the Medium is a principal point of WUM. It follows from the observations of Intergalactic Plasma; Cosmic Microwave Background Radiation (MBR); Far-Infrared Background Radiation. Inter-galactic voids discussed by astronomers are in fact examples of the Medium in its purest. Cosmic MBR is part of the Medium; it then follows that the Medium is the absolute frame of

reference. Relative to MBR rest frame, Milky Way galaxy and Sun are moving with the speed of 552 and 370 km/s respectively [1].

The Medium consists of stable elementary particles with lifetimes longer than the age of the World: DMPs in the Dark Epoch and protons, electrons, photons, neutrinos, and DMPs in the Luminous Epoch (see Sections 3.7, 3.8 and 3.9). For all particles under consideration we use the following characteristics:

- Type of particle (fermion or boson);
- "Mass" that is equivalent to "Rest energy" with the constant c^2 ;
- Electrical charge.

The total energy density of the Medium is 2/3 of the overall energy density of the World. Superclusters, Galaxies, Extrasolar systems, planets, moons, etc. are made of the same particles. The energy density of Macroobjects adds up to 1/3 of the total energy density of the World throughout the World's evolution [1].

In WUM, Time and Space are closely connected with Mediums' impedance and gravitomagnetic parameter. It follows that neither Time nor Space could be discussed in absence of the Medium. The gravitational parameter G that is proportional to the Mediums' energy density can be introduced only for the Medium filled with Matter. In frames of WUM, the Gravitation is a result of simple interactions of DMF4 with Matter that work cooperatively to create a more complex interaction. DMF4 particles are responsible for the Le Sage's mechanism of the gravitation [1].

As the conclusion, **Gravity, Space and Time** are all emergent phenomena [1]. In this regard, it is worth to recall the Albert Einstein quote: "*When forced to summarize the theory of relativity in one sentence: time and space and gravitation have no separate existence from matter*".

3.6. Inter-Connectivity of Primary Cosmological Parameters

The constancy of the universe fundamental constants, including Newtonian constant of gravitation and Planck mass, is now commonly accepted, although has never been firmly established as a fact. All conclusions on the (almost) constancy of the Newtonian parameter of gravitation are model-dependent.

A commonly held opinion states that gravity has no established relation to other fundamental forces, so it does not appear possible to calculate it from other constants that can be measured more accurately, as is done in some other areas of physics. WUM holds that there indeed exist relations between all primary cosmological parameters that depend on dimensionless time-varying quantity Q: Newtonian parameter of gravitation; Hubble's parameter; Age of the World; the Worlds' radius of curvature in the fourth spatial dimension; Critical energy density; Concentration of Intergalactic Plasma; Minimum Energy of Photons; Temperature of the Microwave Background Radiation; Temperature of the Far-Infrared Background Radiation peak [1].

Comparison of the calculated cosmological parameters based on the average value of the gravitational parameter with experimentally measured parameters is presented in **Table 3.**

Table 3. Theoretical and experimental values of the primary cosmological parameters.

Parameter	Theory	Experiment	Ref.
Hubble's parameter, $km/s\ Mpc$	68.7457	69.32 ± 0.8 $69.1^{+0.4}_{-0.6}$ 69.8 ± 1.9	[38] [39] [40]
CMB temperature, K	2.72518	2.72548 ± 0.00057	[41]
Concentration of Intergalactic plasma, m^{-3}	0.25480	$\lesssim 0.27$	[42]
Proton relative energy density	0.048014655	0.049 ± 0.013	[8]
Minimum energy of photons, $\times 10^{-14} eV$	1.8743	$\lesssim 2.2$	[43]
Far-Infrared Background peak, K	28.955	29	[44]

Note that the precision of the most parameters value has increased by three orders of magnitude. We are not aware of any other model that allows calculation of CMB temperature with such accuracy [1].

The remarkable agreement of the calculated values of the primary cosmological parameters with the observational data gives us considerable confidence in the Model. We propose to introduce Q as a new Fundamental Parameter tracked by CODATA and use its value in calculation of all Q-dependent parameters [1].

3.7. Dark Epoch

As we mentioned in Introduction, the Angular Momentum problem is one of the most critical problem in any Cosmological model that must be solved. To be consistent with the Law of Conservation of Angular Momentum a Model must answer the following questions:

- How did Galaxies and Extra Solar systems obtain their substantial orbital and rotational angular momenta;
- Why are all Macroobjects rotating;
- How did Milky Way give birth to different Extra Solar systems in different times;
- The beginning of the Milky Way (MW) galaxy was about 13.8 billion years. The age of MW is about the Age of the World. What is the origin of MW huge angular momentum? We must discuss the Beginning of the MW;
- The beginning of the Solar System (SS) was 4.6 billion years. What is the origin of SS angular momentum? We must discuss the Beginning of the SS;
- Why is the orbital momentum of Jupiter much larger than rotational momentum of the Sun. There is no possible means by which the angular momentum from the Sun could be transferred to the planets;
- In the theory of planetary formation, all planets, being made of the same ingredients, should have the same composition, yet they don't.

In our opinion, there is the only one mechanism that can provide angular momenta to Macroobjects – Rotational Fission of overspinning Prime Objects. From the point of view of Fission model, the prime object is transferring some of its rotational angular momentum to orbital and rotational momenta of satellites. It follows that **the rotational momentum of the prime object should exceed the orbital momentum of its satellite**. In frames of WUM, Prime Objects are DM Cores of Superclusters, which must accumulate tremendous angular momenta before the Birth of the Luminous World. It means that it must be some long enough time in the history of the World, which we named "Dark Epoch" [1].

Dark Epoch started at the Beginning of the World and lasted for about 0.4 billion years. WUM is a classical model, therefore classical notions can be introduced only when the very first ensemble of particles was created at the cosmological time $\cong 10^{-18}s$. At time $\tau \gg 10^{-18}s$ density fluctuations could happen in the Medium of the World filled with DMPs: DMF1, DMF2, DIRACs, ELOPs, DMF3 and DMF4. The heaviest Dark Matter particles DMF1 could collect into a cloud with distances between particles smaller than the range of the weak interaction R_W . As the result of the weak interaction, clumps of DMF1 will arise. Larger clumps will attract smaller clumps of DMPs and initiate a process of expanding the DM clump followed by growth of surrounding shells made up of other DMPs, up to the maximum mass of the shell made up of DMF4 at the end of Dark Epoch (0.4 billion years).

The process described above is the formation of the DM Core of a Supercluster. DMPs supply not only additional mass ($\propto \tau^{3/2}$) to Cores, but also additional angular momentum ($\propto \tau^2$) fueling the overspinning of Dark Matter Cores. In our opinion, all Supercluster Cores had undergone rotational fission at approximately the same cosmological time [1].

3.8. Rotational Fission

According to WUM, the rotational angular momentum of overspinning (surface speed at equator exceeding escape velocity) objects before rotational fission equals to [1]:

$$L_{rot} = \frac{4\sqrt{2}}{15}\frac{1+5\delta}{1+3\delta}G^{0.5}M^{1.5}R^{0.5}$$

where M is a mass of overspinning object, R is its radius, δ is the density ratio inside of the object: $\delta = \rho_{min}/\rho_{max}$. Parameters G, M, R for Macroobjects Cores are time-varying: $G \propto \tau^{-1}$, $M \propto \tau^{3/2}$ and $R \propto \tau^{1/2}$. It follows that the rotational angular momentum of Cores L_{rot} is proportional to τ^2.

Local Supercluster (LS) is a mass concentration of galaxies containing the Local Group, which in turn contains the MW galaxy. At least 100 galaxy groups and clusters are located within its diameter of 1.1×10^8 light-years. Considering parameters of DMF4 shell (see **Table 2**), we calculate the rotational angular momentum L_{rot}^{LSC} of LS Core before rotational fission:

$$L_{rot}^{LSC} = 3.7 \times 10^{77} J\ s$$

MW is gravitationally bounded with LS [13]. Let's compare L_{rot}^{LSC} with an orbital momentum of Milky Way L_{orb}^{MW} calculated based on the distance of 65 million light-years from LS Core and orbital speed of about 400 km/s [13]:

$$L_{orb}^{MW} = 2.5 \times 10^{71}\ J\ s$$

It means that as the result of rotational fission of LS Core, approximately $\sim 10^6$ galaxies like Milky Way could be generated at the same time. Considering that density of galaxies in the LS falls off with the square of the distance from its center near the Virgo Cluster, and the location of MW on the outskirts of the LS [45], the actual number of created galaxies could be much larger.

The mass-to-light ratio of the LS is about 300 times larger than that of the Solar ratio. Similar ratios are obtained for other superclusters [46]. These facts support the rotational fission mechanism proposed above. In 1933, Fritz Zwicky investigated the velocity dispersion of Coma cluster and found a surprisingly high mass-to-light ratio ($\sim$500). He concluded: *if this would be confirmed, we would get the surprising result that dark matter is present in much greater amount than luminous matter* [47]. These ratios are one of the main arguments in favor of presence of large amounts of Dark Matter in the World.

Analogous calculations for MW Core based on parameters of DMF3 shell (see **Table 2**) produce the following value of rotational angular momentum L_{rot}^{MWC} [1]:

$$L_{rot}^{MWC} = 2.4 \times 10^{60}\ J\ s$$

which far exceeds the orbital momentum of the Solar System L_{orb}^{SS} calculated based on the distance from the galactic center of 26.4 kly and orbital speed of about 220 km/s

$$L_{orb}^{SS} = 1.1 \times 10^{56}\ J\ s$$

As the result of rotational fission of MW Core 13.8 billion years ago, approximately $\sim 10^4$ Extrasolar systems like Solar System could be created at the same time. Considering that MW has grown inside out (in the present Epoch, most old stars can be found in the middle, more recently formed ones on the outskirts [48]), the number of generated Extrasolar systems could be much larger. Extrasolar system Cores can give birth to planetary cores, which in turn can generate cores of moons by the same Rotational Fission mechanism [1].

The oldest known star HD 140283 (Methuselah star) is a subgiant star about 190 light-years away from Earth for which a reliable age has been determined [49]. H. E. Bond, *et al.* found its age to be $14.46 \pm 0.8\ Gyr$ that does not conflict with the age of the Universe, $13.77 \pm 0.06\ Gyr$, based on the microwave background and Hubble constant [49]. It means that this star must have formed between 13.66 and 13.83 Gyr, amount of time that is too short for formation of second generation of stars according to prevailing theories.

In WUM this discovery can be explained by generation of the Core of HD 140283 by overspinning Core of the MW 13.8 billion years ago.

In frames of the developed Rotational Fission model, it is easy to explain hyper-runaway stars unbound from the Milky Way with speeds of up to $\sim 700\ km/s$ [50]: they were launched by overspinning Core of the Large Magellan Cloud with the speed higher than the escape velocity [1].

S. E. Koposov, *et al.* present the discovery of the fastest Main Sequence hyper-velocity star S5-HVS1 with mass about 2.3 solar masses that is located at a distance of ~ 9 kpc from the Sun. When integrated backwards in time, the orbit of the star points unambiguously to the Galactic Centre, implying that S5-HVS1 was kicked away from Sgr A* with a velocity of ~ 1800 km/s and travelled for 4.8 Myr to the current location. So far, this is the only hyper-velocity star confidently associated with the Galactic Centre [51].

In frames of the developed Model this discovery can be explained by Gravitational Burst of the overspinning Core of the Milky Way 4.8 million years ago, which gave birth to S5-HVS1 with the speed higher than the escape velocity of the Core (see Section 3.9).

A. Irrgang, *et al.* present the discovery of a new extreme runaway star, PG 1610+062 challenging classical ejection mechanisms [52]. A kinematic analysis, based on the spectrophotometric distance (17.3 kpc) shows that PG 1610+062 was shot into the halo $\sim$ 41 Myr ago from a region with a Galactocentric radius of $\sim$ 6.5 kpc, which possibly coincided with the location of the now nearby Carina-Sagittarius spiral arm at a velocity of 550 ± 40 km/s which is beyond the classical limits [52].

In frames of WUM, this discovery can be explained by a Gravitational Burst of the overspinning Core of the globular cluster M55 in the constellation Sagittarius. M55 is at a distance of about 17.6 kly away from Earth. It has a mass of about 2.69×10^5 times that of the Sun and estimated age 12.3 Gyr.

C. J. Clarke, *et al.* observed CI Tau, a young 2 million years old star. CI Tau is located about 500 light-years away in a highly-productive stellar 'nursery' region of the galaxy. They discovered that the Extrasolar System contains four gas giant planets that are only 2 million years old [53], amount of time that is too short for formation of gas giants according to prevailing theories.

In frames of the developed Rotational Fission model, this discovery can be explained by Gravitational Burst of the overspinning Core of the Milky Way two million years ago, which gave birth to CI Tau system with DM cores of all planets generated at the same time.

To summarize,

- The rotational fission of macroobject Cores is the most probable process that can generate satellite cores with large orbital and rotational momenta in very short time;
- Macrostructures of the World form from the top (superclusters) down to galaxies, extrasolar systems, planets, and moons;
- Gravitational waves can be a product of rotational fission of overspinning Macroobject Cores;
- The Big Bang discussed in the Standard cosmological model is, in our view, the transition from Dark Epoch to Luminous Epoch.

3.9. Luminous Epoch

Luminous Epoch spans from 0.4 billion years up to the present Epoch (during 13.8 billion years). According to WUM, Cores of all Macroobjects (MOs) of the World (Superclusters, Galaxies, Extrasolar systems) possess the following properties [1]:

- Their Nuclei are made up of DMFs and contain other particles, including Dark Matter and Ordinary matter, in shells surrounding the Nuclei;
- DMPs are continuously absorbing by Cores of all MOs. Ordinary Matter (about 7.2% of the total Matter in the World) is a byproduct of DMPs annihilation. It is re-emitted by Cores of MOs continuously;
- Nuclei and shells are growing in time: size $\propto \tau^{1/2}$; mass $\propto \tau^{3/2}$; and rotational angular momentum $\propto \tau^2$, until they reach the critical point of their stability, at which they detonate. Satellite cores and their orbital L_{orb} and rotational L_{rot} angular momenta released during detonation are produced by Overspinning Core (OC). The detonation process does not destroy OC; it's rather gravitational hyper-flares;
- Size, mass, composition, L_{orb} and L_{rot} of satellite cores depend on local density fluctuations at the edge of OC and cohesion of the outer shell. Consequently, the diversity of satellite cores and their rotation have a clear explanation.

WUM refers to OC detonation process as Gravitational Burst (GB), analogous to Gamma Ray Burst. In frames of WUM, the repeating GBs can be explained the following way:

- As the result of GB, the OC loses a small fraction of its mass and a large part of its rotational angular momentum;
- After GB, the Core absorbs new DMPs. Its mass increases $\propto \tau^{3/2}$, and its angular momentum L_{rot} increases much faster $\propto \tau^2$, until it detonates again at the next critical point of its stability. Consequently, the birth to different Extra Solar systems in different times has a clear explanation;
- Afterglow of GBs is a result of processes developing in the Nuclei and shells after detonation;

- In case of Extrasolar systems, a star wind is the afterglow of star detonation: star Core absorbs new DMPs, increases its mass $\propto \tau^{3/2}$ and gets rid of extra L_{rot} by star wind particles;
- Solar wind is the afterglow of Solar Core detonation 4.6 billion years ago. It creates the bubble of the Heliosphere continuously;
- In case of Galaxies, a galactic wind is the afterglow of repeating galactic Core detonations. In Milky Way it continuously creates two Dark Matter Fermi Bubbles.

3.10. Dark Matter Fermi Bubbles

In November 2010, the discovery of two Fermi Bubbles (FBs) emitting gamma- and X-rays was announced. FBs extend for about 25 kly above and below the center of the galaxy [54]. The outlines of the bubbles are quite sharp, and the bubbles themselves glow in nearly uniform gamma rays over their colossal surfaces. Gamma-ray spectrum measured by the Fermi Large Area Telescope remains unconstrained up to around 1 TeV [55]. Years after the discovery of FBs, their origin and the nature of the gamma-ray emission remain unresolved.

M. Su and D. P. Finkbeiner [56] identify a gamma-ray cocoon feature in the southern Fermi bubble, a jet-like feature along the cocoon's axis of symmetry, and another directly opposite the Galactic center in the north. Both the cocoon and jet-like feature have a hard spectrum from 1 to 100 GeV. If confirmed, these jets are the first resolved gamma-ray jets ever seen.

G. Ponti, *et al.* report prominent X-ray structures on intermediate scales (hundreds of parsecs) above and below the plane, which appear to connect the Galactic Centre region to the Fermi bubbles. They propose that these structures, which they term the Galactic Centre 'chimneys', constitute exhaust channels through which energy and mass, injected by a quasi-continuous train of episodic events at the Galactic Centre, are transported from the central few parsecs to the base of the FBs [57].

D. Hooper and T. R. Slatyer discuss two emission mechanisms in the FBs: inverse Compton scattering and annihilating DM [58]. In their opinion, the second emission mechanism must be responsible for the bulk of the low-energy, low-latitude emission. The spectrum and angular distribution of the signal is consistent with that predicted from ~10 GeV DMPs annihilating to leptons. This component is similar to the excess GeV emission previously reported by D. Hooper from the Galactic Center [59].

It is worth to note that a similar excess of gamma-rays was observed in the central region of the Andromeda galaxy (M31). A. McDaniel, T. Jeltema, and S. Profumo calculated the expected emission across the electromagnetic spectrum in comparison with available observational data from M31 and found that the best fitting models are with the DMP mass 11 GeV [60].

In frames of WUM, the Galactic Center Gamma-Ray Excess at energy about 10 GeV is consistent with the annihilation of the particles DMF2 with mass 9.6 GeV.

According to H.-Y. K. Yang, M. Ruszkowski, and E. G. Zweibel, for understanding the physical origin of the FBs, three major questions need to be answered [61]:

- First, what is the emission mechanism? The bubbles can either be hadronic, where the gamma rays are produced by inelastic collisions between cosmic-ray protons and the thermal nuclei via decay of neutral pions, or leptonic, where the gamma rays are generated by inverse-Compton scattering of the interstellar radiation field by cosmic-ray electrons;
- Second, what activity at the Galactic Center triggered the event – are the bubble associated with nuclear star formation or active galactic nucleus activity?

- Third, where are the Cosmic rays accelerated? They could either be accelerated at the Galactic Center and transported to the surface of the bubbles or accelerated in-situ by shocks or turbulence. Note however that not all combinations of the above three considerations would make a successful model because of constraints given by the **hard spectrum of the observed bubbles**.

WUM explains FBs the following way [1]:

- Core of MW galaxy is made up of DM particles: DMF1 (1.3 TeV), DMF2 (9.6 GeV), and DMF3 (3.7 keV). The second component (DMF2) explains the excess GeV emission reported by Dan Hooper from the Galactic Center [59]. Core rotates with surface speed at equator close to the escape velocity between Gravitational Bursts (GBs), and over the escape velocity at the moments of GBs;
- Bipolar astrophysical jets (which are astronomical phenomena where outflows of matter are emitted as an extended beams along the axis of rotation [62]) of DMPs are ejected from the rotating Core into the Galactic halo along the rotation axis of the Galaxy;
- Due to self-annihilation of DMF1 and DMF2, these beams are gamma-ray jets [56].
- The prominent X-ray structures on intermediate scales (hundreds of parsecs) above and below the plane (named the Galactic Centre 'chimneys' [57]) are the result of the self-annihilation of DMF3;
- FBs are bubbles with boundary between them and Intergalactic Medium that has a surface energy density equals to the basic unit of surface energy density $\sigma_0 = hc/a^3$;
- These bubbles are filled with DM particles: DMF1, DMF2, and DMF3. In our Model, FBs are Macroobjects with a mass M_{FB} and diameter D_{FB} , which are proportional to: $M_{FB} \propto Q^{3/2}$ and $D_{FB} \propto Q^{3/4}$ respectively. According to WUM, diameter of FBs equals to:
$$D_{FB} = L_{DMF3} \times Q^{3/4} = \frac{a}{\alpha^2} \times Q^{3/4} = 28.6\ kly$$
where L_{DMF3} is Compton length of particles DMF3 with mass $m_{DMF3} = \alpha^2 m_0$. The calculated diameter is in good agreement with the measured size of the FBs 25 kly [53] and 32.6 kly [55].
- With Nikola Tesla's principle at heart – *There is no energy in matter other than that received from the environment* – we calculate mass M_{FB} :
$$M_{FB} = \frac{\pi D_{FB}^2 \sigma_0}{c^2} = \frac{\pi m_0}{\alpha^4} \times Q^{3/2} \cong 3.6 \times 10^{41} kg$$
Recall that the mass of Milky Way galaxy M_{MW} is about: $M_{MW} \cong 3.2 \times 10^{42} kg$;
- Weak interaction between DMF3 particles provides integrity of Fermi Bubbles. FBs made up of DMF3 particles resembles a honeycomb filled with DMF1 and DMF2;
- FBs radiate X-rays due to the annihilation of DMF3 particles;
- Gamma rays up to 1 TeV [52] are the result of annihilation of DMF1 (1.3 TeV) and DMF2 (9.6 GeV) in Dark Matter Objects (DMOs) whose density is sufficient for the annihilation of DMPs to occur. DMOs are much smaller than stars in the World, have a high concentration in FBs and provide nearly uniform gamma ray glow over their colossal surfaces. The total flux of the gamma radiation from FBs is the sum of the contributions of all individual DMOs;
- The Core of the Milky Way supplies FBs with new DMPs through the galactic wind, explaining the brightness of FBs remaining fairly constant during the time of observations. FBs are built continuously throughout the lifetime of Milky Way (13.8 By).

In our view, FBs are DMP clouds containing uniformly distributed clumps of Dark Matter Objects, in which DMPs annihilate and radiate X-rays and gamma rays. Dark Matter Fermi Bubbles constitute a principal proof of the World-Universe Model.

3.11. Hypersphere World

The physical laws we observe appear to be independent of the Worlds' curvature in the fourth spatial dimension due to the very small value of the dimension-transposing gravitomagnetic parameter of the Medium [1]. Consequently, direct observation of the Worlds' curvature would appear to be a hopeless goal.

One way to prove the existence of the Worlds' curvature is direct measurement of truly large-scale parameters of the World: Gravitational, Hubble's, Temperature of the Microwave Background Radiation. Conducted at various points of time, these measurements would give us varying results, providing insight into the curved nature of the World. Unfortunately, the accuracy of the measurements is quite poor. Measurement errors far outweigh any possible "curvature effects", rendering this technique useless in practice. To be conclusive, the measurements would have to be conducted billions of years apart .

In WUM, Local Physics is linked with the large-scale structure of the Hypersphere World through the dimensionless quantity Q . The proposed approach to the fourth spatial dimension agrees with Mach's principle: "*Local physical laws are determined by the large-scale structure of the universe*". Applied to WUM, it follows that all parameters of the World depending on Q are a manifestation of the Worlds' curvature in the fourth spatial dimension.

Conclusion

In the Conclusion we postulate the principal role of Angular Momentum and Dark Matter in Cosmological theories of the World.

Dark Matter is abundant:

- 2.4 % of Ordinary Matter is in Superclusters, Galaxies, Stars, Planets, etc.
- 4.8 % of Ordinary Matter is in the Medium of the World;
- The remaining 92.8 % of mass is Dark Matter;
- WUM predicts existence of DM particles with 1.3 TeV, 9.6 GeV, 70 MeV, 340 keV, 3.7 keV, and 0.2 eV masses.

Based on the totality of the results obtained by WUM [1], we suggest adopting existence of Dark Matter in the World from the Classical Physics point of view.

To be consistent with the Law of Conservation of Angular Momentum we develop New Physics of the World:

- The Model introduces Dark Epoch (spanning from the Beginning of the World for 0.4 billion years) when only Dark Matter Particles existed, and Luminous Epoch (ever since for 13.8 billion years) when Dark Matter and Ordinary Matter exist;
- The main players of the World are overspinning DM Cores of Superclusters, which accumulated tremendous rotational angular momenta during Dark Epoch and transferred it to DM Cores of Galaxies during their Rotational Fission;
- Big Bang discussed in Standard Cosmology is a transition from Dark Epoch to Luminous Epoch due to Rotational Fission of Overspinning DM Supercluster's Cores;
- Dark Matter Core of Milky Way galaxy was born 13.8 billion years ago as the result of the Rotational Fission of the Local Supercluster DM Core;

- DM Cores of Extrasolar systems, planets and moons were born as the result of Gravitational Bursts of the Milky Way DM Core in different times (4.6 billion years ago for the Solar system);
- Proposed Weak Interaction between DMPs provides the integrity of DM Cores of all Macroobjects.

The Hypersphere World-Universe Model successfully describes primary cosmological parameters and their relationships, ranging in scale from cosmological structures to elementary particles. WUM allows for precise calculation of their values that were only measured experimentally earlier and makes verifiable predictions.

WUM does not attempt to explain all available cosmological data, as that is an impossible feat for any one manuscript. Nor does WUM pretend to have built an all-encompassing theory that can be accepted as is. The Model needs significant further elaboration, but in its present shape, it can already serve as a basis for a new Physics proposed by Paul Dirac in 1937. The Model should be developed into the well-elaborated theory by all physical community.

Acknowledgements

I am a Doctor of Sciences in Physics. I belong to the school of physicists established by Alexander Prokhorov – Nobel Prize Laureate in Physics. I am an author of more than 150 published papers, mostly in the area of Laser Physics. I am eternally grateful to Prof. A. M. Prokhorov and Prof. A. A. Manenkov, whose influence on my scientific life has been decisive.

For the past 18 years I have been developing a model I dubbed the World-Universe Model and published a serious of papers in the Journal of High Energy Physics, Gravitation and Cosmology (JHEPGC). I am much obliged to Prof. C. Corda for publishing my manuscripts in JHEPGC.

Many thanks to my long-term friend Felix Lev for stimulating discussions of history and philosophy of Physics and important comments on the Model. Special thanks to my son Ilya Netchitailo who questioned every aspect of the Model, gave valuable suggestions and helped shape it to its present form.

References

[1] Netchitailo, V. (2019) Dark Matter Cosmology and Astrophysics. *Journal of High Energy Physics, Gravitation and Cosmology*, **5**, 999-1050. doi: 10.4236/jhepgc.2019.54056.

[2] The Four Pillars of the Standard Cosmology. http://www.damtp.cam.ac.uk/research/gr/public/bb_pillars.html.

[3] Shortcomings of the Standard Cosmology. http://www.damtp.cam.ac.uk/research/gr/public/bb_problems.html.

[4] Couronne, I. and Ahmed, I. (2019) Top cosmologist's lonely battle against 'Big Bang' theory. https://phys.org/news/2019-11-cosmologist-lonely-big-theory.html.

[5] Silk, J. (2018) Towards the Limits of Cosmology. Foundations of Physics, **48**, 1305.

[6] Conover, E. (2019) Debate over the universe's expansion rate may unravel physics. Is it a crisis? ScienceNews. https://www.sciencenews.org/article/debate-universe-expansion-rate-hubble-constant-physics-crisis

[7] Verde, L., Treu, T., and Riess, A. G. (2019) Tensions between the Early and the Late Universe. arXiv:1907.10625.

[8] Keane, E.F., *et al.* (2016) A Fast Radio Burst Host Galaxy. https://doi.org/10.1038/nature17140.

[9] Wikipedia. Big Bang nucleosynthesis. https://en.wikipedia.org/wiki/Big_Bang_nucleosynthesis#cite_ref-13.
[10] M. Anders, *et al.* (2014) First Direct Measurement of the $^{2}H(\alpha,\gamma)^{6}Li$ Cross Section at Big Bang Energies and the Primordial Lithium Problem. Physical Review Letters, **113**, 042501.
[11] Burbidge, E.M., Burbidge, G.R., Fowler, W.A. and Hoyle, F. (1957) Synthesis of the Elements in Stars. Reviews of Modern Physics, **29**, 547.
[12] Lopez-Corredoira, M. (2017) Tests and problems of the standard model in Cosmology. arXiv:1701.08720.
[13] NASA (2015) The Cosmic Distance Scale. https://imagine.gsfc.nasa.gov/features/cosmic/local_supercluster_info.html.
[14] Karachentsev, I. (1987) Double Galaxies. 7.1. The Orbital and Internal Angular Momentum of Galaxies in Pairs. Izdatel'stvo Nauka. Moscow. https://ned.ipac.caltech.edu/level5/Sept02/Keel/Keel7.html.
[15] Toth, V. T. (2019) Is a black hole technically 2-dimensional? Quora. https://mail.google.com/mail/u/0/?tab=rm&ogbl#inbox/FMfcgxwGBmrfKchQCdbTTjWvmLcpPCpl.
[16] Cahill, D. (2014) Radio galaxy discovery near Earth spurs more questions. https://phys.org/news/2014-05-radio-galaxy-discovery-earth-spurs.html.
[17] Van Dokkum, P., *et al.* (2019) A High Stellar Velocity Dispersion and ~100 Globular Clusters for the Ultra Diffuse Galaxy Dragonfly 44. arXiv:1606.06291.
[18] Narayan, R., McClintock, J. E., and Yi, I. (1995) A New Model for Black Hole Soft X-ray Transients in Quiescence. arXiv:9508014.
[19] Gebhardt, K., Rich, R. M., and Luis Ho, L. (2002) A 20 Thousand Solar Mass Black Hole in the Stellar Cluster G1. arXiv:0209313.
[20] Chomiuk, L., *et al.* (2013) A Radio-Selected Black Hole X-ray Binary Candidate in the Milky Way Globular Cluster M62. arXiv:1306.6624.
[21] Giesers, B., *et al.* (2018) A detached stellar-mass black hole candidate in the globular cluster NGC 3201. arXiv:1801.05642.
[22] Liu, J., *et al.* (2019) A wide star-black-hole binary system from radial-velocity measurements. arXiv:1911.11989.
[23] Mersini-Houghton, L. (2014) Back-reaction of the Hawking radiation flux on a gravitationally collapsing star II. arXiv:1409.1837.
[24] Leane R. K. and Slatyer T. R. (2019) Revival of the Dark Matter Hypothesis for the Galactic Center Gamma-Ray Excess. Phys. Rev. Lett. **123**, 241101.
[25] Spolyar, D., Freese, K. and Gondolo, P. (2007) The Effect of Dark Matter and the First Stars: A New Phase of Stellar Evolution. AIP Conference Proceedings , 990, 42.
[26] Freese, K., Rindler-Daller, T., Spolyar, D., and Valluri, M. (2015) Dark Stars: A Review. arXiv:1501.02394.
[27] Lee, B.W. and Weinberg, S. (1977) Cosmological lower bound on heavy-neutrino masses. Phys. Rev. Lett. **39**, 165.
[28] Dicus, D.A., Kolb, E.W., and Teplitz, V.L. (1977) Cosmological upper bound on heavy-neutrino lifetimes. Phys. Rev. Lett. **39**, 168.
[29] Dicus, D.A., Kolb, E.W., and Teplitz, V.L. (1978) Cosmological implications of massive, unstable neutrinos. Astrophys. J. **221**, 327.
[30] Gunn, J.E., *et al.* (1978) Some astrophysical consequences of the existence of a heavy stable neutral lepton. Astrophys. J. **223**, 1015.
[31] Stecker, F.W. (1978) The cosmic gamma-ray background from the annihilation of primordial stable neutral heavy leptons. Astrophys. J. **223**, 1032.
[32] Zeldovich, Ya.B., Klypin, A.A., Khlopov, M.Yu., and Chechetkin, V.M. (1980) Astrophysical constraints on the mass of heavy stable neutral leptons. Sov. J. Nucl. Phys**. 31**, 664.
[33] Corda, C. (2009) Interferometric detection of gravitational waves: the definitive test for General Relativity. Int. J. Mod. Phys. **18**, 2275.

[34] Bertone, G. and Tait, T. M. P. (2018) A New Era in the Quest for Dark Matter. arXiv:1810.01668.
[35] Boehm, C., Fayet, P., Silk, J. (2003) Light and Heavy Dark Matter Particles. arXiv:0311143.
[36] Mehrgan, K., *et al.* (2019) A 40-billion solar mass black hole in the extreme core of Holm 15A, the central galaxy of Abell 85. arXiv:1907.10608.
[37] Riemann, B. (1854) On the Hypotheses which lie at the Bases of Geometry. Translated by William Kingdon Clifford .Nature, Vol. VIII. Nos. 183, 184, pp. 14–17, 36, 37.
[38] Bennett, C.L., *et al.* (2013) Nine-Year Wilkinson Microwave Anisotropy Probe (WMAP) Observations: Final Maps and Results. arXiv:1212.5225.
[39] Abbott, T. M. C., *et al.* (2017) Dark Energy Survey Year 1 Results: A Precise H0 Measurement from DES Y1, BAO, and D/H Data. arXiv:1711.00403.
[40] Freedman, W. L., *et al.* (2019) The Carnegie-Chicago Hubble Program. VIII. An Independent Determination of the Hubble Constant Based on the Tip of the Red Giant Branch. arXiv:1907.05922.
[41] Fixsen, D.J. (2009) The Temperature of the Cosmic Microwave Background. arXiv:0911.1955.
[42] Mirizzi, A., Raffelt, G.G., and Serpico, P.D. (2006) Photon-Axion Conversion in Intergalactic Magnetic Fields and Cosmological Consequences. arXiv:0607415.
[43] Bonetti, L., *et al.* (2017) FRB 121102 Casts New Light on the Photon Mass. arXiv:1701.03097.
[44] Lagache, G., *et al.* (1999) First detection of the Warm Ionized Medium Dust Emission. Implication for the Cosmic Far-Infrared Background. arXiv: 9901059.
[45] Tully, R.B. (1982) The Local Supercluster. Astrophysical Journal, **257**, 389. Bibcode:1982ApJ...257..389T. doi:10.1086/159999.
[46] Heymans, C., *et al.* (2008) The dark matter environment of the Abell 901/902 supercluster: a weak lensing analysis of the HST STAGES survey. arXiv:0801.1156.
[47] Zwicky, F. (1933) Die Rotverschiebung von extragalaktischen Nebeln. Helvetica Physica Acta, **6**, 110.
[48] Ness, M., *et al.* (2015) The Cannon: A data-driven approach to Stellar Label Determination. The Astrophysical Journal, **808**, 1. doi:10.1088/0004-637X/808/1/16.
[49] Bond, H. E., *et al.* (2013) HD 140283: A Star in the Solar Neighborhood that Formed Shortly After the Big Bang. arXiv:1302.3180.
[50] Marchetti, T., Rossi, E.M., Brown. A.G.A. (2018) Gaia DR2 in 6D: Searching for the fastest stars in the Galaxy. *Monthly Notices of the Royal Astronomical Society*, sty2592 https://doi.org/10.1093/mnras/sty2592.
[51] Koposov, S. E., *et al.* (2019) The Great Escape: Discovery of a nearby 1700 km/s star ejected from the Milky Way by Sgr A*. arXiv:1907.11725.
[52] A. Irrgang, A., *et al.* (2019) PG 1610+062: a runaway B star challenging classical ejection Mechanisms. arXiv:1907.06375.
[53] Clarke, C.J., *et al.* (2018) High-resolution Millimeter Imaging of the CI Tau Protoplanetary Disk: A Massive Ensemble of Protoplanets from 0.1 to 100 au. The Astrophysical Journal Letters, **866**, L6.
[54] Aguilar, D.A. and Pulliam, C. (2010) Astronomers Find Giant, Previously Unseen Structure in our Galaxy. Harvard-Smithsonian Center for Astrophysics. Release No. 2010-22.
[55] Yang, L. and Razzaque, S. (2019) Constraints on very high energy gamma-ray emission from the Fermi Bubbles with future ground-based experiments. arXiv:1811.10970v1.
[56] Su, M. and Finkbeiner, D.P. (2012) Evidence for Gamma-Ray Jets in the Milky Way. arXiv:1205.5852.
[57] Ponti, G., *et al.* (2019) An X-ray chimney extending hundreds of parsecs above and below the Galactic Centre. Nature **567**, 347–350.
[58] Hooper, D. and Slatyer, T.R. (2013) Two Emission Mechanisms in the Fermi Bubbles: A Possible Signal of Annihilating Dark Matter. arXiv:1302.6589.
[59] Hooper, D. and Goodenough, L. (2011) Dark matter annihilation in the Galactic Center as seen by the Fermi Gamma Ray Space Telescope. Physics Letters B, **697**, 412. doi:10.1016/j.physletb.2011.02.029.
[60] McDaniel, A., Jeltema, T. and Profumo, S. (2018) A Multi-Wavelength Analysis of Annihilating Dark Matter as the Origin of the Gamma-Ray Emission from M31. arXiv:1802.05258.

[61] Yang, H.Y.K., Ruszkowski, M., and Zweibel, E.G. (2018) Unveiling the Origin of the Fermi Bubbles. arXiv1802.03890.
[62] Beall, J.H. (2015) A Review of Astrophysical Jets. Proceedings of Science: 58. Bibcode: 2015mbhe.confE..58B . Retrieved 19 February 2017.

World-Universe Model Predictions

Abstract

In 2013, World-Universe Model (WUM) proposed principally different way to solve the problem of Newtonian Constant of Gravitation measurement precision. WUM revealed a self-consistent set of time-varying values of Primary Cosmological parameters of the World: Gravitation parameter, Hubble's parameter, Age of the World, Temperature of the Microwave Background Radiation, and the concentration of Intergalactic plasma. Based on the inter-connectivity of these parameters, WUM solved the Missing Baryon problem and predicted the values of the following Cosmological parameters: gravitation G, concentration of Intergalactic plasma, relative energy density of protons in the Medium, and the minimum energy of photons, which were experimentally confirmed in 2015 – 2018. Between 2013 and 2018, the relative standard uncertainty of G measurements decreased x6. The set of values obtained by WUM was recommended for consideration in CODATA Recommended Values of the Fundamental Physical Constants 2014.

Keywords. "World-Universe Model"; "Dimensionless Time-Varying Parameter Q"; "Gravitational Parameter"; "Hubble's Parameter"; "Age of the World"; "Temperature of Microwave Background Radiation"; "Temperature of Far-Infrared Background Radiation Peak"; "Medium of the World"; "Inter-Connectivity of Primary Cosmological Parameters"; "Multicomponent Dark Matter"; "Weak Interaction"; "Intergalactic Plasma"; "Neutrinos"; "CODATA"

1. Introduction

> *It doesn't make any difference how beautiful your guess is, it doesn't make any difference how smart you are, who made the guess, or what his name is. If it disagrees with experiment, it's wrong. That's all there is to it.*
>
> Richard Feynman

The very first "World-Universe Model" paper was published on viXra on March 2013. At that time great results were achieved:

- The cosmic Far-Infrared Background (FIRB) was announced in 1999. FIRB is part of the Cosmic Infrared Background with wavelengths near 100 microns that is the peak power wavelength of the black-body radiation at temperature $T_{FIRB} = 29\ K$ [1];
- Microwave Background Radiation (MBR) temperature $T_{MBR} = 2.72548 \pm 0.00057\ K$ was measured in 2009 [2];
- Nine-Year Wilkinson Microwave Anisotropy Probe (WMAP) Observations were published in 2013. The WMAP mission has resulted in a highly constrained ΛCDM cosmological model with precise and accurate parameters in agreement with a host of other cosmological measurements [3] (see Section 2.1).

In 2013, the most important for the Cosmology, Newtonian constant of gravitation G, proved too difficult to measure [4] (see analysis in Section 2.2). Its measurement precision was the worst among all Fundamental physical constants. In 2013 WUM proposed principally different way to solve the problem of G measurement precision and made some predictions of values of Primary Cosmological parameters [5], [6] (see Section 3.1).

2. Status of Primary Cosmological Parameters in 2013

2.1. WMAP Mission Results

The Big Bang Model (BBM) offers a comprehensive explanation for a broad range of observed phenomena. The framework for the BBM relies on General Relativity and on simplifying assumptions such as homogeneity and isotropy of space. The Lambda Cold Dark Matter (ΛCDM) model is a parametrization of the BBM in which the universe contains three major components: first, a Cosmological constant Λ associated with Dark Energy; second, the postulated Cold Dark Matter (CDM); and third, Ordinary Matter.

The ΛCDM model is based on six parameters: baryon density Ω_B , dark matter density Ω_{DM} , dark energy density Ω_Λ , scalar spectral index, curvature fluctuation amplitude, and reionization optical depth. The values of these six parameters are mostly not predicted by current theory; other possible parameters are fixed at "natural" values e.g. total density equals to 1.00, neutrino masses are small enough to be negligible.

WMAP team, following the ΛCDM model, found the best ΛCDM fit parameters and based on them derived Cosmological parameters including Age of the Universe $A_\tau = 13.772 \pm 0.059\ Gyr$ and Hubble parameter $H_0 = 69.32 \pm 0.8\ km/s\ Mpc$.

2.2. Newtonian Constant of Gravitation

Table 1, borrowed from CODATA Recommended Values of the Fundamental Physical Constants, 2010, summarizes the results of measurements of the Newtonian constant of gravitation [4].

Observe that the values of G vary significantly depending on Method. The disagreement in the values of G obtained by the various teams far exceeds the standard uncertainties provided with the values. Detailed analysis of these results shows that there are three groups of measurements. Inside each such group, the measurements are not mutually exclusive; however, measurements outside of a group contradict the entire group:

- The first such group consists of six measurements with the average value of

$$G_1 = 6.67401 \times 10^{-11}\ m^3 kg^{-1} s^{-2}$$

and relative standard uncertainty 28.5 ppm (ppm is one part per million);

- The second one consists of four measurements with the average value of

$$G_2 = 6.67250 \times 10^{-11}\ m^3 kg^{-1} s^{-2}$$

and relative standard uncertainty 24 ppm;

- The third one consists of one measurement with the value of

$$G_3 = 6.67539 \times 10^{-11}\ m^3 kg^{-1} s^{-2}$$

and relative standard uncertainty 40 ppm. The measurements falling into three groups are mutually exclusive; it is therefore likely that one group of measurements is correct, and the others are not.

Table 1. Summary of the results of measurements of the Newtonian constant of gravitation G relevant to the 2010 adjustment.

Source	Method	Value ($10^{-11}m^3kg^{-1}s^{-2}$)	Rel. stand. uncert. ppm
Luther and Towler (1982)	Fiber torsion balance, dynamic mode	6.67248(43)	64
Karagioz and Izmailov (1996)	Fiber torsion balance, dynamic mode	6.6729(5)	75
Bagley and Luther (1997)	Fiber torsion balance, dynamic mode	6.67398(70)	100
Gundlach and Merkowitz (2000,2002)	Fiber torsion balance, dynamic compensation	6.674255(92)	14
Quinn *et al*. (2001)	Strip torsion balance, compensation mode, static deflection	6.67559(27)	40
Kleinevoss (2002); Kleinevoss *et al*. (2002)	Suspended body, displacement	6.67422(98)	150
Armstrong and Fitzgerald (2003)	Strip torsion balance, compensation mode	6.67387(27)	40
Hu, Guo, and Luo (2005)	Fiber torsion balance, dynamic mode	6.67228(87)	130
Schlamminger *et al*. (2006)	Stationary body, weight change	6.67425(12)	19
Luo *et al*. (2009); Tu *et al*. (2010)	Fiber torsion balance, dynamic mode	6.67349(18)	27
Parks and Faller (2010)	Suspended body, displacement	6.67234(14)	21

3. Ordinary Matter

3.1. Fundamental Parameter Q. Recommended Values of the Newtonian Parameter of Gravitation, Hubble's Parameter, Age of the World, and Temperature of the Microwave Background Radiation

The constancy of the Universe Fundamental constants, including Newtonian constant of gravitation G, is now commonly accepted, although has never been firmly established as a fact. All conclusions on the constancy of G are model-dependent [5]. In our opinion, it is impossible to either prove or disprove the constancy of G. Consequently, variability of G with time can legitimately be explored. Alternative cosmological models describing the Universe with time-varying G are widely discussed in literature (see e.g. [5] and references therein).

WUM is based on two parameters: dimensionless Rydberg constant $\alpha = (2aR_\infty)^{1/3}$, where R_∞ is Rydberg constant, a is the basic unit of size (classical electron radius equals to: $a_0 = a/2\pi$); and a dimensionless time-varying parameter Q, which is a measure of a Size R and Age A_τ of the World: $Q = R/a = A_\tau/t_0$, where $t_0 = a/c$ is the basic unit of time and c is the gravitodynamic constant.

In the present Epoch, the calculated value of Q based on the average value of the Gravitational parameter in 2018 is:

$$Q = 0.759972 \times 10^{40}$$

A commonly held opinion states that gravity has no established relation to other fundamental forces, so it does not appear possible to calculate it indirectly from other constants that can be measured more accurately, as is done in some other areas of physics. WUM holds that there indeed exist relations between all Q-dependent, time-varying parameters: Newtonian Parameter of Gravitation G, Hubble's parameter H_0, Age of the World A_τ, Temperature of the microwave background radiation T_{MBR}, Critical energy density of the World ρ_{cr}, Photon minimum energy E_{ph}, etc. [5]. In frames of WUM, all Primary Cosmological parameters are inter-connected [7].

In accordance with WUM, the primary parameters of the World can be expressed as follows [5]:

- Newtonian parameter of gravitation G

$$G = \frac{a^2 c^4}{8\pi h c} \times Q^{-1}$$

- Hubble's parameter H_0

$$H_0 = \frac{c}{a} \times Q^{-1}$$

- Age of the World A_τ

$$A_\tau = \frac{a}{c} \times Q$$

- Temperature of the microwave background radiation T_{MBR}

$$T_{MBR} = \frac{E_0}{k_B}\left(\frac{15\alpha}{2\pi^3}\frac{m_e}{m_p}\right)^{1/4} \times Q^{-1/4}$$

where k_B is Boltzmann constant; m_p is the mass of a proton; m_e is the mass of an electron and a basic unit of energy E_0 equals to $E_0 = hc/a = 0.070025267\ GeV$, where h is Plank constant.

In 2013, the following two parameters were measured with the best precision: G (120 ppm) and T_{MBR} (210 ppm). At that time, we could calculate the value of Q_G based on the average value of G_{2010}:

$$Q_G = 0.760000 \times 10^{40}$$

and using Q_G, substantially increase the precision of other parameters. With the help of WUM, more precise measurement of T_{MBR} can help us narrow down the correct group of G measurements. The right group of the measurements of G can be selected once the relative standard uncertainty of the measurement of T_{MBR} becomes significantly better than 30 ppm, but it is not the case. Then the choice of the correct group of G measurements would appear to be a hopeless goal.

In frames of WUM, we succeeded to find the following equation for Fermi Coupling parameter G_F [6]:

$$\frac{G_F}{(\hbar c)^3} = \sqrt{30}\left(2\alpha\frac{m_e}{m_p}\right)^{1/4}\frac{m_p}{m_e}\frac{1}{E_0^2} \times Q^{-1/4}$$

where $\hbar$ is Dirac constant: $\hbar = h/2\pi$. We used the average value of G_F with relative standard uncertainty 4.3 ppm in 2010 and calculated the value of parameter Q_F

$$Q_F = 0.759960 \times 10^{40}$$

Then the value of the predicted parameter $\boldsymbol{G}$ in this case equals to

$$\boldsymbol{G} = 6.67420 \times 10^{-11}\ m^3 kg^{-1} s^{-2}$$

that is close to the value of G_1 for the first group

$$G_1 = 6.67401 \times 10^{-11}\ m^3 kg^{-1} s^{-2}$$

WUM calculates the value of the temperature of the microwave background radiation:

$$T_{MBR} = 2.72522\ K$$

that is in excellent agreement with experimentally measured value [2]:

$$T_{MBR} = 2.72548 \pm 0.00057\ K$$

We are not aware of any other model that allows calculation of MBR temperature with such accuracy.

WUM calculates the value of the Hubble's parameter:

$$H_0 = 68.7494\ km/s\ Mpc$$

which is in good agreement with the derived by WMAP team value [3]:

$$H_0 = 69.32 \pm 0.8\ \ km/s\ Mpc$$

and with the newest value of

$$H_0 = 69.6 \pm 0.8\ (\pm 1.1\%\ stat) \pm 1.7\ (\pm 2.4\%\ sys)\ \ km/s\ Mpc$$

found by W. L. Freedman, *et al.* using the revised (and direct) measurement of the LMC (Large Magellanic Cloud) TRGB (Tip of the Red Giant Branch) extinction [8].

It is worth to note that the situation with the measurement accuracy of the Hubble's parameter in 2019 [9] looks the same as it was with the measurement accuracy of the gravitation parameter in 2013. We hope that WUM will prove helpful in determining the correct methods of measurement of the Hubble's parameter.

WUM calculates the Age of the World:

$$A_\tau = 14.2226\ Gyr$$

that is much longer than the value derived by WMAP team

$$A_\tau = 13.772 \pm 0.059\ Gyr$$

In frames of WUM, the difference between them $0.45\ Gyr$ is the longevity of Dark Epoch [7].

To summarize: parameters G, H_0, A_τ, and T_{MBR} are all inter-connected. The first group of G_1 measurements is correct.

When these results were obtained, we sent the following letter to every member of the CODATA Task Group on Fundamental Physical Constants and every participant of the Royal Society Meeting [10]:

In 1937, Paul Dirac proposed a new basis for cosmology: the hypothesis of a variable gravitational "constant"; and later added the notion of continuous creation of matter in the World. My World – Universe Model follows these ideas, albeit introducing a different mechanism of matter creation. The

proposed Model provides a mathematical framework based on a few basic assumptions, that allows to calculate the primary parameters of the World (its size, age, Hubble's parameter, the temperature of the cosmic microwave background radiation, masses of neutrinos and dark matter particles, etc.), in good agreement with the most recent measurements and observations. The Model published on viXra http://vixra.org/abs/1303.0077 v7*.*

Recently I published on viXra http://vixra.org/abs/1312.0179 *v2 a new paper which gives the self-consistent set of Q-dependent, time varying values of the basic parameters of the World: Fermi Coupling parameter, Newtonian parameter of Gravitation, Hubble's parameter, Age of the World, and Temperature of the Microwave Background Radiation. It describes in detail the adjustment of the values of the parameters based on the World – Universe Model. The obtained set of values is recommended for consideration in CODATA Recommended Values of the Fundamental Physical Constants 2014.*

Terry Quinn in the paper "Outcome of the Royal Society meeting on G held at Chicheley Hall on 27 and 28 February 2014 to discuss 'The Newtonian constant of gravitation, a constant too difficult to measure?' concluded [11]:

"*Thus, instead of simply calling for new determinations of G, it is suggested that an international advisory board be created, made up largely of those who have already carried out a G experiment, to advise on the choice of method or methods, on the design of the experiment, on its construction and finally on the interpretation of the data and calculation of the results. This would be in contrast to the present situation in which outside criticism and comments can be brought to bear only when the experiment is finished and published when it is too late to affect the outcome. It is only by proceeding in this way that one might hope to obtain results that are demonstrably reliable*".

At the time, CODATA stated the following value of G_{2010} :

$$G_{2010} = 6.67384 \times 10^{-11}\ m^3 kg^{-1} s^{-2}$$

with relative uncertainty of 120 ppm. To the best of our knowledge, no breakthrough in G measurement methodology has been achieved since. Nevertheless, in 2015 CODATA recommended a more precise value of the Newtonian constant of gravitation

$$G_{2014} = 6.67408 \times 10^{-11}\ m^3 kg^{-1} s^{-2}$$

with relative standard uncertainty 47 ppm [12]. In 2018 the recommendation improved further:

$$G_{2018} = 6.67430 \times 10^{-11}\ m^3 kg^{-1} s^{-2}$$

with relative standard uncertainty 22 ppm [13]. Since 2013, the relative standard uncertainty of G measurements reduced from 120 ppm to 22 ppm!

The variations of the average values of G_{2014} and G_{2018} around the predicted value of $\boldsymbol{G}$ are:

$$\frac{G_{2018}}{G_{2014}} = \boldsymbol{G}^{+0.00010}_{-0.00012}$$

Compare this result with the variations of the average values of G_2 and G_3 around the average value of G in 2010:

$$\frac{G_3}{G_2} = G^{+0.00155}_{-0.00134}$$

which are by order of magnitude larger than the variations of G_{2014} and G_{2018} around the predicted value of $\boldsymbol{G}$.

It seems that CODATA considered the WUM recommendation that the first group of G_1 measurements is correct. In any case, the predicted by WUM in 2013 value of the Gravitational parameter is in an excellent agreement with its accepted value in 2014 [12] and in 2018 [13].

In 2014, WUM calculated the stationary temperature of Cosmic Large Grains based on the thermo-equilibrium that corresponds to the FIRB temperature peak [14]:

$$T_{FIRB} = \frac{E_0}{k_B}\left(\frac{15\alpha}{4\pi^5}\right)^{1/4} \times Q^{-1/4}$$

and obtained $T_{FIRB} = 28.955\ K$, which is in good agreement with experimentally measured value of $29\ K$ [1]. Comparing equations for T_{MBR} and T_{FIRB}, we can find the relation between them [14]:

$$T_{FIRB} = (3\Omega_e)^{-1/4} \times T_{MBR}$$

where Ω_e is the relative energy density of electrons in the Medium of the World in terms of the critical energy density ρ_{cr} [5]:

$$\Omega_e = \frac{2\pi^2\alpha}{3}\frac{m_e}{m_p}$$

3.2. Missing Baryon Problem

The Missing Baryon Problem related to the fact that the observed amount of baryonic matter did not match theoretical predictions. Observations by the Planck spacecraft in 2015, yielded a theoretical value for baryonic matter of 4.85% of the contents of the Universe [15]. However, directly adding up all the known baryonic matter produces a baryonic density slightly less than half of this [16]. The missing baryons are believed to be located in the warm–hot intergalactic medium.

The existence of the Medium of the World is a principal point of WUM. It follows from the observations of Intergalactic Plasma; Cosmic Microwave Background Radiation; Far-Infrared Background Radiation. There is no empty space (vacuum) in WUM. Inter-galactic voids discussed by astronomers are in fact examples of the Medium in its purest [5].

Detailed analysis of Intergalactic plasma carried out in 2013 [5] showed that the concentration of protons n_p and electrons n_e can be found by the following equation:

$$n_p = n_e = \frac{2\pi^2}{a^3}\frac{m_e}{m_p} \times Q^{-1}$$

$\rho_p = n_p E_p$ is the energy density of protons in the Medium. The relative energy density of protons in the Medium Ω_p is then the ratio of ρ_p/ρ_{cr}:

$$\Omega_p = \frac{2\pi^2\alpha}{3} = 0.048014655$$

According to WUM, the relative energy density of baryons in Macroobjects Ω_{MO} is:

$$\Omega_{MO} = \frac{1}{2}\Omega_p = \frac{\pi^2\alpha}{3} = 0.024007318$$

The calculated values of Ω_p and Ω_{MO} are in good agreement with their 2015 estimations [15], [16].

In our opinion, direct measurements of the Intergalactic plasma parameters can be done by investigations of Fast Radio Bursts, which are millisecond duration radio signals originating from distant galaxies. These signals are dispersed according to a precise physical law and this dispersion is a key observable quantity which, in tandem with a redshift measurement, can be used for fundamental physical investigations [17].

The dispersion measure and redshift, carried out in 2016 by E. F. Keane, *et al.*, provide a direct measurement of the cosmic density of ionized baryons in the intergalactic medium Ω_{IGM} [17]:

$$\Omega_{IGM} = 4.9 \pm 1.3\%$$

that is in excellent agreement with the predicted by WUM value of Ω_p. Using the equation for n_e, we calculated the value of photons' time delay [18]:

$$\Delta t_{ph}^{cal} = 2.189 \times (\frac{\nu}{1GHz})^{-2}$$

which is in good agreement with experimentally measured value [17]:

$$\Delta t_{ph}^{exp} = 2.438 \times (\frac{\nu}{1GHz})^{-2}$$

To summaries: the values of the Intergalactic plasma parameters predicted by WUM in 2013 are confirmed by experiments conducted in 2016.

3.3. Energy-Varying Photons

Analysis of Intergalactic plasma shows that the value of the lowest plasma frequency ν_{pl} is [5]:

$$\nu_{pl} = \frac{c}{a}(\frac{m_e}{m_p})^{1/2} \times Q^{-1/2} = 4.5322\ Hz$$

Photons with energy smaller than $E_{ph} = h\nu_{pl}$ cannot propagate in plasma, thus $h\nu_{pl}$ is the smallest amount of energy a photon may possess. Following L. Bonetti, *et al.* [19] we can call this amount of energy the rest energy of photons that equals to

$$E_{ph} = \left(\frac{m_e}{m_p}\right)^{1/2} E_0 \times Q^{-1/2} = 1.8743 \times 10^{-14}\ eV$$

The above value, predicted by WUM in 2013, is in good agreement with the value

$$E_{ph} \lesssim 2.2 \times 10^{-14}\ eV$$

obtained by L. Bonetti, *et al.* in 2017 [19]. It is more relevant to call E_{ph} the minimum energy of photons which can pass through the Intergalactic plasma. It is worth to note that E_{ph} is varying in time: $E_{ph} \propto \tau^{-1/2}$.

3.4. Mass-Varying Neutrinos

It is now established that there are three different types of neutrino: electronic ν_e, muonic ν_μ, and tauonic ν_τ. Neutrino oscillations imply that neutrinos have non-zero masses. The neutrino was postulated first by Wolfgang Pauli in 1930 to explain how beta decay could conserve energy, momentum, and angular momentum (spin). But we still don't know the values of neutrino masses.

Experimentalists are measuring Δm^2_{sol} and Δm^2_{atm} , which are mass splitting for solar and atmospheric neutrinos respectively.
The situation with Dark Matter Particles (DMPs) is similar: we can investigate them indirectly by the analysis of gamma-rays and X-rays irradiated as the result of DMPs self-annihilation (see Section 4.1).

In 2013, WUM predicted the following values of neutrino mass eigenstates:

$$m_{\nu_\mu} = m_0 \times Q^{-1/4} \cong 7.5 \times 10^{-3}\ eV/c^2$$

$$m_{\nu_\tau} = 6 m_{\nu_\mu} \cong 4.5 \times 10^{-2}\ eV/c^2$$

$$m_{\nu_e} = \frac{1}{24} m_{\nu_\mu} \cong 3.1 \times 10^{-4}\ eV/c^2$$

where m_0 is a basic unit of mass: $m_0 = h/ac$. The sum of the predicted neutrino masses

$$\Sigma m_\nu \cong 0.053\ eV/c^2$$

is in good agreement with the value of 0.06 eV/c^2 discussed in literature [20]. It is worth to note that m_ν is varying in time: $m_\nu \propto \tau^{-1/4}$.

As the conclusion, in 2013-2014 WUM gave the following results for Ordinary Matter:

- Calculated the values of parameters H_0 , T_{MBR} , T_{FRIB} , that are in good agreement with experimental results;
- Predicted the values of cosmological parameters G , n_p , Ω_p , E_{ph} , which were confirmed experimentally in 2015 – 2018;
- Predicted the values of neutrino masses.

4. Dark Matter

4.1. Multicomponent Dark Matter

Dark Matter (DM) is among the most important open problems in both cosmology and particle physics. Dark Matter Particles (DMPs) might be observed in Centers of Macroobjects has drawn many new researchers to the field in the last forty years [7]. Important cosmological problems like Dark Matter and Dark Energy could be, in principle, solved through extended gravity. This is stressed, for example, in the famous paper of Prof. C. Corda [21].

Two-component DM system consisting of bosonic and fermionic components is proposed for the explanation of emission lines from the bulge of Milky Way galaxy. C. Boehm, P. Fayet, and J. Silk analyze the possibility of two coannihilating neutral and stable DMPs: a heavy fermion for example, like the lightest neutralino ($>$ 100 GeV) and the other one a possibly light spin-0 particle ($\sim$ 100 MeV) [22].

WUM proposes multicomponent DM system consisting of two couples of coannihilating DMPs: a heavy DM fermion – DMF1 (1.3 TeV) and a light spin-0 boson – DIRAC (70 MeV) that is a dipole of Dirac's monopoles; a heavy fermion – DMF2 (9.6 GeV) and a light spin-0 boson – ELOP (340 keV) that is a dipole of preons with electrical charge e/3; a self-annihilating fermion – DMF3 (3.7 keV) and a fermion DMF4 (0.2 eV).

WUM postulates that masses of DMFs and bosons are proportional to m_0 multiplied by different exponents of α and can be expressed with the following formulae [5], [7]:

DMF1 (fermion): $m_{DMF1} = \alpha^{-2} m_0 = 1.3149950\ TeV$

DMF2 (fermion): $m_{DMF2} = \alpha^{-1} m_0 = 9.5959823\ GeV$

DIRAC (boson): $m_{DIRAC} = \alpha^{0} m_0 = 70.025267\ MeV$

ELOP (boson): $m_{ELOP} = 2/3\alpha^{1} m_0 = 340.6660\ keV$

DMF3 (fermion): $m_{DMF3} = \alpha^{2} m_0 = 3.7289402\ keV$

DMF4 (fermion): $m_{DMF4} = \alpha^{4} m_0 = 0.19857111\ eV$

The values of mass of DMF1, DMF2, and DMF3 fall into the ranges estimated in literature for neutralinos, WIMPs, and sterile neutrinos respectively. DMF1, DMF2 and DMF3 partake in the self-annihilation interaction with strength equals to α^{-2}, α^{-1} and α^{2} respectively [5].

The widely discussed models for nonbaryonic DM are based on the Cold DM hypothesis, and corresponding particles are commonly assumed to be WIMPs, which interact via gravity and any other force (or forces), potentially not part of the standard model itself, which is as weak as or weaker than the weak nuclear force, but also non-vanishing in its strength. It follows that a new weak force needs to exist, providing interaction between DMPs. The strength of this force exceeds that of gravity, and its range is considerably greater than that of the weak nuclear force [7].

In WUM, strength of the proposed weak interaction is characterized by the parameter G_W :

$$G_W = G_0 \times Q^{-1/4}$$

where $G_0 = \frac{a^2 c^4}{8\pi hc}$ is an extrapolated value of G at the Beginning of the World (Q=1). In the present Epoch, $Q = 0.759972 \times 10^{40}$, and thus G_W is about 30 orders of magnitude greater than G.

The range of the weak interaction R_W in the present Epoch equals to:

$$R_W = a \times Q^{1/4} = 1.65314 \times 10^{-4}\ m$$

that is much greater than the range of the weak nuclear force. The predicted Weak Interaction between DMPs provides integrity of all DM shells in all Macroobjects. In our view, the foretold weak interaction between particles DMF3 provides integrity of Fermi Bubbles [7].

The signatures of DMPs annihilation with predicted masses of 1.3 TeV, 9.6 GeV, 70 MeV, 340 keV, and 3.7 keV, which are calculated independently of astrophysical uncertainties, are found in spectra of the diffuse gamma-ray background and the emission of various Macroobjects in the World. The correlation between different emission lines in spectra of Macroobjects is connected to their structure, which depends on the composition of the Core and surrounding shells made up of DMPs. Thus, the diversity of Very High Energy gamma-ray sources in the World has a clear explanation [23].

4.2. Predicted Distribution of the World's Energy Density

According to WUM, the total DMF4 relative energy density ρ_{DMF4}, in terms of proton energy density in the Medium of the World $\rho_p = \frac{2\pi^2\alpha}{3}\rho_{cr}$, equals to [7]:

$$\rho_{DMF4} = \frac{45}{\pi}\rho_p = 30\pi\alpha\rho_{cr} = 0.68775927\rho_{cr}$$

Our Model holds that the energy density of all types of self-annihilating DMPs is proportional to ρ_p. In all, there are 5 different types of self-annihilating DMPs: DMF1, DMF2, DIRAC, ELOP, and DMF3. Then the total energy density of DM ρ_{DM} is

$$\rho_{DM} = 5\rho_p = 0.24007327\rho_{cr}$$

The total baryonic energy density ρ_B is:

$$\rho_B = 1.5\rho_p$$

The sum of electron and MBR energy densities ρ_{eMBR} equals to:

$$\rho_{eMBR} = 1.5\frac{m_e}{m_p}\rho_p + 2\frac{m_e}{m_p}\rho_p = 3.5\frac{m_e}{m_p}\rho_p$$

We take energy density of neutrinos ρ_ν to equal:

$$\rho_\nu = \rho_{MBR}$$

For FIRB radiation energy density ρ_{FIRB} we take

$$\rho_{FIRB} = \frac{1}{5\pi}\frac{m_e}{m_p}\rho_p \approx 0.032\rho_{MBR}$$

which corresponds to the value of $0.034\,\rho_{MBR}$ calculated by E. L. Wright [24]. Then the energy density of the World ρ_W in Luminous Epoch equals to the theoretical critical energy density ρ_{cr}

$$\rho_W = \left[\frac{45}{\pi} + 6.5 + \left(5.5 + \frac{1}{5\pi}\right)\frac{m_e}{m_p}\right]\rho_p = \rho_{cr}$$

From this equation we can calculate the value of $1/\alpha$ using electron-to-proton mass ratio m_e/m_p

$$\frac{1}{\alpha} = \frac{\pi}{15}\left[450 + 65\pi + (55\pi + 2)\frac{m_e}{m_p}\right] = 137.03600$$

which is in excellent agreement with the commonly adopted value of 137.035999. It follows that there is a direct correlation between constants α and m_e/m_p expressed by the obtained equation. As shown, m_e/m_p is not an independent constant but is instead derived from α [7].

As the conclusion, according to WUM:

- The World's energy density is inversely proportional to the dimensionless time-varying parameter $Q \propto \tau$ in all cosmological times;
- The particles relative energy densities are proportional to constant α in Luminous Epoch.

5. Hypersphere World-Universe Model

> *The sciences do not try to explain, they hardly even try to interpret, they mainly make models. By a model is meant a mathematical construct, which, with addition of certain verbal interpretations describes observed phenomena. The justification of such a mathematical construct is solely and precisely that it is expected to work.*
>
> John von Newmann

The Hypersphere World-Universe model is the only cosmological model in existence that [7]:

- Is consistent with the Law of conservation of angular momentum, and answers the following questions: why is the orbital momentum of Jupiter larger than rotational momentum of Sun, and how did Milky Way galaxy and Solar system obtain their substantial orbital angular momentum?
- Reveals the Inter-connectivity of primary cosmological parameters of the World (Age, Size, Hubble's parameter, Newtonian parameter of gravitation, Critical energy density, Concentration of Intergalactic Plasma, Temperature of the Microwave Background Radiation, Temperature of the Far-Infrared Background Radiation Peak) and calculates their values, which are in good agreement with experimental results;
- Considers Fermi Bubbles (FBs) built up from Dark Matter Particles (DMPs), and explains X-rays and gamma-rays radiated by FBs as a result of DMPs annihilation;
- Solves Coronal heating problem that relates to the question of why the temperature of the Solar corona is millions of degrees higher than that of the photosphere. In WUM, the Solar corona is made up of DMPs, and the plasma is the result of their annihilation. The Solar corona resembles a honeycomb filled with plasma. The Geocorona and Planetary Coronas possess features similar to these of the Solar Corona;
- Explains the diversity of Very High Energy gamma-ray sources in the World in frames of the proposed Macroobject (MO) Shell Model, which describes Cores of MOs as Nuclei made up of annihilating Dark Matter Fermions (DMFs) surrounded by shells containing other DMPs;
- Explains the diversity of gravitationally-rounded objects (planets and moons in Solar system) and their internal heat through annihilation of DMFs in their Cores.

WUM envisions the following picture of creation and evolution of the World [7]:

- Overspinning (surface speed at equator exceeding escape velocity) DM Cores of Superclusters initiate creation of all World's Macrostructures;
- The outer shells of Supercluster's Cores are composed of DMF4 with mass of 0.2 eV and total energy density of 68.8% of the overall energy density of the World;
- Proposed Weak Interaction between DMPs provides the integrity of Dark Matter (DM) Cores of all MOs;
- DMF4 outer shells of Supercluster's Cores are growing to the critical mass during Dark Epoch lasting from the Beginning of the World (14.22 billion years ago) for 0.45 billion years;
- Luminous Galaxies and Extrasolar Systems arise due to Rotational Fission of Overspinning Supercluster's Cores and annihilation of DMPs;
- Macrostructures of the World form from Superclusters down to Galaxies, Extrasolar systems, planets, and moons. Formation of galaxies and stars is not a process that concluded ages ago; instead, it is ongoing in the Luminous Epoch;
- Luminous Epoch spans from 0.45 billion years up to the present Epoch for 13.77 billion years. The Big Bang discussed in the standard cosmological model is, in our view, the transition from Dark Epoch to Luminous Epoch.

In frames of WUM, Time and Space are closely connected with Mediums' impedance and gravitomagnetic parameter. It follows that neither Time nor Space could be discussed in absence of the Medium. The gravitational parameter G that is proportional to the Mediums' energy density can be introduced only for the Medium filled with Matter. Gravity, Space and Time are all emergent phenomena [7].

WUM confirms the Supremacy of Matter postulated by Albert Einstein: "*When forced to summarize the theory of relativity in one sentence: time and space and gravitation have no separate existence from matter*".

WUM is based on two parameters only: dimensionless Rydberg constant α and dimensionless time-varying quantity Q. In WUM we often use well-known physical parameters, keeping in mind that all of them can be expressed through the Basic Units of time t_0, size a, and energy E_0. For example, $c = a/t_0$ and $h = E_0 \times t_0$. Taking the relative values of physical parameters in terms of the Basic Units we can express all dimensionless parameters of the World through two parameters α and Q in various rational exponents, as well as small integer numbers and π [25].

There are no Fundamental Physical Constants in WUM. In our opinion, constant α and quantity Q should be named "Universe Constant" and "World Parameter" respectively.

The Hypersphere World–Universe Model successfully describes primary cosmological parameters and their relationships, ranging in scale from cosmological structures to elementary particles. WUM predicted in 2013 the values of cosmological parameters G, n_p, Ω_p, E_{ph}, which were confirmed experimentally in 2015 – 2018. The Model allows for precise calculation of values that were only measured experimentally earlier and makes verifiable predictions.

Acknowledgements

I'm grateful to my son Ilya Netchitailo who has reviewed and edited this work.

References

[1] Lagache, G., *et al.* (1999) First detection of the WIM dust emission. Implication for the Cosmic Far-Infrared Background. arXiv:astro-ph/9901059.
[2] Fixsen, D.J. (2009) The Temperature of the Cosmic Microwave Background. arXiv:0911.1955.
[3] C. L. Bennett, *et al.* (2013) Nine-Year Wilkinson Microwave Anisotropy Probe (WMAP) Observations: Final Maps and Results. arXiv:1212.5225v3.
[4] Mohr, P. J., Taylor, B. N., and Newell, D. B. (2012) CODATA Recommended Values of the Fundamental Physical Constants: 2010. arXiv:1203.5425.
[5] Netchitailo V. S. (2013) Word-Universe Model. viXra:1303.0077.
[6] Netchitailo V. S. (2013) Fundamental Parameter Q. Recommended Values of the Newtonian Parameter of Gravitation, Hubble's Parameter, Age of the World, and Temperature of the Microwave Background Radiation. viXra:1312.0179.
[7] Netchitailo, V. (2019) Dark Matter Cosmology and Astrophysics. *Journal of High Energy Physics, Gravitation and Cosmology*, **5**, 999-1050. DOI: 10.4236/jhepgc.2019.54056
[8] Freedman, W. L., *et al.* (2020) Calibration of the Tip of the Red Giant Branch (TRGB). arXiv:2002.01550.
[9] Conover, E. (2019) Debate over the Universe's Expansion Rate May Unravel Physics. Is It a Crisis? ScienceNews.
https://www.sciencenews.org/article/debate-universe-expansion-rate-hubble-constant-physics-crisis.
[10] Quinn, T., Speake, C., and Luo, J. (2014) The Newtonian constant of gravitation, a constant too difficult to measure? The Royal Society Meeting. London, Feb. 27-28. https://royalsociety.org/science-events-and-lectures/2014/gravitation/.
[11] Quinn, T. (2014) Outcome of the Royal Society meeting on G held at Chicheley Hall on 27 and 28 February 2014 to discuss 'The Newtonian constant of gravitation, a constant too difficult to measure?". Phil. Trans. R. Soc. **A 372**. https://doi.org/10.1098/rsta.2014.0286

[12] Mohr, P. J., Newell, D. B., and Taylor, B. N. (2015) CODATA Recommended Values of the Fundamental Physical Constants:2014. arXiv:1507.07956.
[13] NIST (2018) CODATA RECOMMENDED VALUES OF THE FUNDAMENTAL PHYSICAL CONSTANTS: 2018. https://physics.nist.gov/cuu/pdf/wall_2018.pdf.
[14] Netchitailo V. S. (2014) World-Universe Model. Cosmic Far-Infrared Background. viXra:1412.0265.
[15] Ade, P. A. R., *et al.* (2015) Planck 2015 results. XIII. Cosmological parameters. arXiv:1502.01589.
[16] Ferguson, H. C. The Case of the "Missing Baryons". https://archive.stsci.edu/hut/astro2/astro2_science/starburst.html.
[17] Keane, E. F., *et al.* (2016) A Fast Radio Burst Host Galaxy. arXiv:1602.07477.
[18] Netchitailo, V. (2017) Burst Astrophysics. *Journal of High Energy Physics, Gravitation and Cosmology*, **3**, 157-166. DOI: 10.4236/jhepgc.2017.32016.
[19] Bonetti, L., *et al.* (2017) FRB 121102 Casts New Light on the Photon Mass. arXiv:1701.03097.
[20] Battye, R.A. and Moss, A. (2013) Evidence for Massive Neutrinos from CMB and Lensing Observations. arXiv: 1308.5870.
[21] Corda, C. (2009) Interferometric Detection of Gravitational Waves: The Definitive Test for General Relativity. International Journal of Modern Physics , 18, 2275-2282.
[22] Boehm, C., Fayet, P., and Silk, J. (2003) Light and Heavy Dark Matter Particles. arXiv:0311143.
[23] Netchitailo V. S. (2014) World-Universe Model. Multicomponent Dark Matter. Cosmic Gamma-Ray Background. viXra:1406.0018.
[24] Wright, E.L. (2001) Cosmic InfraRed Background Radiation. http://www.astro.ucla.edu/~wright/CIBR/.
[25] Netchitailo, V. (2020) World-Universe Model – Alternative to Big Bang Model. *Journal of High Energy Physics, Gravitation and Cosmology*, **6**, 133-158. DOI**:** 10.4236/jhepgc.2020.61012.

World-Universe Model. Self-Consistency of Fundamental Physical Constants

Abstract

Every four years the Committee on Data for Science and Technology (CODATA) provides a self-consistent set of values of the basic constants and conversion factors of physics recommended for international use. In 2013, the World-Universe Model (WUM) proposed a principally different depiction of the World as an alternative to the picture of the Big Bang Model. This article makes a detailed analysis of the self-consistency of Fundamental Physical Constants through the prism of WUM. The performed analysis suggests: discontinuing using the notion "Vacuum" and its characteristics (Speed of Light in Vacuum, Characteristic Impedance of Vacuum, Vacuum Magnetic Permeability, Vacuum Electric Permittivity); correcting the numerical value and relative standard uncertainty of Hartree energy; accepting the exact numerical values of Planck constant and Elementary charge. WUM recommends the predicted value of Newtonian Constant of Gravitation (x8 more accurate than the 2018 value) to be considered in CODATA Recommend Values of the Fundamental Physical Constants 2022.

Keywords

"World-Universe Model"; "Fundamental Physical Constants"; "Self-Consistency"; "Medium of World"; "Maxwell's Equations"; "Newtonian Constant of Gravitation"; "Rydberg Constant"; "Hartree Energy"; "Planck Constant"; "Elementary Charge"; "Characteristic Impedance"; "Fermi Coupling Constant"

1. Introduction

> *It doesn't make any difference how beautiful your guess is, it doesn't make any difference how smart you are, who made the guess, or what his name is. If it disagrees with experiment, it's wrong. That's all there is to it.*
>
> Richard Feynman

The very first manuscript "World-Universe Model" (WUM) was published on viXra in March 2013. At that time great results in Cosmology were achieved:

- The cosmic Far-Infrared Background was announced in 1999 [1];
- Microwave Background Radiation temperature was measured in 2009 [2];
- Nine-Year Wilkinson Microwave Anisotropy Probe Observations were published in 2012 [3].

At the same time, the most important for the Cosmology, Newtonian constant of gravitation G, proved too difficult to measure [4]. Its measurement precision was the worst among all Fundamental physical constants.

To resolve the problem T. Quinn, C. Speake, and J. Luo organized the Royal Society meeting named "The Newtonian constant of gravitation, a constant too difficult to measure?" in London on Feb. 2014 [5]. According to Jun Luo: "*The Newtonian gravitational constant G holds an important place in physics. Though there have been about 300 measurements of G since the first laboratory*

measurement by Cavendish over 200 years ago, its measurement precision is the worst among all the fundamental physics constants".

At that time, CODATA stated the following value of the gravitational constant G:

$$G(2010) = 6.67384 \times 10^{-11} m^3 kg^{-1} s^{-2}$$

with Relative Standard Uncertainty (RSU): 1.2×10^{-4}.

Terry Quinn in the paper "Outcome of the Royal Society meeting on G held at Chicheley Hall on 27 and 28 February 2014 to discuss 'The Newtonian constant of gravitation, a constant too difficult to measure?' concluded [6]:

"*Thus, instead of simply calling for new determinations of G, it is suggested that an international advisory board be created, made up largely of those who have already carried out a G experiment, to advise on the choice of method or methods, on the design of the experiment, on its construction and finally on the interpretation of the data and calculation of the results. This would be in contrast to the present situation in which outside criticism and comments can be brought to bear only when the experiment is finished and published when it is too late to affect the outcome. It is only by proceeding in this way that one might hope to obtain results that are demonstrably reliable*".

2. Newtonian Constant of Gravitation

In 2013 WUM proposed a principally different way to solve the problem of G measurement precision and made some predictions of values of Primary Cosmological Parameters (PCPs). WUM revealed a self-consistent set of time-varying values of PCPs: Gravitation parameter, Hubble's parameter, Age of the World, Temperature of the Microwave Background Radiation, the concentration of Intergalactic plasma, and the minimum energy of photons that can pass through the Intergalactic plasma [7], [8].

Based on the inter-connectivity of these parameters, WUM solved the Missing Baryon problem and predicted the values of PCPs, which were experimentally confirmed in 2015 – 2018. The set of values obtained by WUM was recommended for consideration in CODATA Recommended Values of the Fundamental Physical Constants 2014 [9].

According to WUM, the predicted value of the gravitational constant G^*_{2014} equals to :

$$G^*_{2014} = 6.67420 \times 10^{-11} m^3 kg^{-1} s^{-2}$$

To the best of our knowledge, no breakthrough in G measurement methodology has been achieved since [10]. Nevertheless, in 2015 CODATA recommended a more precise value of the Newtonian constant of gravitation:

$$G(2014) = 6.67401 \times 10^{-11} m^3 kg^{-1} s^{-2}$$

with RSU: 4.7×10^{-5}. In 2018 the recommendation improved further:

$$G(2018) = 6.67430 \times 10^{-11} m^3 kg^{-1} s^{-2}$$

with RSU: 2.2×10^{-5}. These values are very close to the predicted value by WUM in 2013. Since 2013, the relative standard uncertainty of G measurements reduced x6. It seems that CODATA considered the WUM recommendation of the predicted value of G and used it for G(2014) and G(2018) without any reference or explanation of their methodology.

3. Self-Consistency of Fundamental Physical Constants

Every four years the Committee on Data for Science and Technology (CODATA) provides a self-consistent set of values of the basic constants and conversion factors of physics recommended for international use.

Table 1, borrowed from CODATA Recommended Values of the Fundamental Physical Constants, 2010, 2014, and 2018 summarizes the results of measurements of Universal, Electromagnetic, and Atomic and Nuclear constants. Observe that the most of Fundamental Physical Constants have more precise values with each adjustment. However, there are a few results that prompt some questions.

1.1. Characteristic Impedance of Vacuum, Vacuum Electric Permittivity, Vacuum Magnetic Permeability, Speed of Light in Vacuum

In 2010 and 2014 these constants had exact values that equal to the theoretical values in vacuum with the value of the electrodynamic constant c equals to the exact value of speed of light in vacuum. Whereas, in 2018 these constants have different numerical values with RSU: 1.5×10^{-10}. By definition, constants Z_0 and ε_0 were calculated based on the value of μ_0 according to the following equations: $Z_0 = \mu_0 c$ and $\varepsilon_0 = (\mu_0 c^2)^{-1}$ with the exact value of speed of light in vacuum c.

Observe that the value of $\mu_0(2018)$ is larger than $\mu_0(2014)$. It means that there is a relative permeability of the Medium of the World μ_r and the magnetic permeability of the Medium μ_M equals to:

$$\mu_M = \mu_r \mu_0$$

The calculated value of μ_r is:

$$\mu_r = 1.00000000054$$

According to WUM, there is a relative electric permittivity of the Medium of the World ε_r and the electric permittivity of the Medium ε_M equals to:

$$\varepsilon_M = \varepsilon_r \varepsilon_0$$

Then, the electrodynamic constant of the Medium c_M can be calculated by the following equation:

$$c_M = (\mu_M \varepsilon_M)^{-1/2} = (\mu_r \mu_0 \varepsilon_r \varepsilon_0)^{-1/2}$$

The existence of the Medium of the World is a principal point of WUM. It consists of Intergalactic plasma, Microwave background radiation, cosmic Far-Infrared background, Dark Matter particles including magnetic dipole DIRAC and electric dipole ELOP. Cosmic Maxwell's equations should consider the macroscopically averaged electric dipole and magnetic dipole moment densities of the Medium in the presence of applied fields [11].

1.2. Rydberg Constant, Hartree Energy, Planck Constant

As of 2018, Rydberg Constant R_∞ is the most accurately measured Fundamental physical constant. Hartree Energy E_h can be calculated by the following equation:

$$E_h = hcR_\infty$$

The RSU of its numerical value depends on the RSU of the numerical value of Planck constant h and RSU of the electrodynamic constant c. CODATA supposed that c is the speed of light in vacuum

with the exact numerical value. Considering the exact numerical value of Planck constant, CODATA gave the RSU of E_h : 1.9×10^{-12} that equals to the RSU of R_∞ .

In our view, it is not correct because the electrodynamic constant c discussed in Section 3.1. has an RSU $\sim 10^{-10}$ and consequently, E_h should have the RSU $\sim 10^{-10}$.

Table 1. Summary of the results of measurements of the Fundamental Physical Constants relevant to the 2010, 2014, and 2018 adjustments.

Fundamental Physical Constant	Numerical Value. Relative Standard Uncertainty, 2010	Numerical Value. Relative Standard Uncertainty, 2014	Numerical Value. Relative Standard Uncertainty, 2018
Characteristic Impedance of Vacuum Z_0 , Ω	376.730 313 461 exact	376.730 313 461 exact	376.730 313 668 1.5×10^{-10}
Newtonian Constant of Gravitation G, $\times 10^{-11}\ m^3 kg^{-1} s^{-2}$	6.673 84 1.2×10^{-4}	6.674 08 4.7×10^{-5}	6.674 30 2.2×10^{-5}
Planck constant h , $\times 10^{-34}\ J\ Hz^{-1}$	6.626 069 57 4.4×10^{-8}	6.626 070 040 1.2×10^{-8}	6.626 070 15 exact
Speed of Light in Vacuum $c, m\ s^{-1}$	299 792 458 exact	299 792 458 exact	299 792 458 exact
Vacuum Electric Permittivity ε_0 , $\times 10^{-12}\ F\ m^{-1}$	8.854 187 8176 exact	8.854 187 8176 exact	8.854 187 8128 1.5×10^{-10}
Vacuum Magnetic Permeability μ_0 , $\times 10^{-6}\ N\ A^{-2}$	1.256 637 061 44 exact	1.256 637 061 44 exact	1.256 637 062 12 1.5×10^{-10}
Elementary charge C, $\times 10^{-19}$	1.602 176 565 2.2×10^{-8}	1.602 176 6208 6.1×10^{-9}	1.602 176 634 exact
Electron Charge to Mass Quotient $-e/m_e$, $\times 10^{11}\ C\ kg^{-1}$	$-1.758\ 820\ 088$ 2.2×10^{-8}	$-1.758\ 820\ 024$ 6.2×10^{-9}	$-1.758\ 820\ 01076$ 3.0×10^{-10}
Fermi Coupling Constant $G_F/(\hbar c)^3$, $\times 10^{-5}\ GeV^{-2}$	1.166 364 4.3×10^{-6}	1.166 3787 5.1×10^{-7}	1.166 3787 5.1×10^{-7}
Fine-Structure Constant α , $\times 10^{-3}$	7.297 352 5698 3.2×10^{-10}	7.297 352 5664 2.3×10^{-10}	7.297 352 5693 1.5×10^{-10}
Hartree Energy E_h , $\times 10^{-18}\ J$	4.359 744 34 4.4×10^{-8}	4.359 744 650 1.2×10^{-8}	4.359 744 722 2071 1.9×10^{-12}
Rydberg Constant R_∞ , m^{-1}	10 973 731.568 539 5.0×10^{-12}	10 973 731.568 508 5.9×10^{-12}	10 973 731.568 160 1.9×10^{-12}

1.3. Elementary Charge, Characteristic Impedance of Vacuum

The relation used by CODATA to determine elementary charge is:

$$e^2 = \frac{2h\alpha}{\mu_0 c}$$

As of 2018, the Elementary charge e, Planck constant h, and speed of light in vacuum c have the exact numerical values. It means that the ratio α/μ_0 must be a constant. No explanation for this calculation is provided.

In our view, we should use the following relation:

$$Z_0 = \frac{2h}{e^2}\alpha$$

The RSU of the numerical value of α is: 1.5×10^{-10}. It means that the RSU of the numerical value of Z_0 must be the same. Z_0 cannot have the exact value as it was supposed in 2010 and 2014.

1.4. Fermi Coupling Constant, Newtonian Constant of Gravitation

Considering a more precise value of Fermi Coupling constant (see **Table 1**) we calculate the value of the predicted parameter G^*_{2018} [8]:

$$G^*_{2018} = 6.674536 \times 10^{-11} m^3 kg^{-1} s^{-2}$$

which is x8 more accurate than G^*_{2014}.

2. Conclusion

The detailed analysis of the self-consistency of Fundamental physical constants based on the developed World-Universe Model shows that it is the right time to:

- discontinue using the notion "Vacuum" and its characteristics:
  - Speed of Light in Vacuum;
  - Characteristic Impedance of Vacuum;
  - Vacuum Magnetic Permeability;
  - Vacuum Electric Permittivity;
- correct the numerical value and relative standard uncertainty of Hartree energy;
- accept the exact numerical values of Planck constant and Elementary charge;
- recommend for consideration in CODATA Recommended Values of the Fundamental Physical Constants 2022 the predicted value of the Newtonian Constant of Gravitation G^*_{2018}.

Acknowledgements

I'm grateful to my son Ilya Netchitailo who has reviewed and edited this work.

References

[1] Lagache, G., *et al.* (1999) First detection of the WIM dust emission. Implication for the Cosmic Far-Infrared Background. arXiv:astro-ph/9901059.
[2] Fixsen, D.J. (2009) The Temperature of the Cosmic Microwave Background. arXiv:0911.1955.
[3] C. L. Bennett, *et al.* (2012) Nine-Year Wilkinson Microwave Anisotropy Probe (WMAP) Observations: Final Maps and Results. arXiv:1212.5225v3.
[4] Mohr, P. J., Taylor, B. N., and Newell, D. B. (2012) CODATA Recommended Values of the Fundamental Physical Constants: 2010. arXiv:1203.5425.

[5] Quinn, T., Speake, C., and Luo, J. (2014) The Newtonian constant of gravitation, a constant too difficult to measure? The Royal Society Meeting. London, Feb. 27-28. https://royalsociety.org/science-events-and-lectures/2014/gravitation/.
[6] T. Quinn (2014) Outcome of the Royal Society meeting on G held at Chicheley Hall on 27 and 28 February 2014 to discuss 'The Newtonian constant of gravitation, a constant too difficult to measure?". Phil. Trans. R. Soc. **A 372**. https://doi.org/10.1098/rsta.2014.0286 .
[7] Netchitailo V. S. (2013) Word-Universe Model. viXra:1303.0077.
[8] Netchitailo V. S. (2013) Fundamental Parameter Q. Recommended Values of the Newtonian Parameter of Gravitation, Hubble's Parameter, Age of the World, and Temperature of the Microwave Background Radiation. viXra:1312.0179.
[9] Netchitailo, V. (2020) World-Universe Model Predictions. *Journal of High Energy Physics, Gravitation and Cosmology*, **6**, 282-297. doi: 10.4236/jhepgc.2020.62022.
[10] Mohr, P. J., Newell, D. B., and Taylor, B. N. (2015) CODATA Recommended Values of the Fundamental Physical Constants: 2014. arXiv:1507.07956.
[11] Netchitailo, V. (2017) Analysis of Maxwell's Equations. Cosmic Magnetism. *Journal of High Energy Physics, Gravitation and Cosmology*, **4**, 1-7. https://doi.org/10.4236/jhepgc.2018.41001.